Electronic Supplementary Material (ESI) for ChemComm.

Supporting Information

Synthesis and catalytic application of donor-free bismuthenium cation

Nilanjana Sen[a], Pallavi Mukherjee[b#], Yadram Meena[a], Srinu Tothadi[c] Swapan K. Pati[*b]
Shabana Khan[*a]

Table of Contents

[S1]. Crystal Data and Structure Refinement for 3

Crystallography reflections were collected on a Bruker Smart Apex Duo diffractometer at 150 K using Mo Kα radiation (λ = 0.71073 Å) for **3**. The structures were solved by direct method and refined by full-matrix least-squares methods against F2 (SHELXL-2014/6). Crystallographic data (including structure factors) for the structure reported in this paper have been deposited with the Cambridge Crystallographic Data Centre as supplementary publication CCDC no. of compound **3** is 2322619.

Table [S1]. Data collection parameters for compound **3**.

	3
Chemical formula	$C_{32}H_{52}Bi_2F_{12}N_4Sb_2$
Formula weight	1382.23g/mol
Temperature	100(2) K
Wavelength	0.71073 Å
Crystal system	Monoclinic
Space group	*C 2/c*
Unit cell dimensions	*a* = 36.971(6) Å
	b = 11.0199(18) Å
	c = 21.471(4) Å
	α = 90°
	β = 101.205(5) °
	γ = 90°
Volume	8581(2) Å^3
Z	8
Density (calculated)	2.140 g/cm^3
Absorption coefficient	9.504 mm^{-1}
F(000)	5184
Theta range for data collection	2.21 to 28.18°
Index ranges	-48<=h<=44, -14<=k<=14, -27<=l<=27
Reflections collected	64711
Independent reflections	9829 [R(int) =0.0766]
Coverage of independent reflections	99.9%
Function minimized	Σ w(Fo2 - Fc2)2
Data / restraints / parameters	9829 / 0 / 483
Goodness-of-fit on F2	2.557
Δ/σ max	0.012

Final R indices	8398 data; [I>2σ(I)] R1 = 0.1193, wR2 = 0.3342
	all data, R1 = 0.1317, wR2 = 0.3399
Largest diff. peak and hole	0.282 and -0.045 eÅ-3
R.M.S. deviation from mean	0.007eÅ-3

[S2]. Molecular structure of compound 2.

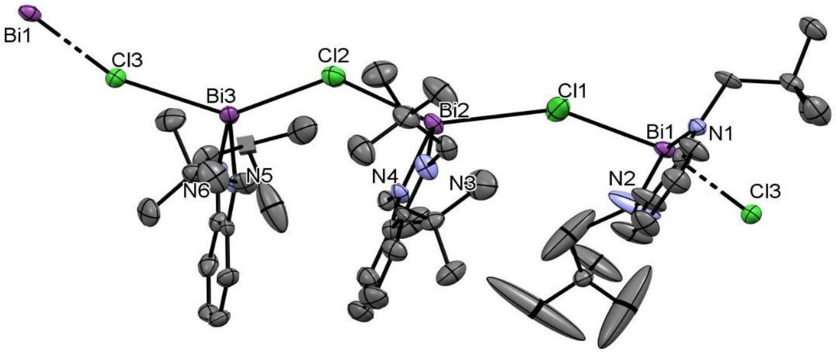

Figure S1a. The molecular structure of **2** with anisotropic displacement parameters is depicted at the 50% probability level. Hydrogen atoms are not shown for clarity.

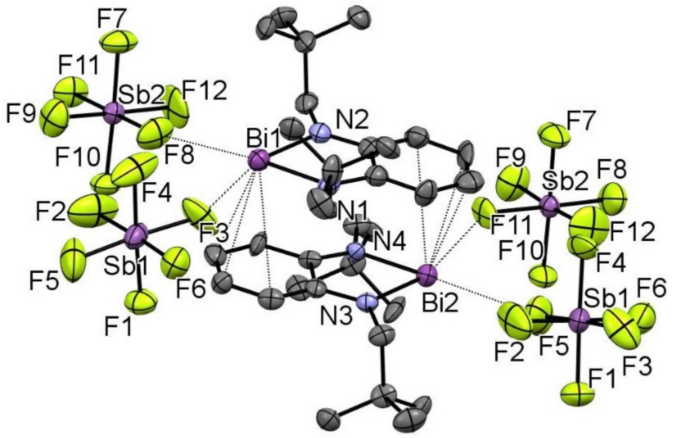

Figure S1b. Representation of the interactions of the central cationic bismuth with the adjacent fluorine atoms and π-stacking in **3**. Hydrogen atoms are not shown for clarity.

It has been observed that **3** exhibits a different pattern of cation-cation interaction in the solid state which is similar to that of the previously reported stibenium cation by Khan and coworkers.[1] The molecular structure reveals that the bismuth center comprises π-stacked dimers which are antiparallel to each other in orientation and the Bi center displays an intermolecular π interaction with the arene ring of the adjacent moiety in η^3 fashion (Bi···C4 is 3.468 Å, Bi···C5 is 3.364 Å, Bi···C6 is 3.540 Å).

Experimental Section

Synthesis of compound 2. Compound **1** (1 gm, 4.11 mmol) was taken in a 100 ml Schlenk flask, and 60 ml Et_2O was added to it at room temperature. Subsequently, the flask was cooled to -70 °C, and *n*BuLi (3.29 ml of 2.5 M solution) was added slowly. The reaction mixture was slowly allowed to come to room temperature and left on stirring for 6 h. The reaction mixture was cooled again to 0°C and was transferred to another Schlenk flask containing THF (20 ml) solution of $BiCl_3$ (1.294 g, 4.11 mmol). The reaction was left on stirring overnight. The solution was filtered and concentrated until it formed crystalline particles on the surface of the flask. The concentrated solution of **2** was stored at 0 °C, which resulted in the formation of violet-red colored crystals of **2**. Yield (%): 61.2% (300mg) ^1H NMR (400 MHz, $CDCl_3$, 298 K): δ 1.05 (s, 18H, ^{t}Bu group), 2.86 (s, 4H, $-CH_2$), 6.69-6.80 (m, 4H, Ph) ppm. $^{13}C\{^1H\}$ NMR (100.613 MHz, $CDCl_3$, 298 K): δ 1.1, 27.9, 31.6, 56.5, 112.2, 119.3, 138.4 ppm.

Synthesis of compound 3. To the mixture of compound **2** (403 mg, 1 mmol) and $AgSbF_6$ (344 mg, 1 mmol) in a 100 ml Schlenk flask, 40 ml DCM was added. The reaction mixture was kept on stirring overnight at room temperature. The solution was then filtered and concentrated to 5 ml, and a few drops of *n*-pentane were added. The solution was stored at 0 °C for crystallization. Yield (%): 66.3% (400mg) ^1H NMR (400 MHz, $CDCl_3$, 298 K): δ 1.10 (s, 18H, ^{t}Bu group), 3.05 (s, 4H, $-CH_2$), 6.69-6.80 (m, 4H, Ph) ppm. $^{13}C\{^1H\}$ NMR (100.613 MHz, $CDCl_3$, 298 K): δ 1.1, 25.7, 27.3, 31.4, 60.9, 68.1, 120.1, 126.2, 134.8 ppm. $^{19}F\{^1H\}$ (100.613 MHz, $CDCl_3$, 298 K) δ -169.42 ppm. HRMS: Calcd. for $[C_{16}H_{26}BiN_2SbF_6]$: *m/z* 690.0842. Found *m/z* 690.5701 $[M^+]$

[S3]. ^{1}H, ^{13}C, ^{19}F NMR spectra of compounds 2 and 3.

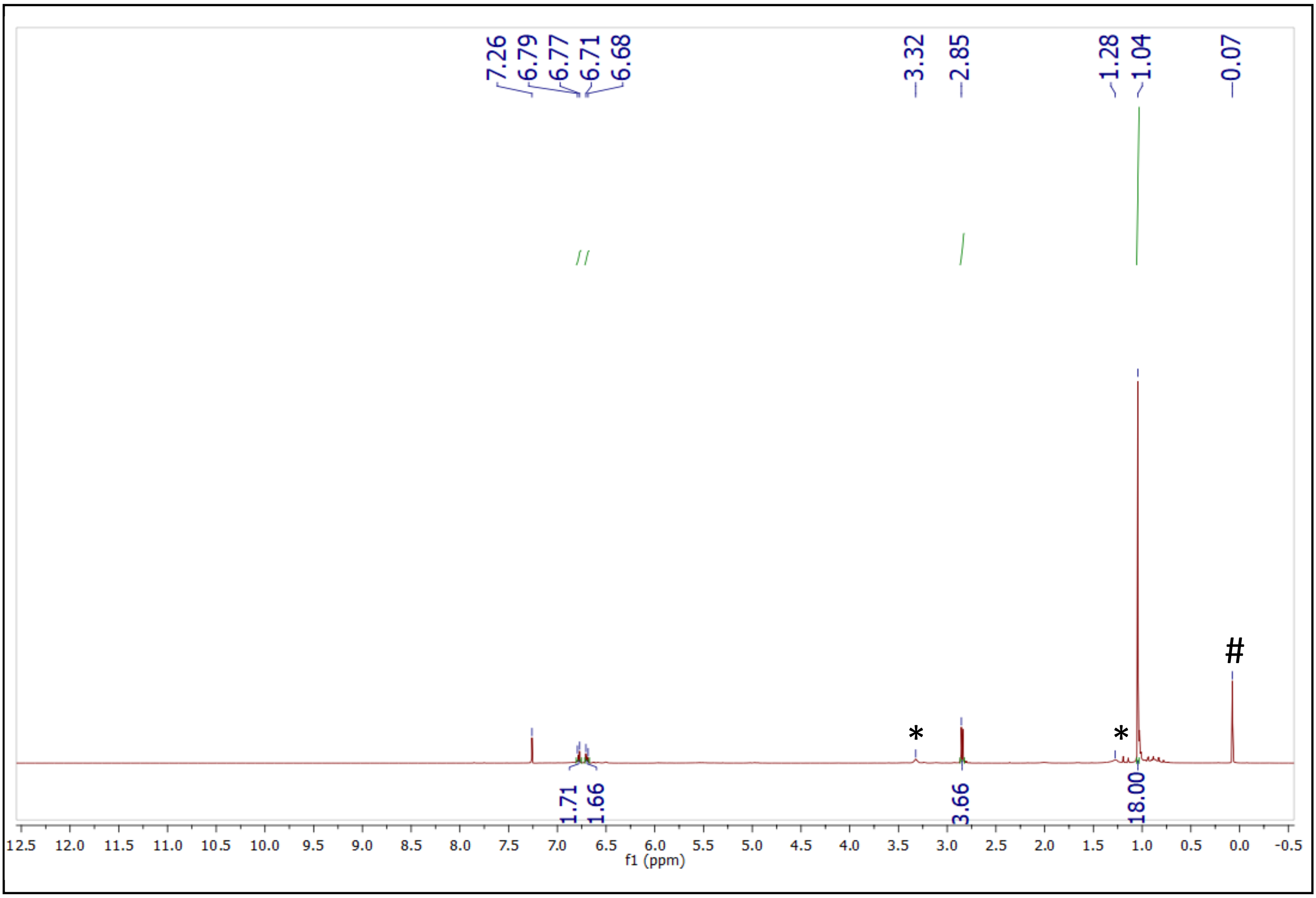

Figure S2. ^{1}H NMR spectrum of compound **2** in $CDCl_3$ (* - Diethyl ether, # - Grease).

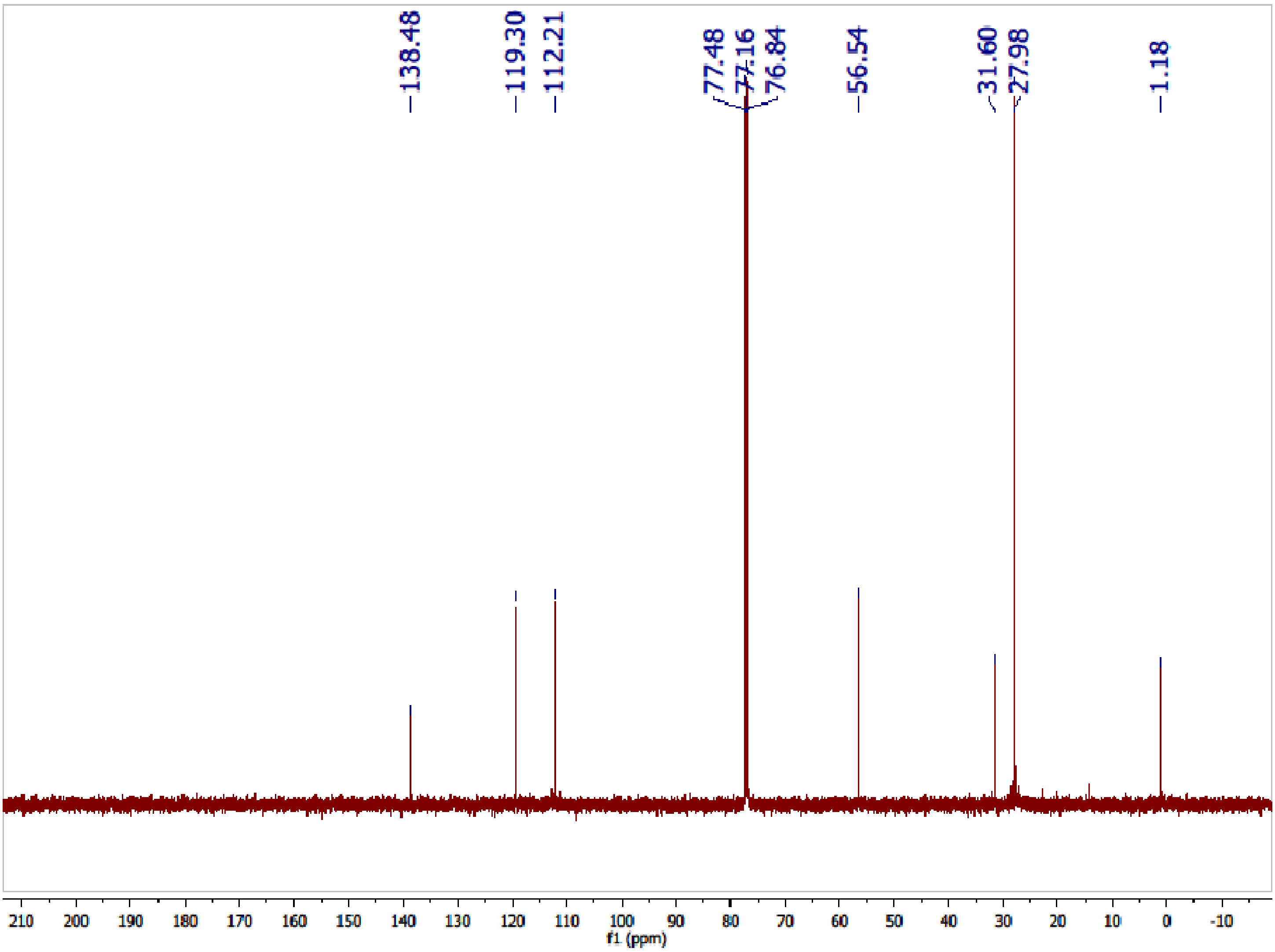

Figure S3. ^{13}C NMR spectrum of compound **2** in $CDCl_3$.

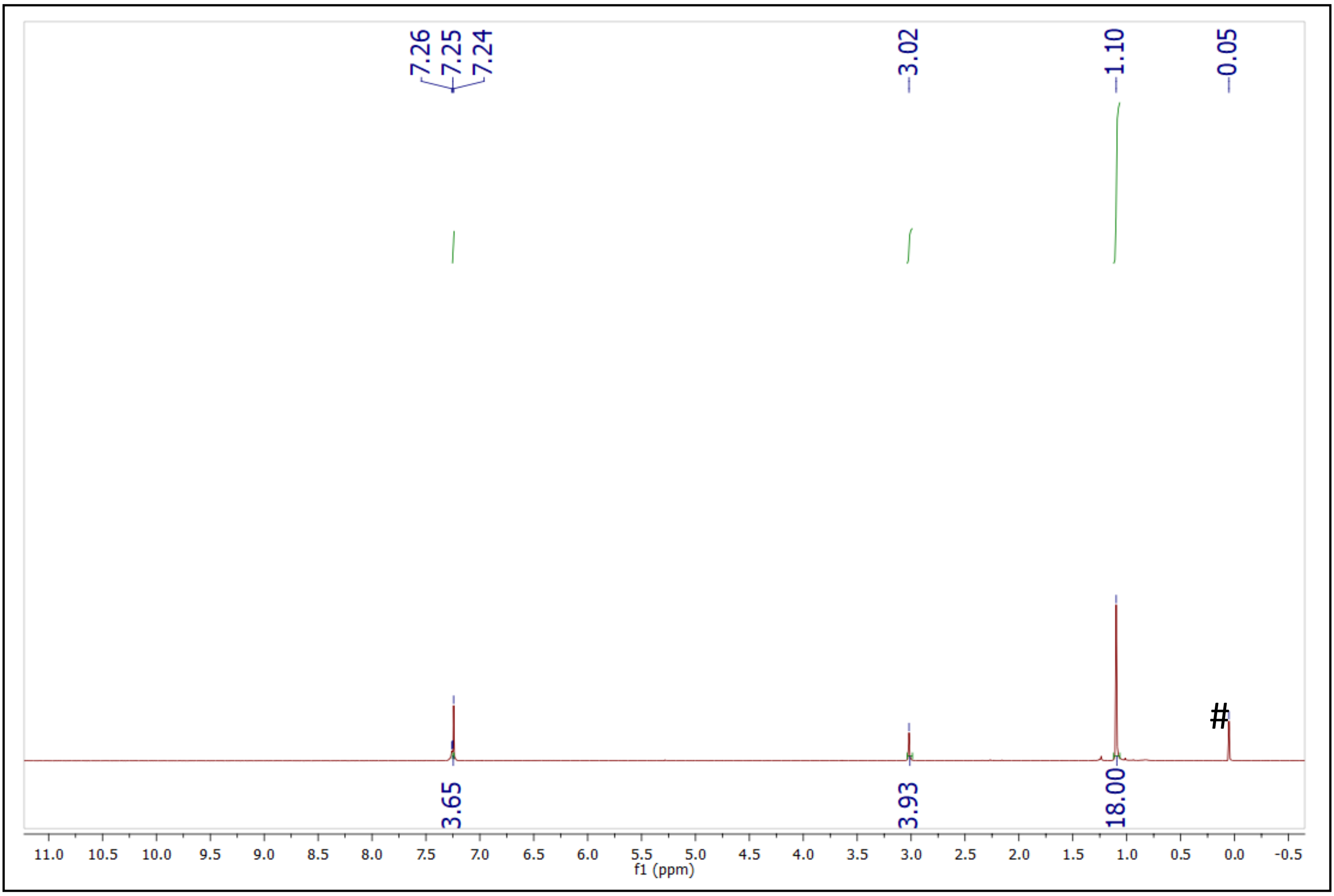

Figure S4. ^{1}H NMR spectrum of compound **3** in $CDCl_3$ (# - Grease).

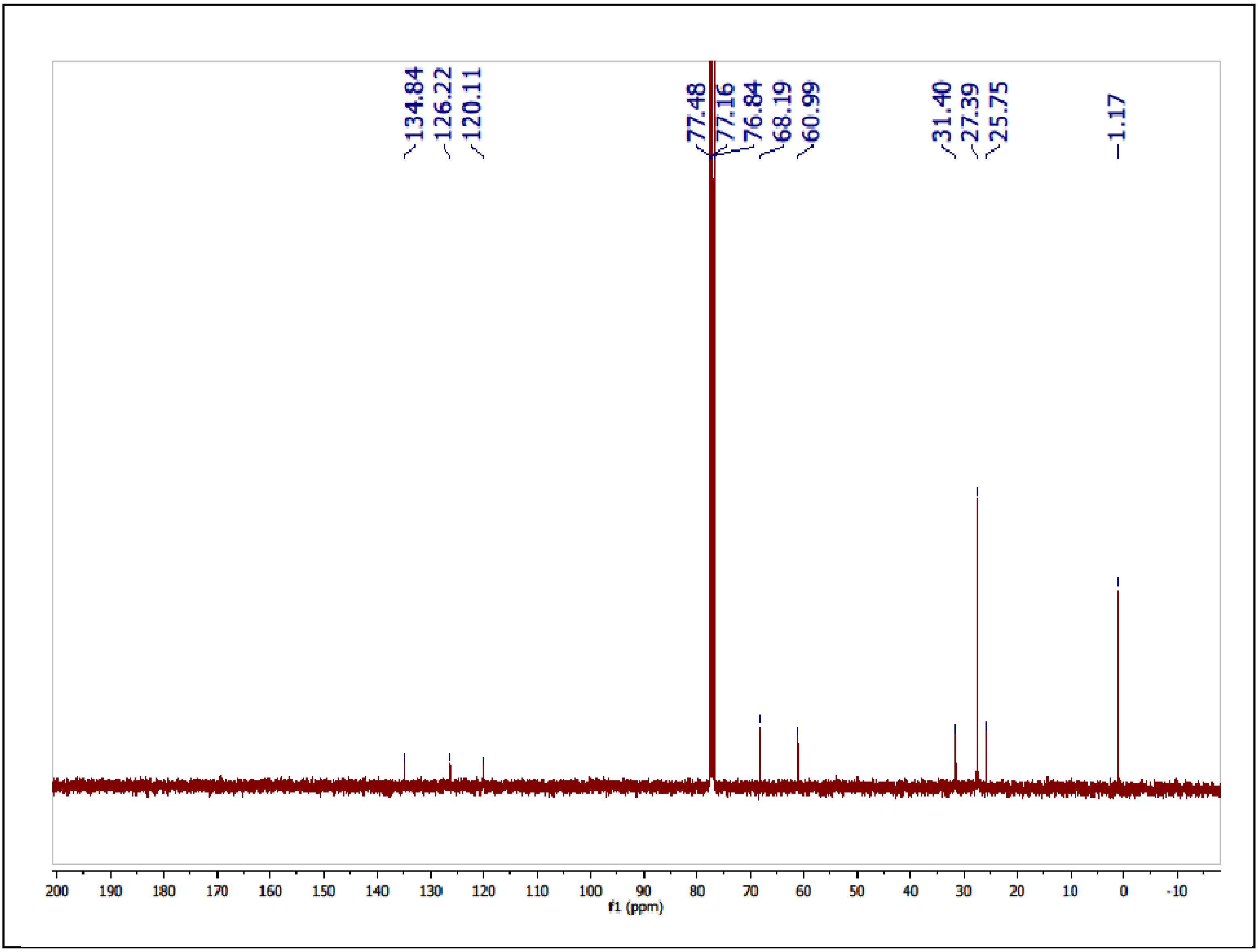

Figure S5. ^{13}C NMR spectrum of compound **3** in $CDCl_3$.

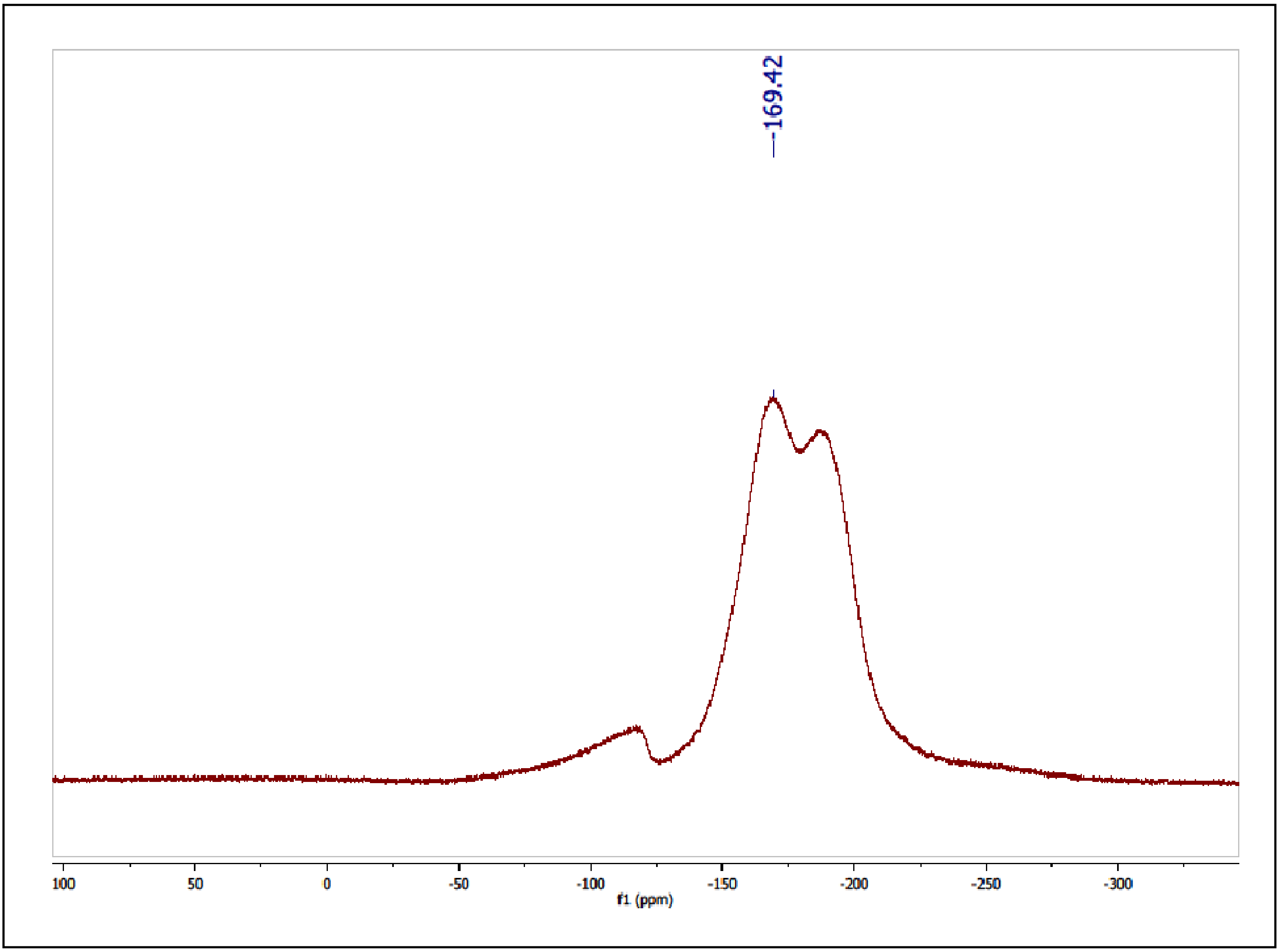

Figure S6. ^{19}F NMR spectrum of compound **3** in $CDCl_3$.

[S4]. Photophysical properties and UV-Vis absorption spectra of compounds 2 and 3.

Compound	**Absorption Wavelength (nm)**		
	THF	DCM	ACN
2 (experimental value)	298, 498	299, 560	299, 557
2 (computed value)	294, 507.7	293, 506	289, 498.3
3 (experimental value)	290, 500	299, 496	289, 528
3 (computed value)	301, 510	300.8, 509.7	299.8, 506

Table S2. UV-Vis spectroscopic data of compounds **2** and **3**.

Our both the compounds being highly colored; hence we were motivated to study the photophysical properties of these compounds. We recorded the UV-Vis absorption in three different solvents THF, DCM, and ACN (300μL of the concentration) (Figure S7). Compound **2** exhibits a dark purple color, and the observed UV-Vis spectrum appears at 299 nm and 560 nm in DCM, 298 nm and 498 nm in THF, 299 nm and 557 nm in ACN. Compound **3** also appeared to be dark violet and from UV-Vis spectrometry study it is observed that two peaks at 290 nm and 500 nm appear in THF, 299 nm and 496 nm in DCM, 289 nm and 528 nm in ACN. We have performed the TD-DFT calculations with B3LYP-D3 exchange-correlation functional and lanl2dz basis set for Bi and 6-311+G(d,p) for lighter atoms. The results reveal that the absorptions are due to the charge transfer from the p-electron density of the aromatic ring to the vacant *p* orbital of the bismuth atom (**Figure S8**).

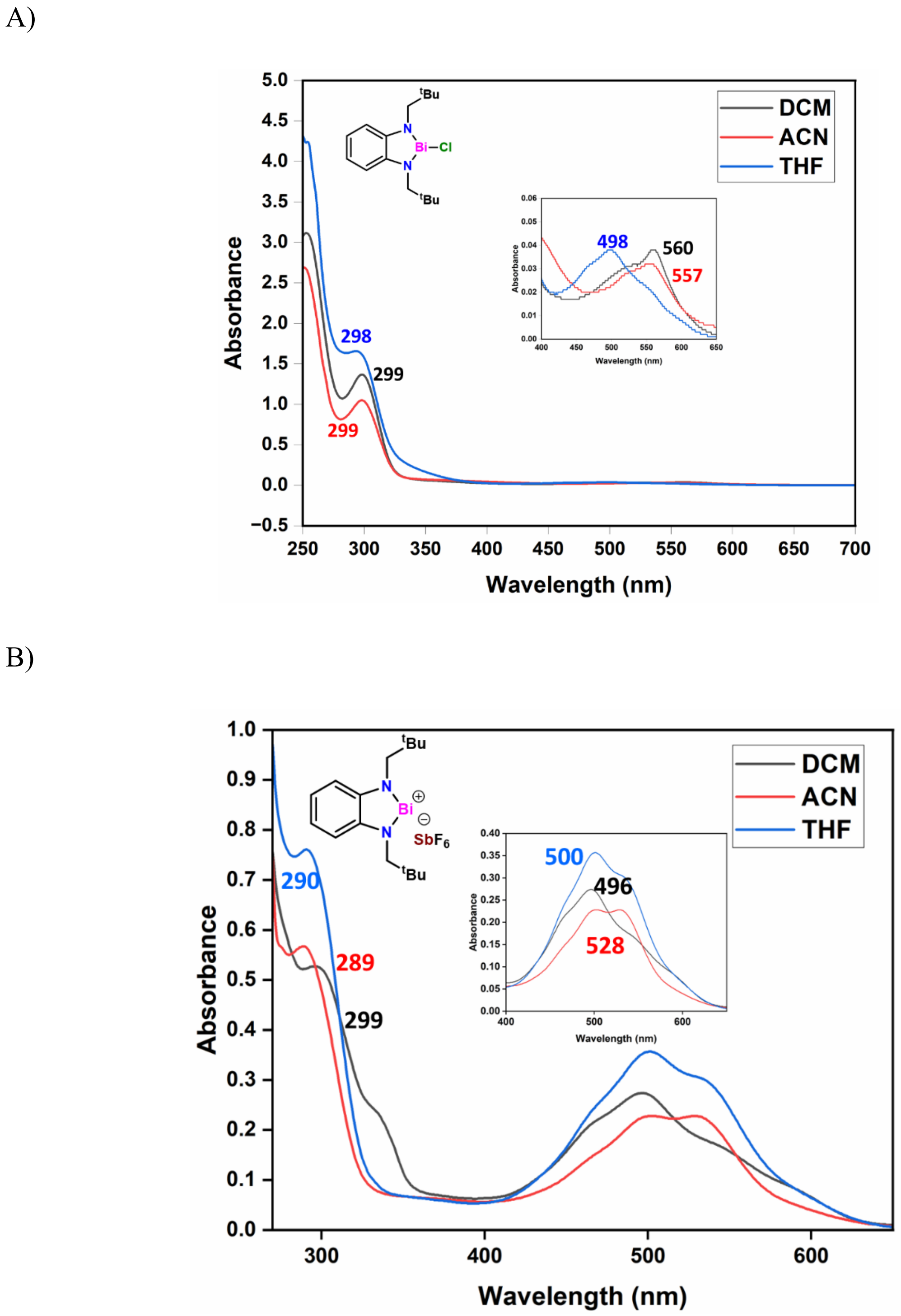

Figure S7a. UV-Vis absorption spectra of compounds A) **2** and B) **3** (300μL of the concentration).

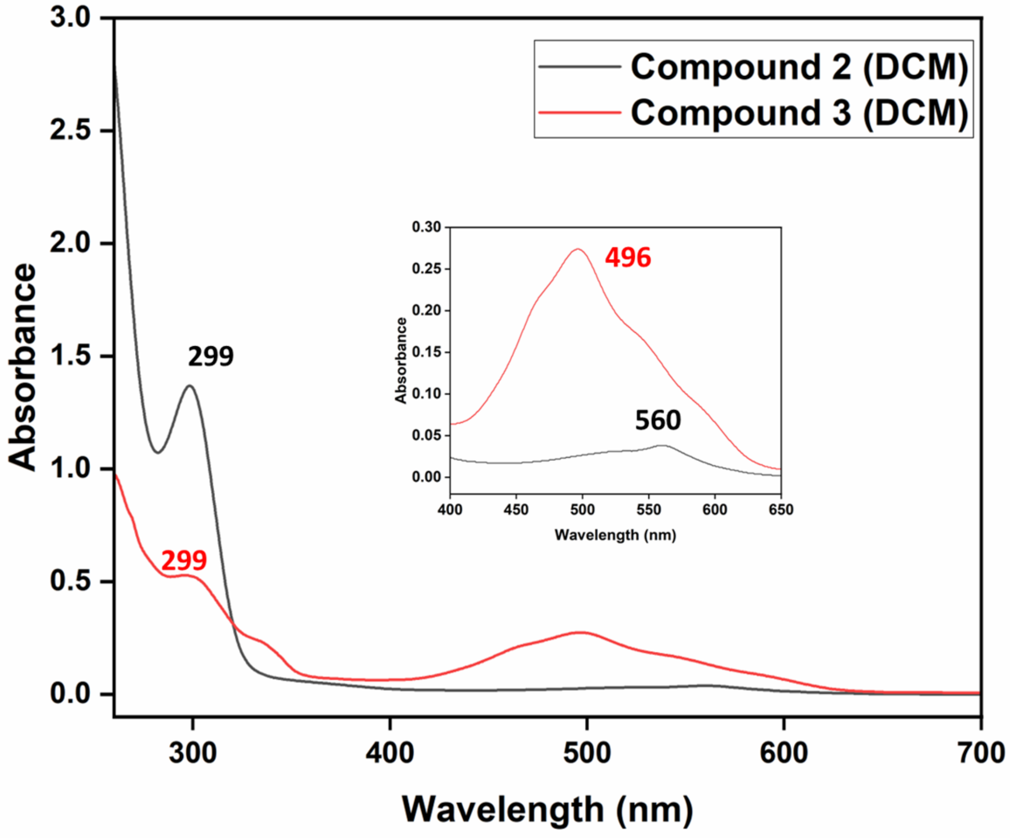

Figure S7b. Combined UV-Vis absorption spectra of compounds **2** and **3** in DCM (300µL of the concentration).

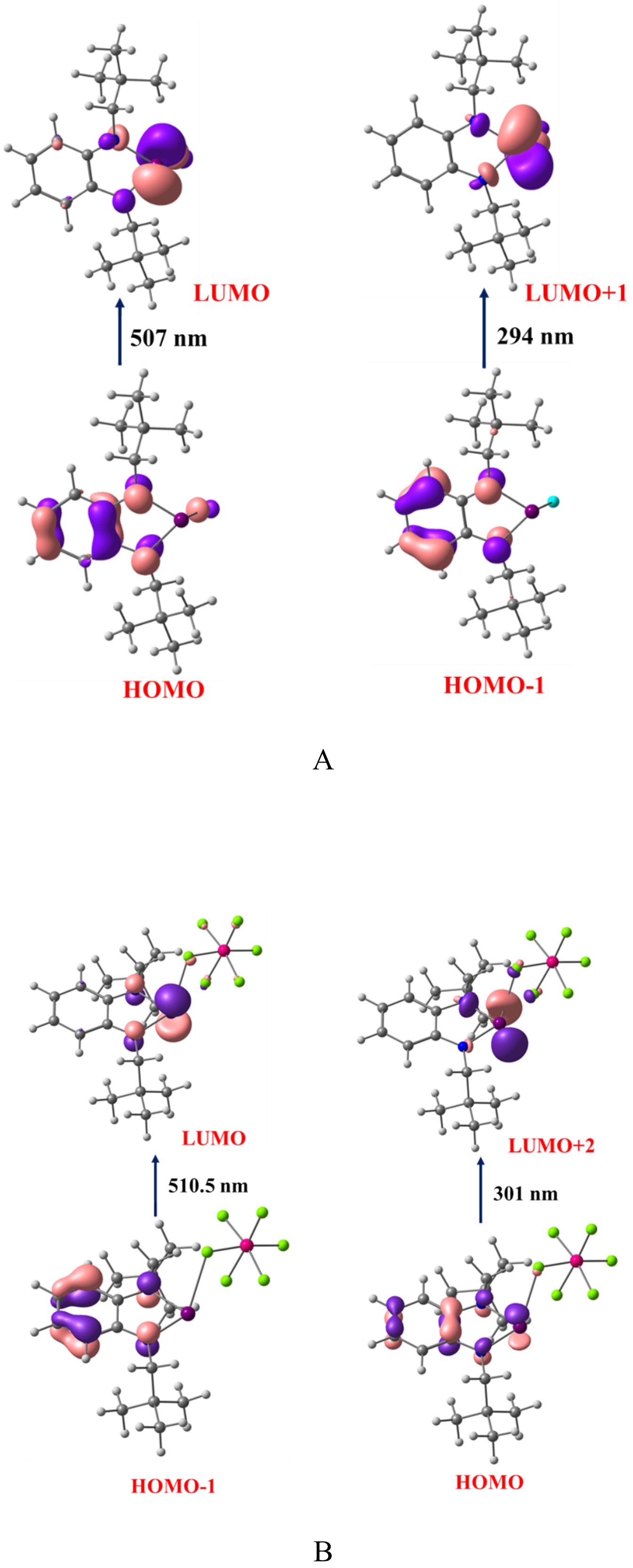

Figure S8. Calculated transitions for the main absorption of a) **2** and b) **3**.

[S5]. ^{31}P NMR Spectra of compounds 2 and 3 with $OPEt_3$ (1:1 reaction).

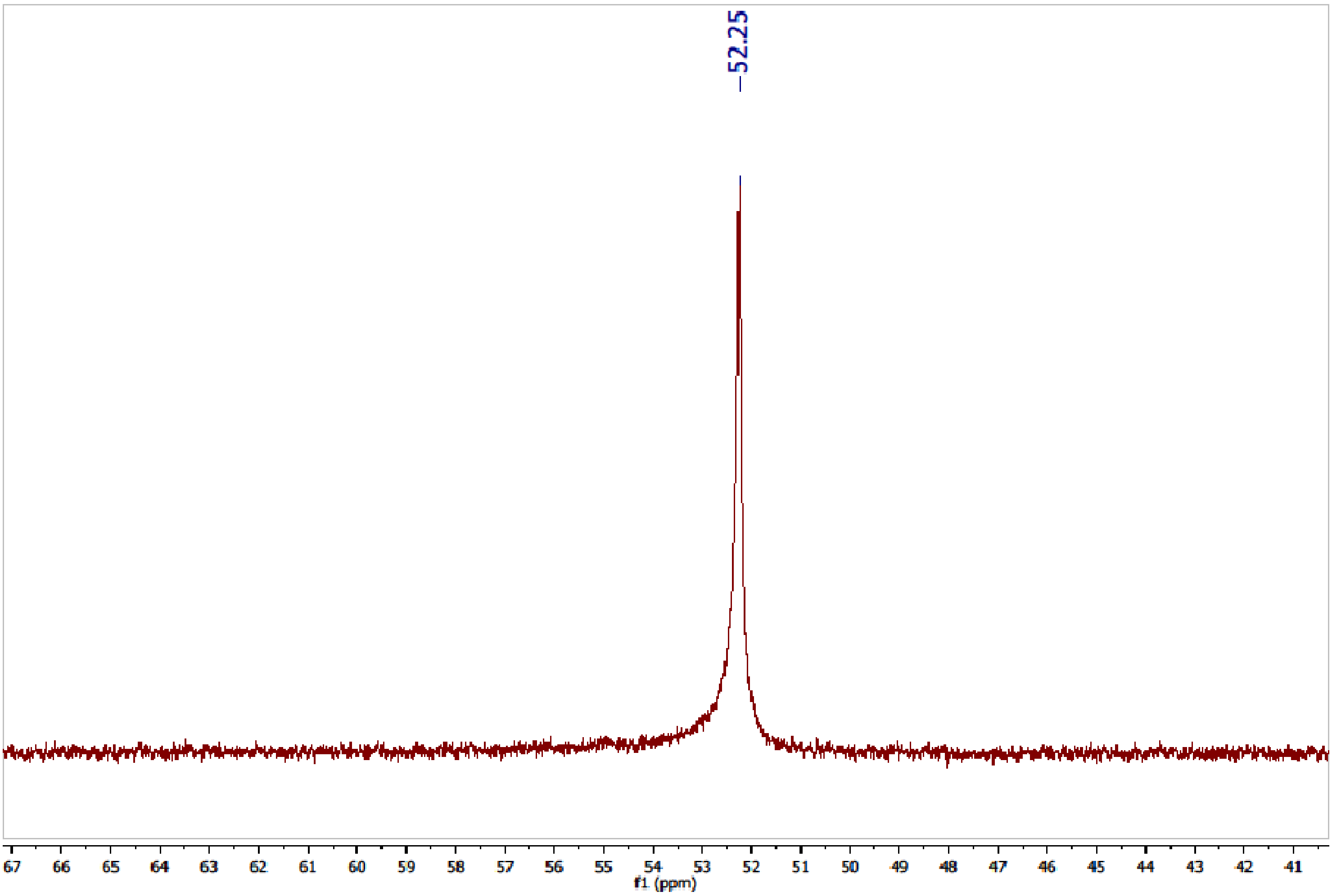

Figure S9. ^{31}P NMR spectrum of compound **2** and $OPEt_3$ in $CDCl_3$.

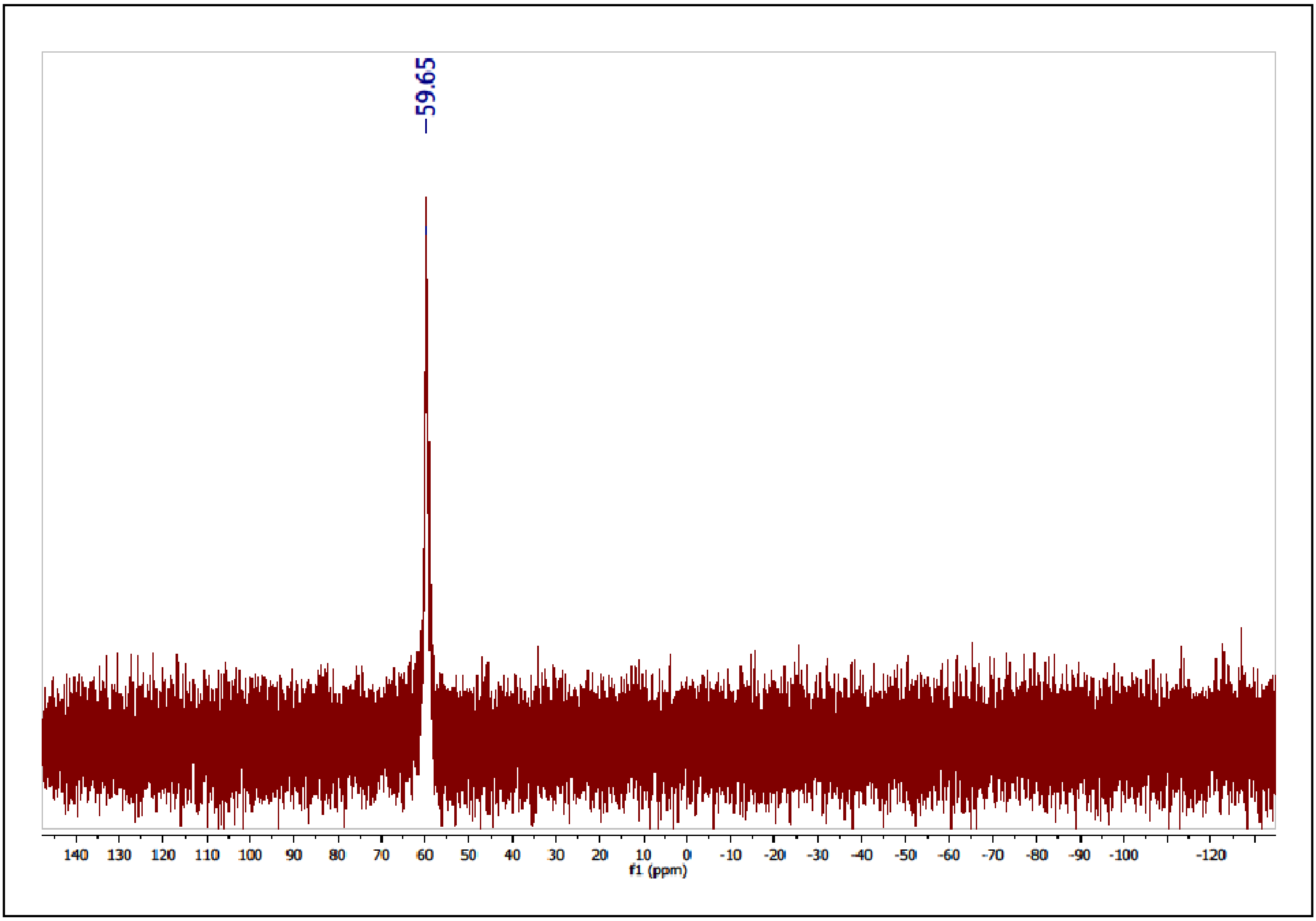

Figure S10. ^{31}P NMR spectrum of compound **3** and OPEt$_3$ in CDCl$_3$.

[S6]. General procedure for the cyanosilylation of ketones.

The desired cyanosilylation reaction of differently substituted aromatic/aliphatic ketones was carried out in Schlenk tubes. A similar equivalence of trimethyl silyl cyanide, TMSCN (0.38 mmol), and the desired ketone (0.25 mmol) were poured into a Schlenk tube, and then the exact equivalence of catalyst **3** (0.1 mol%) was added to the same tube and allowed to stir for a 15 mins at room temperature. Later, the reaction mixture was subjected to ^{1}H and ^{13}C NMR experiments using mesitylene as an internal standard to obtain the definite yield of the cyanosilylated product.

Calculation of the stock solution of 10 mol% of 0.25mmol the catalyst in DCM

Molecular weight of catalyst = 690g/mol

10 mol% of 0.25 mmol catalyst = 17.25mg

0.1 mol% of 0.25 mmol catalyst = 0.1725 mg

17.25 mg of the catalyst taken in 10 ml of DCM (Stock solution)

0.1725 mg of catalyst = (10×0.1725)/17.25 = 0.1ml or 100μl

Table S3. Optimization table for cyanosilylation of acetophenone by catalyst **3**.

Entry	Catalyst	Mol (%)	Time (Mins)	TMSCN (Equiv.)	Temperature	Yield (%)
1	3	0.5	30	1.5	RT	>99
	3	0.5	15	1.5	RT	>99
2	3	0.25	30	1.5	RT	>99
	3	0.25	15	1.5	RT	>99
3	3	0.1	30	1.5	RT	>99
	3	0.1	15	1.5	RT	>99
4	3	0.05	30	1.5	RT	<50
5	2	0.1	15	1.5	RT	Traces
6	-		15	1.5	RT	No conversion
7	$AgSbF_6$	0.1	15	1.5	RT	<15%
8	$AgSbF_6$	0.5	15	1.5	RT	50%
9	$NaBAr^F$	0.1	15	1.5	RT	No conversion

[S7]. Standardization of reaction conditions for cyanosilylation reaction of ketones with trimethyl silyl cyanide using catalyst 3.

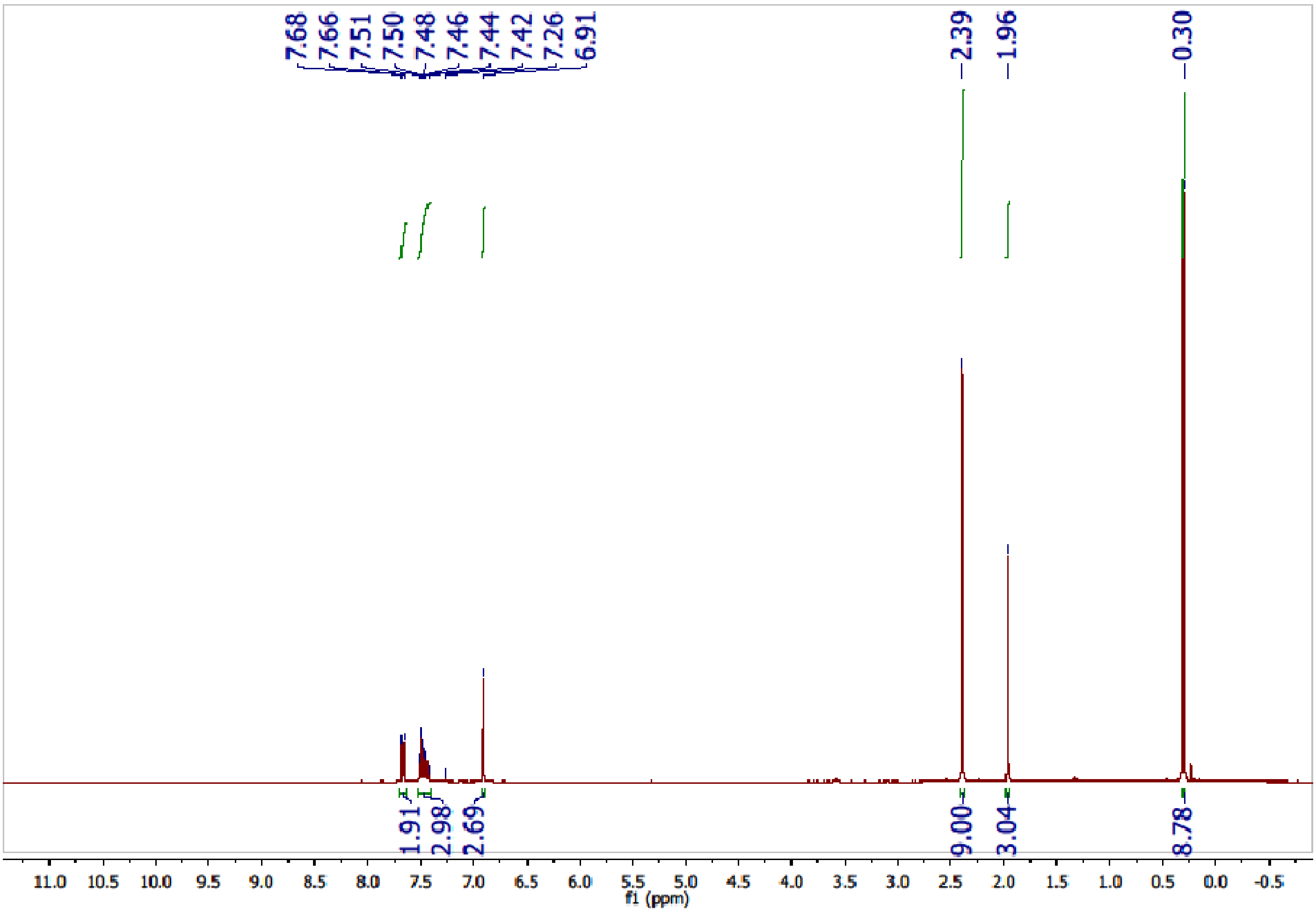

Figure S11. ^{1}H NMR spectrum of cyanosilylation of acetophenone with TMSCN with 0.5 mol% of catalyst loading within 30 mins.

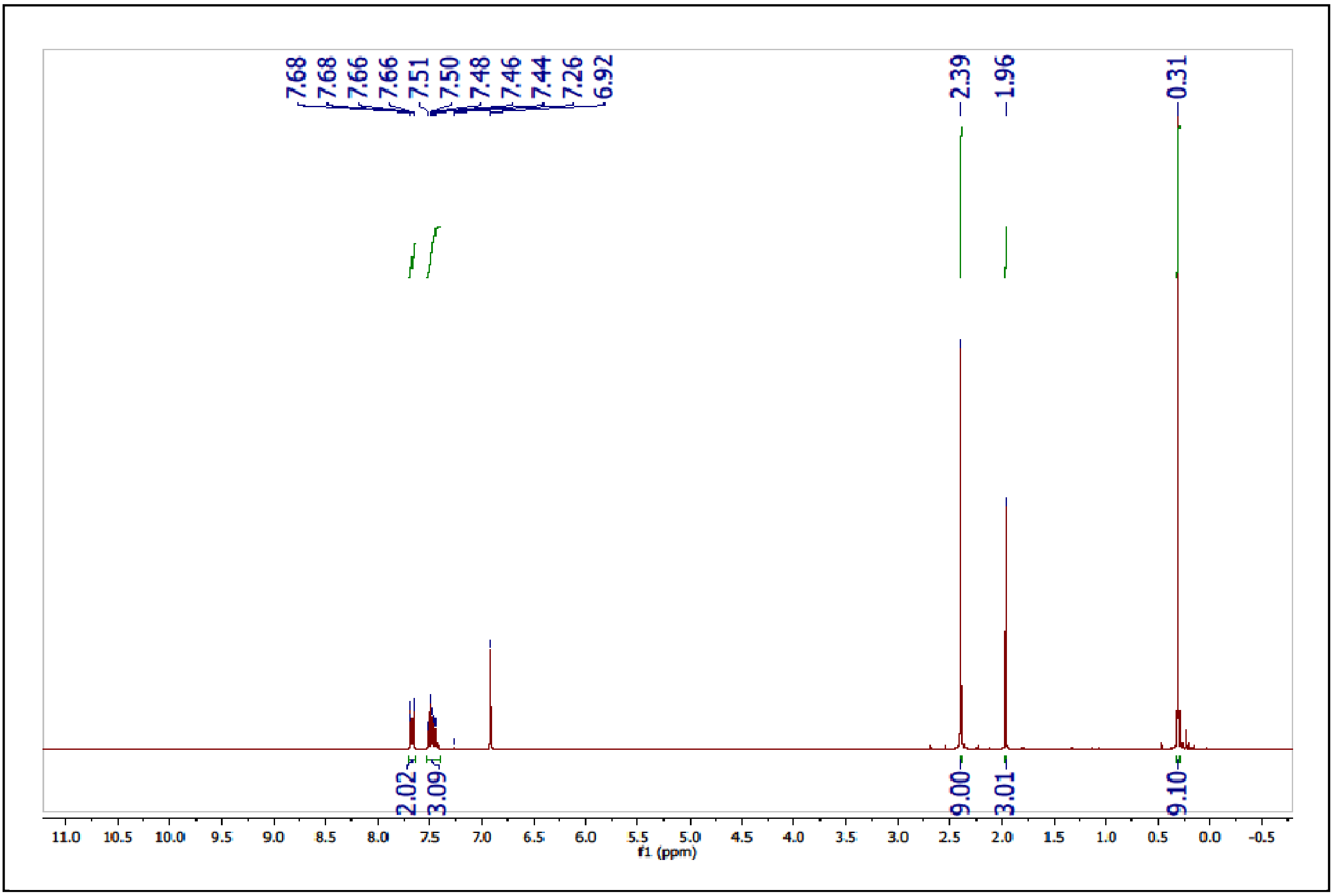

Figure S12. ^{1}H NMR spectrum of cyanosilylation of acetophenone with TMSCN with 0.5 mol% of catalyst loading within 15 mins.

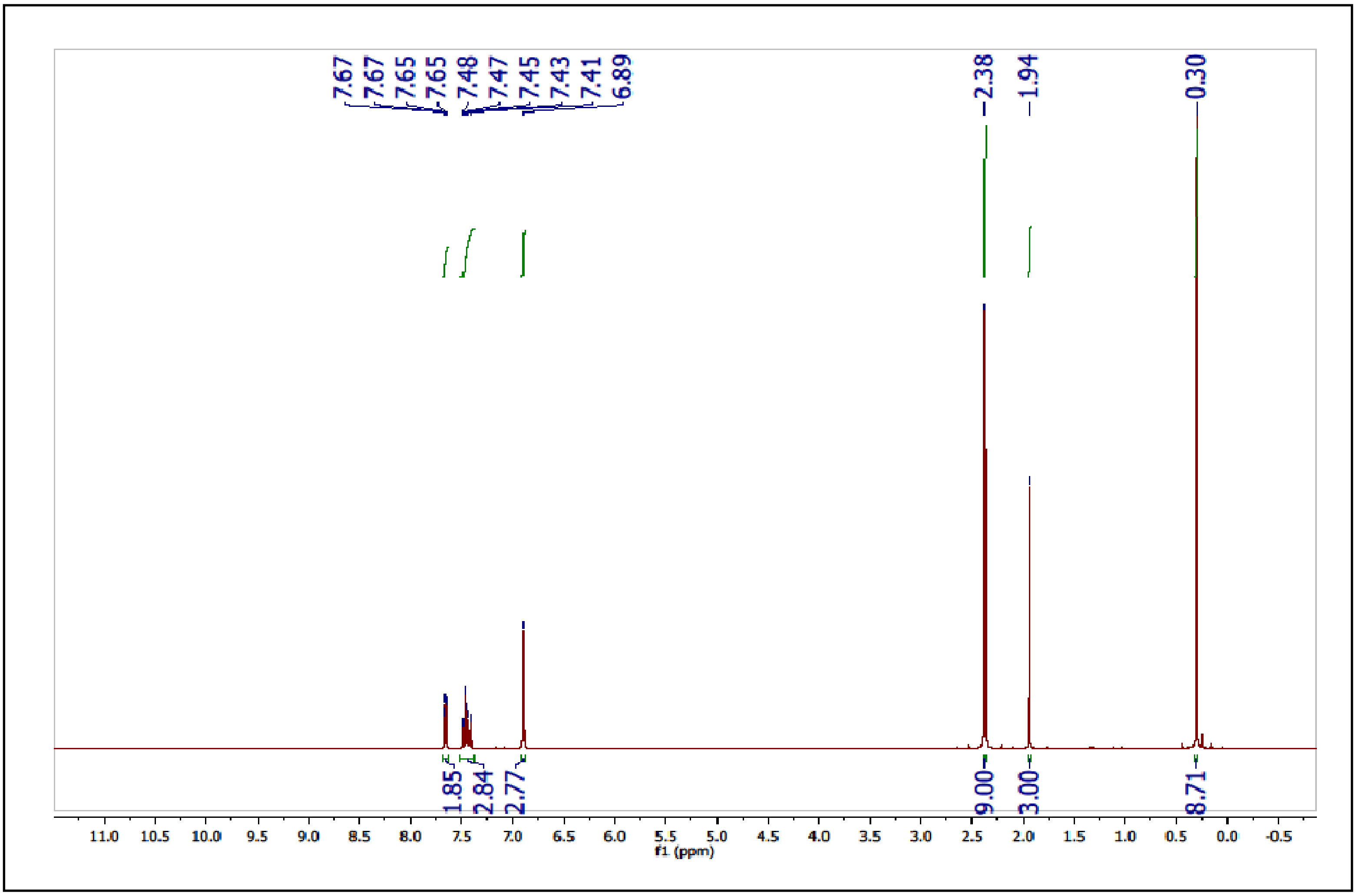

Figure S13. ^{1}H NMR spectrum of cyanosilylation of acetophenone with TMSCN with 0.25 mol% of catalyst loading within 30 mins.

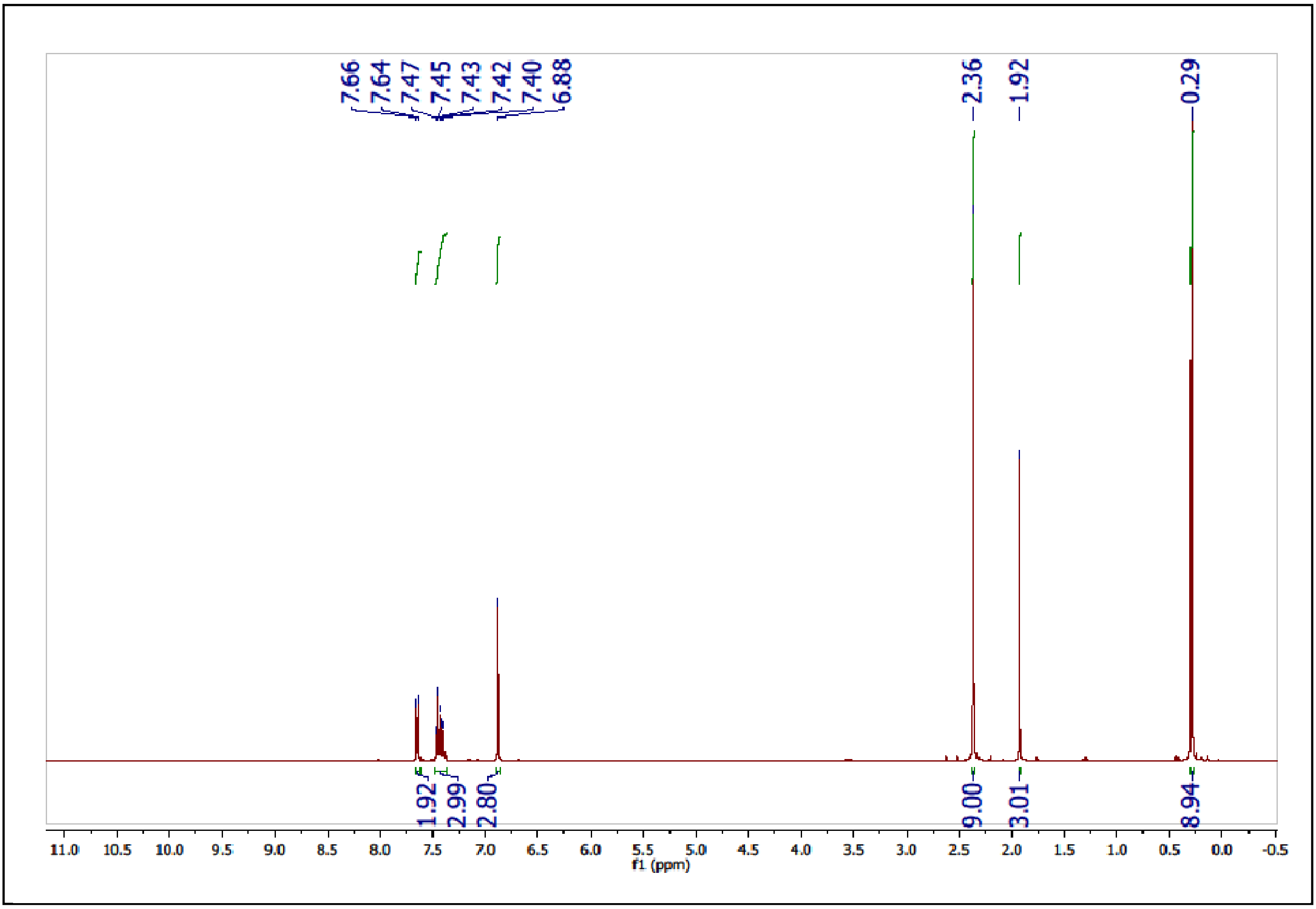

Figure S14. ^{1}H NMR spectrum of cyanosilylation of acetophenone with TMSCN with 0.25 mol% of catalyst loading within 15 mins.

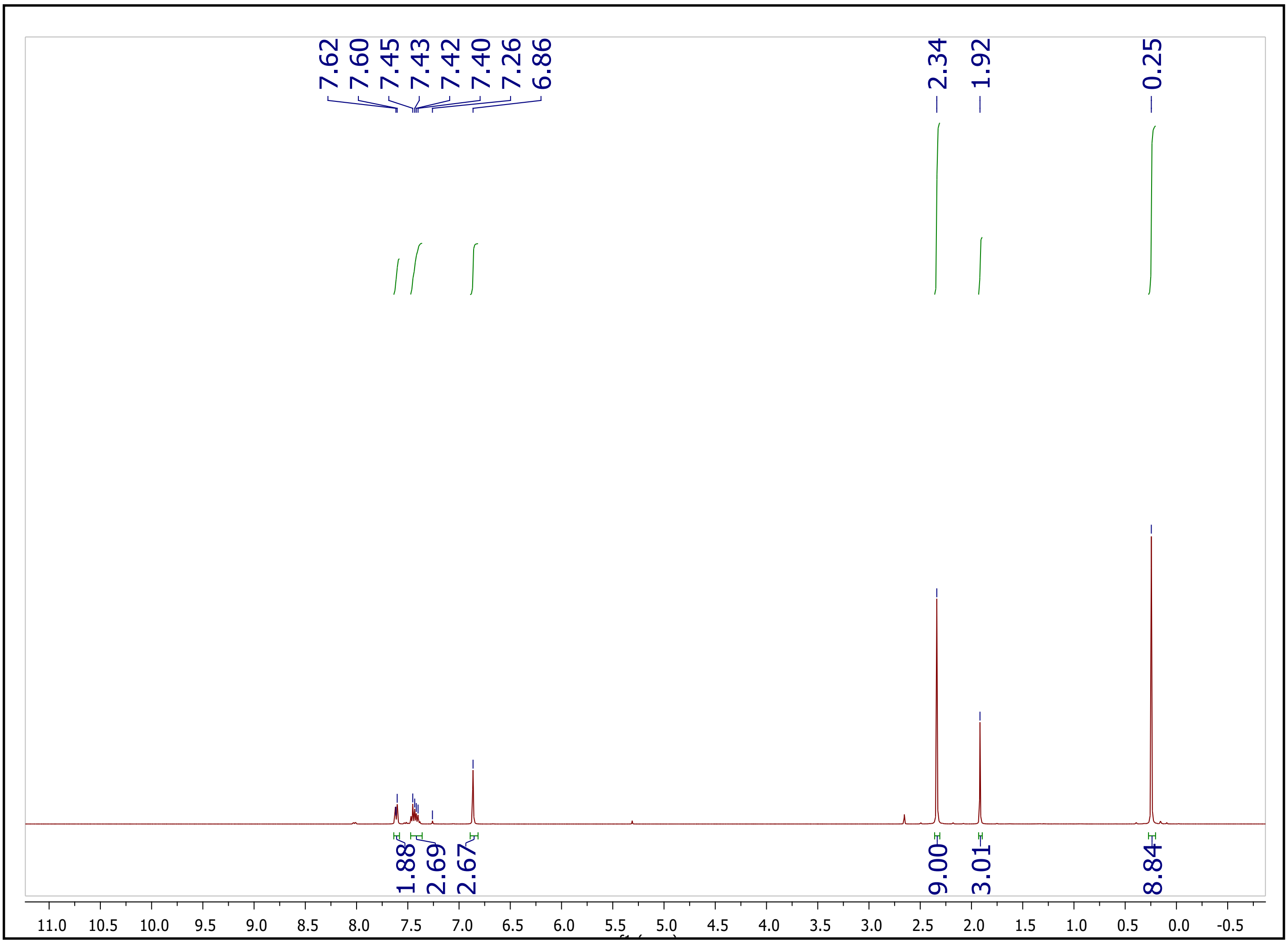

Figure S15. ^{1}H NMR spectrum of cyanosilylation of acetophenone with TMSCN with 0.1 mol% of catalyst loading within 15 mins.

[S8]. ^{1}H and ^{13}C NMR spectra for cyanosilylation products of ketones by compound 3.

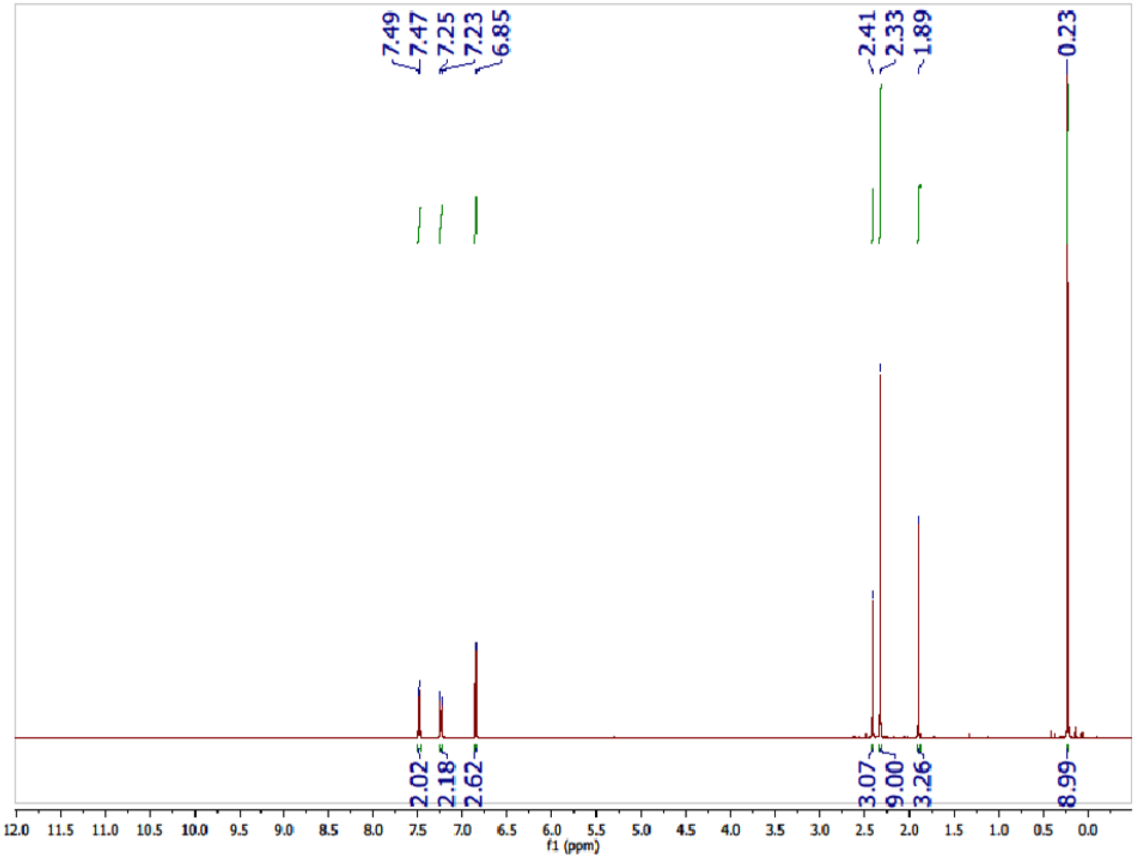

Figure S16. ^{1}H NMR spectrum of **5b** (Solvent: $CDCl_3$, IS: Mesitylene).

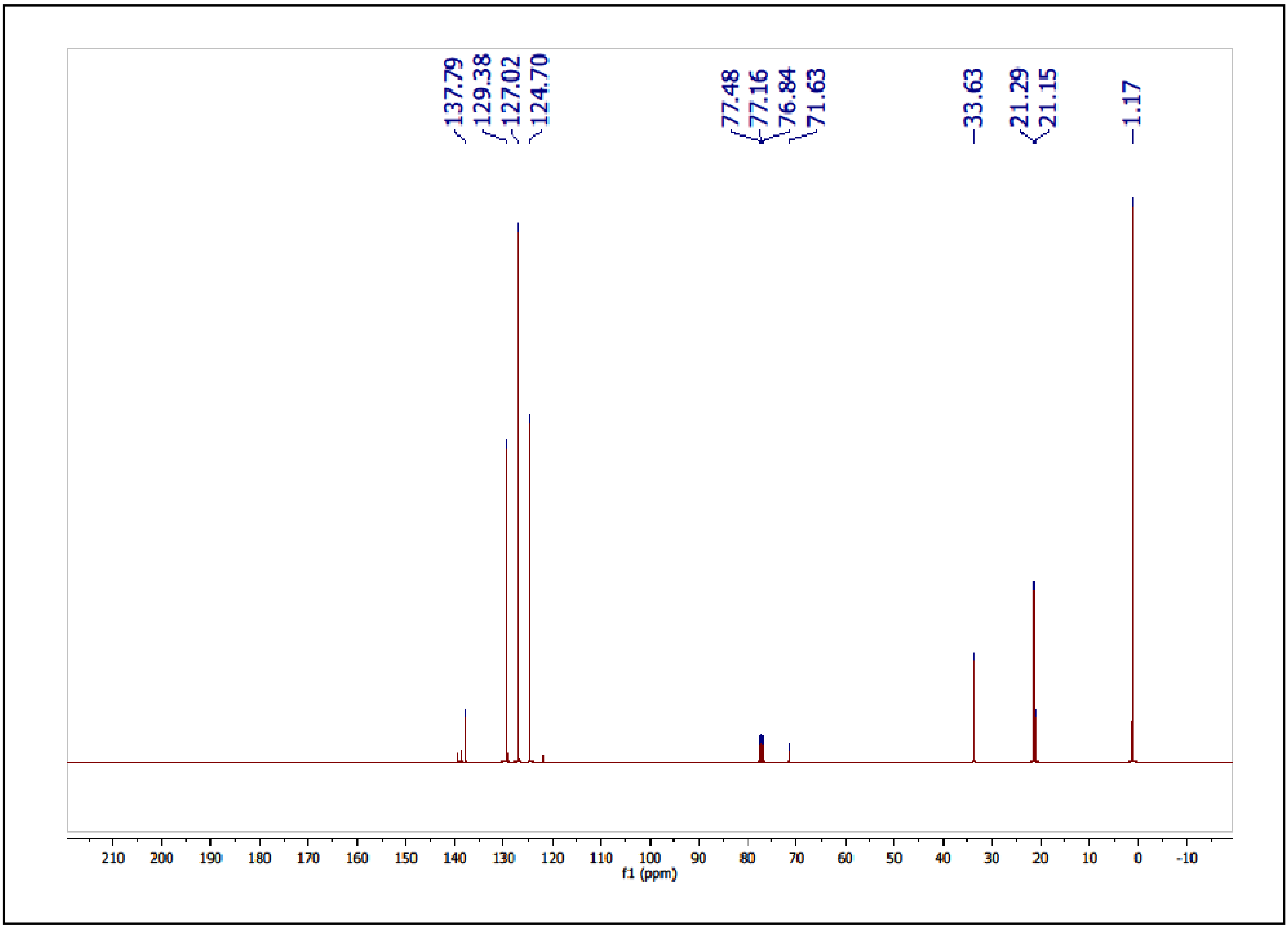

Figure S17. ^{13}C NMR spectrum of **5b** (Solvent: $CDCl_3$, IS: Mesitylene).

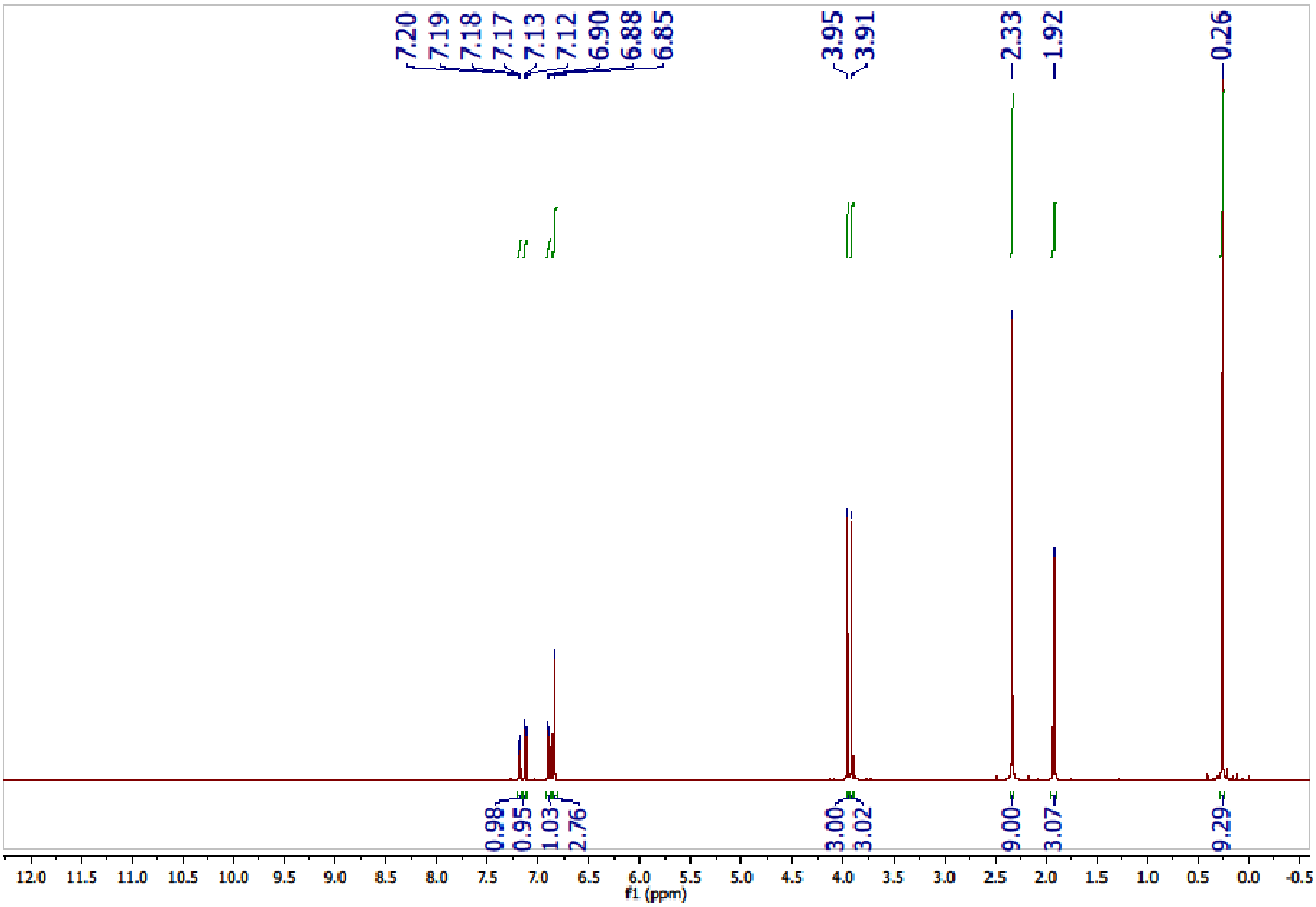

Figure S18. ^{1}H NMR spectrum of **5c** (Solvent: $CDCl_3$, IS: Mesitylene).

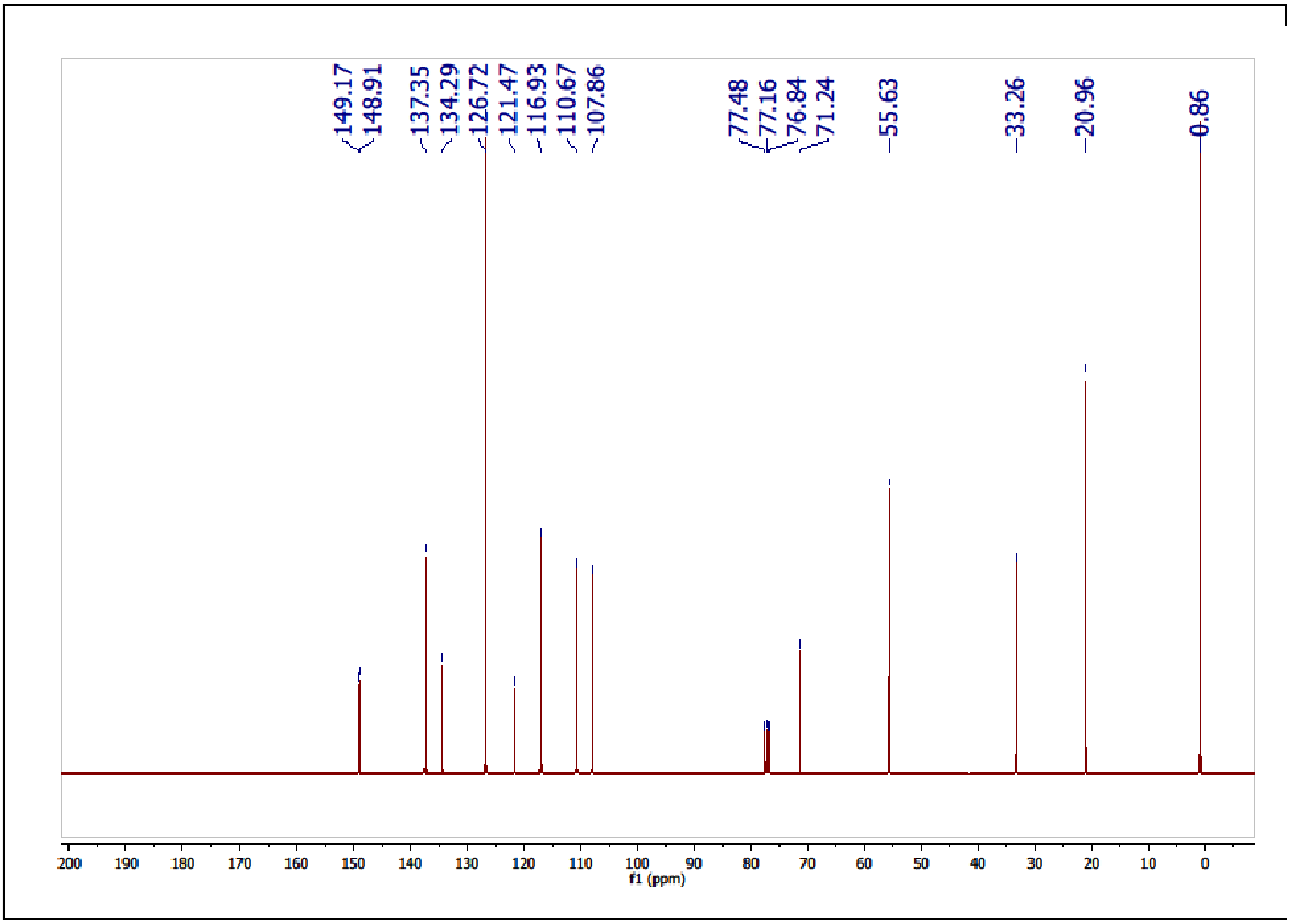

Figure S19. ^{13}C NMR spectrum of **5c** (Solvent: $CDCl_3$, IS: Mesitylene).

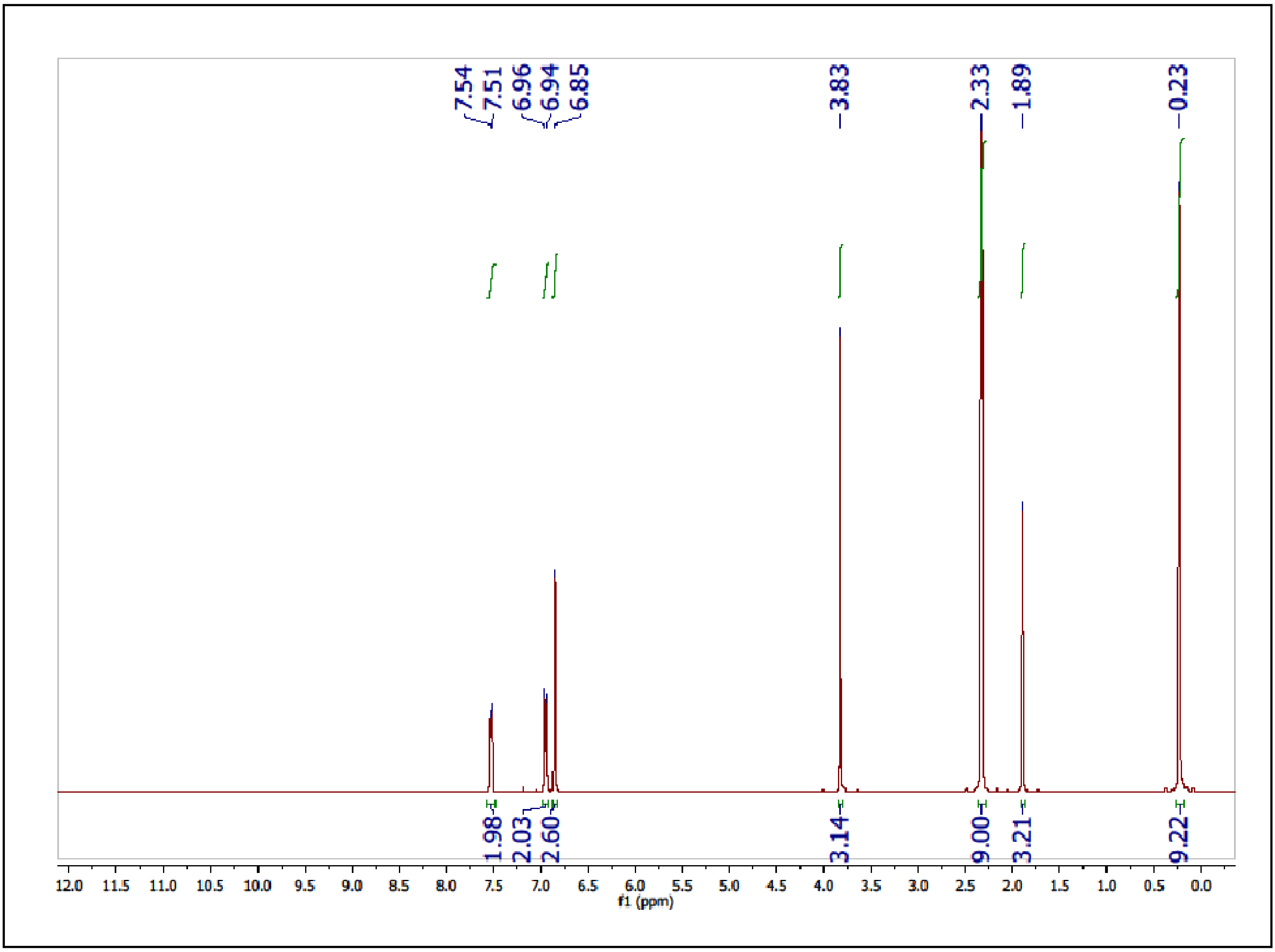

Figure S20. ^{1}H NMR spectrum of **5d** (Solvent: $CDCl_3$, IS: Mesitylene).

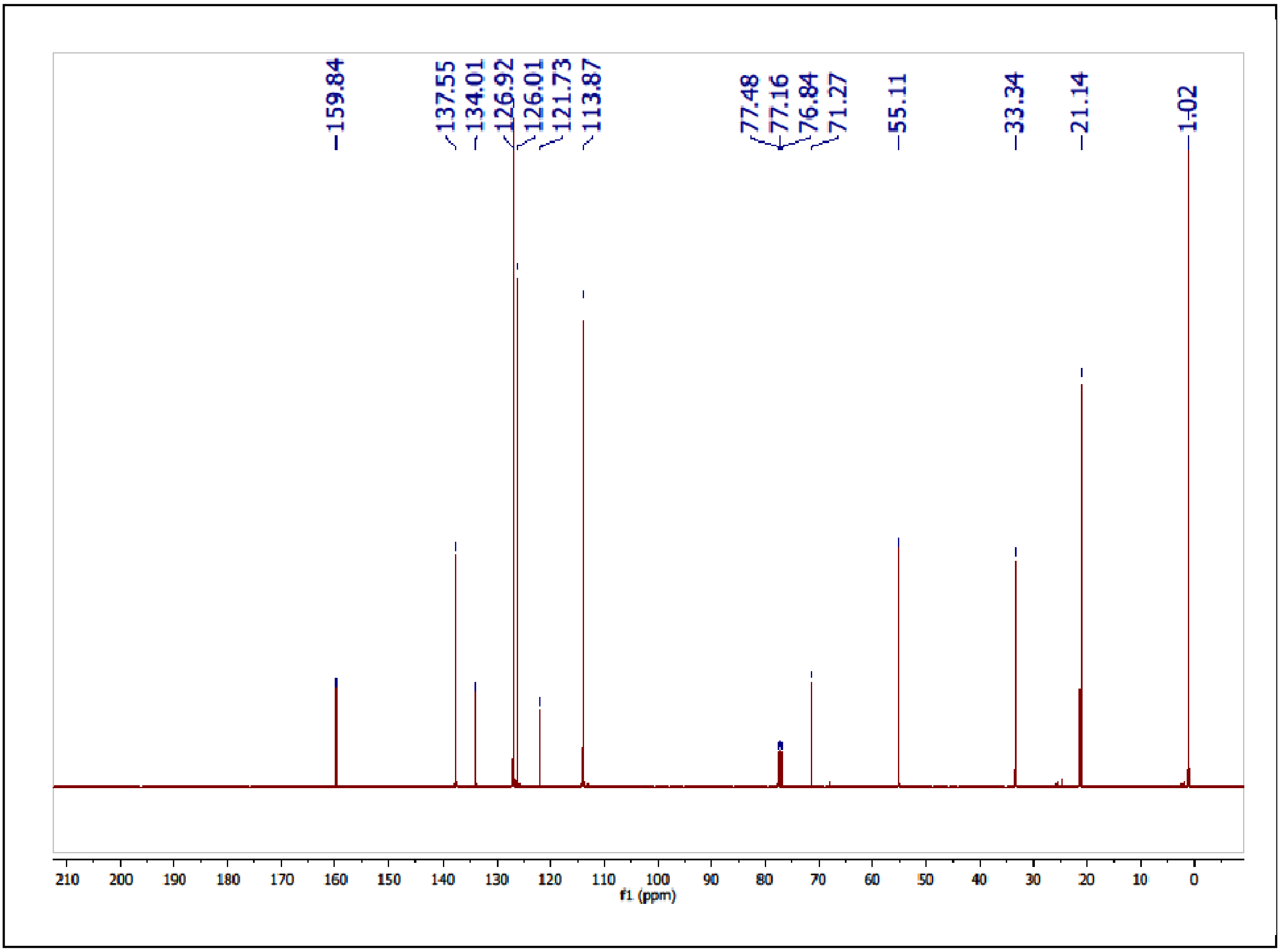

Figure S21. ^{13}C NMR spectrum of **5d** (Solvent: $CDCl_3$, IS: Mesitylene).

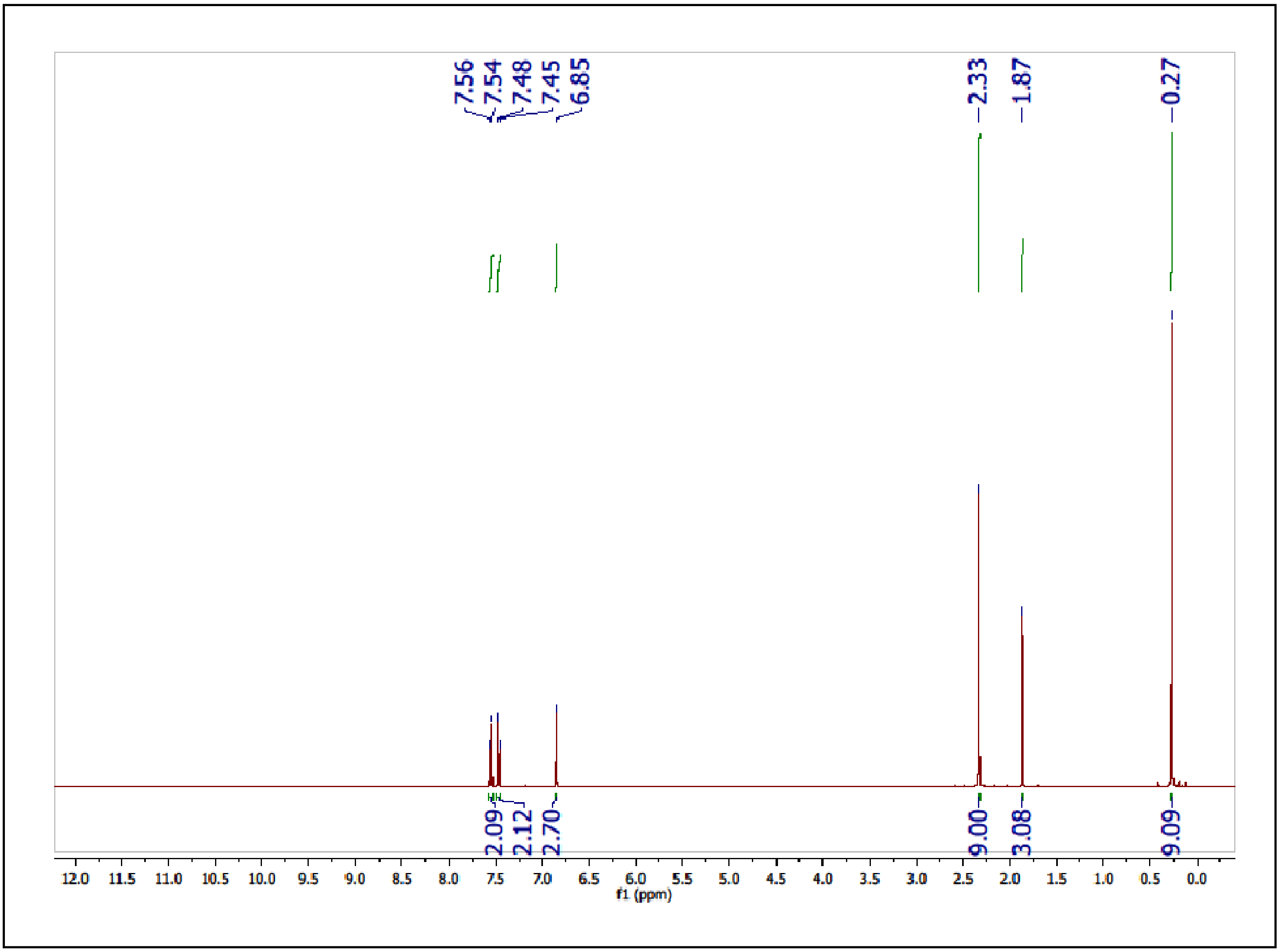

Figure S22. ^{1}H NMR spectrum of **5e** (Solvent: $CDCl_3$, IS: Mesitylene).

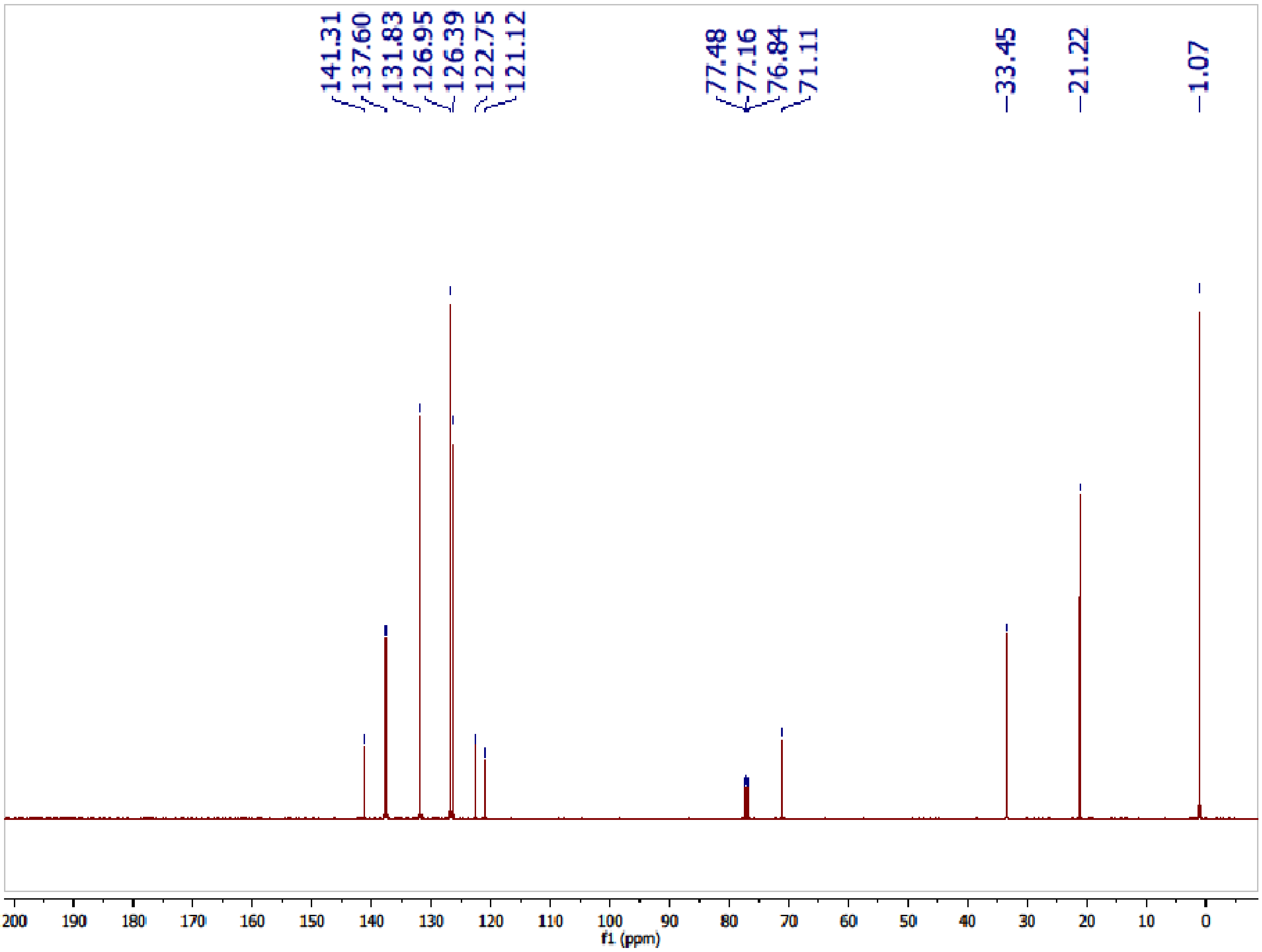

Figure S23. ^{13}C NMR spectrum of **5e** (Solvent: $CDCl_3$, IS: Mesitylene).

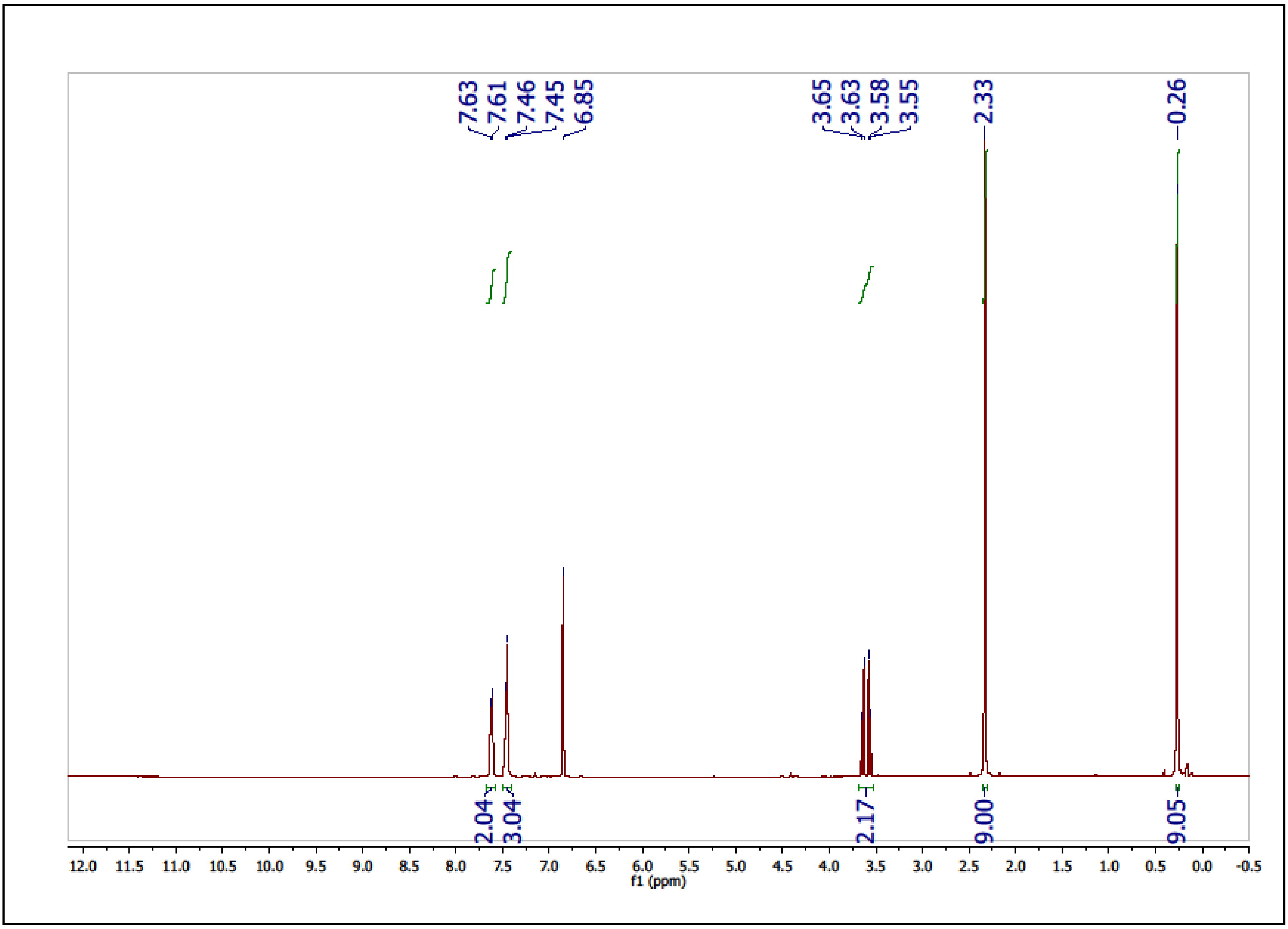

Figure S24. ^{1}H NMR spectrum of **5f** (Solvent: $CDCl_3$, IS: Mesitylene).

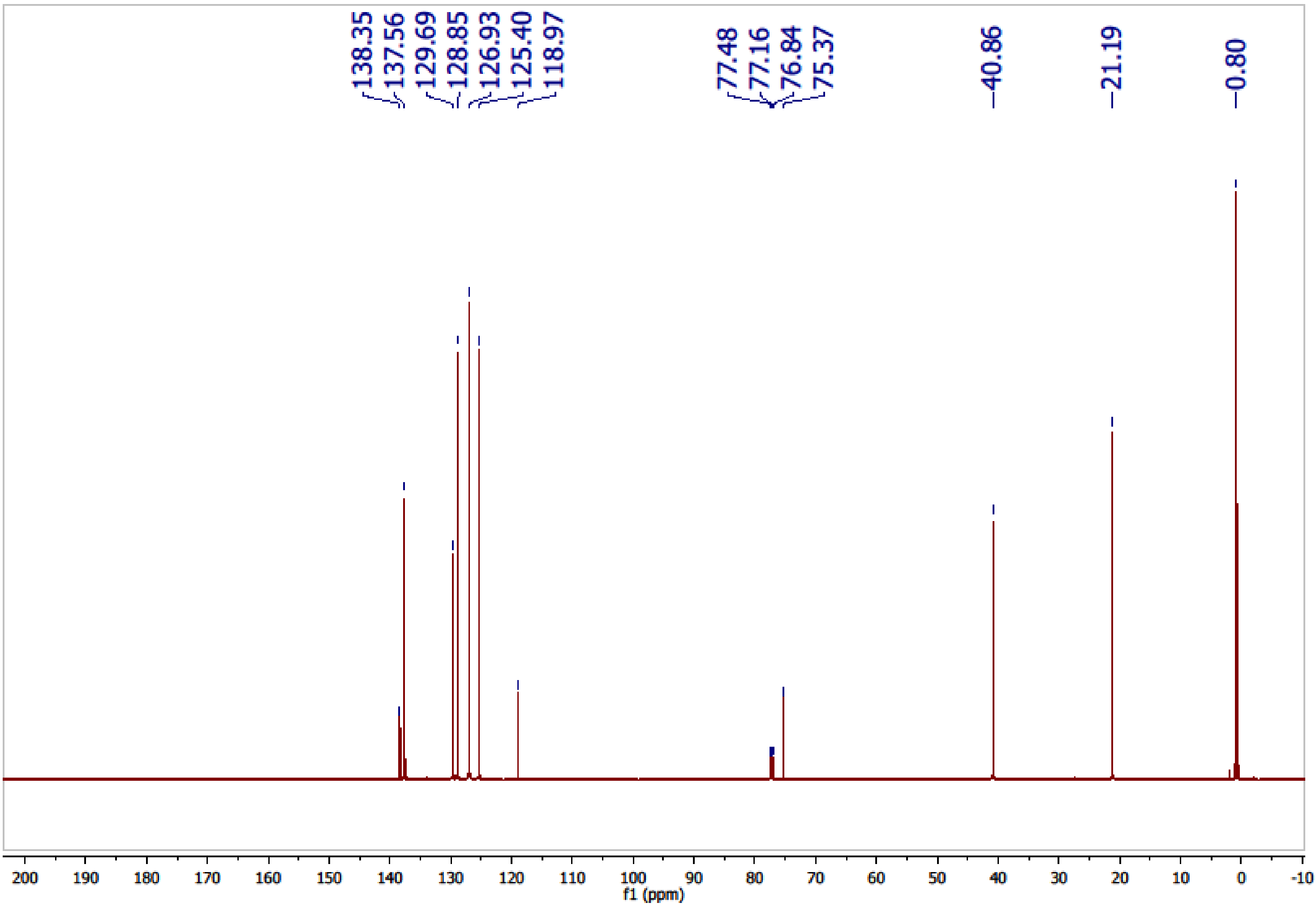

Figure S25. ^{13}C NMR spectrum of **5f** (Solvent: $CDCl_3$, IS: Mesitylene).

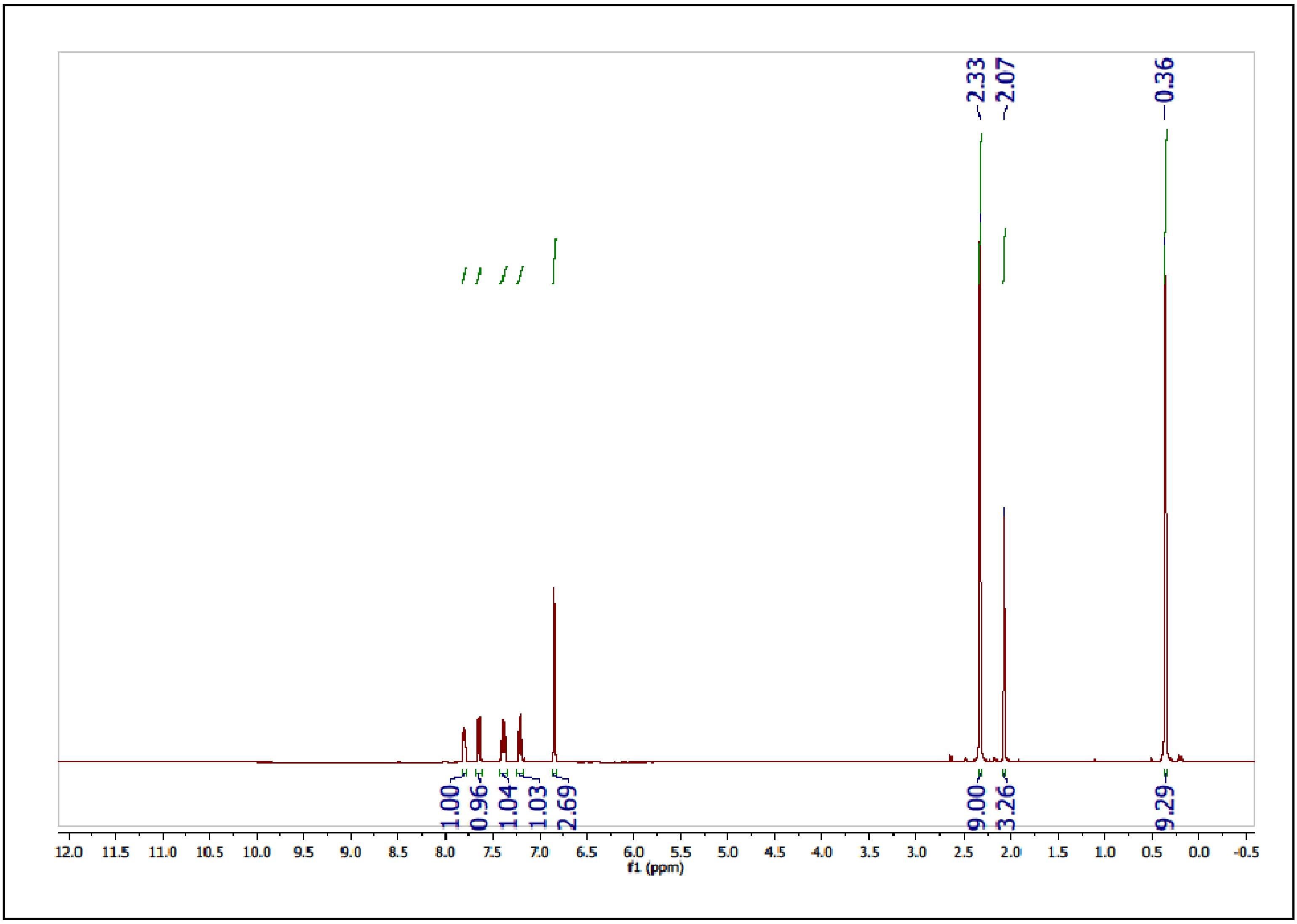

Figure S26. ^{1}H NMR spectrum of **5g** (Solvent: $CDCl_3$, IS: Mesitylene).

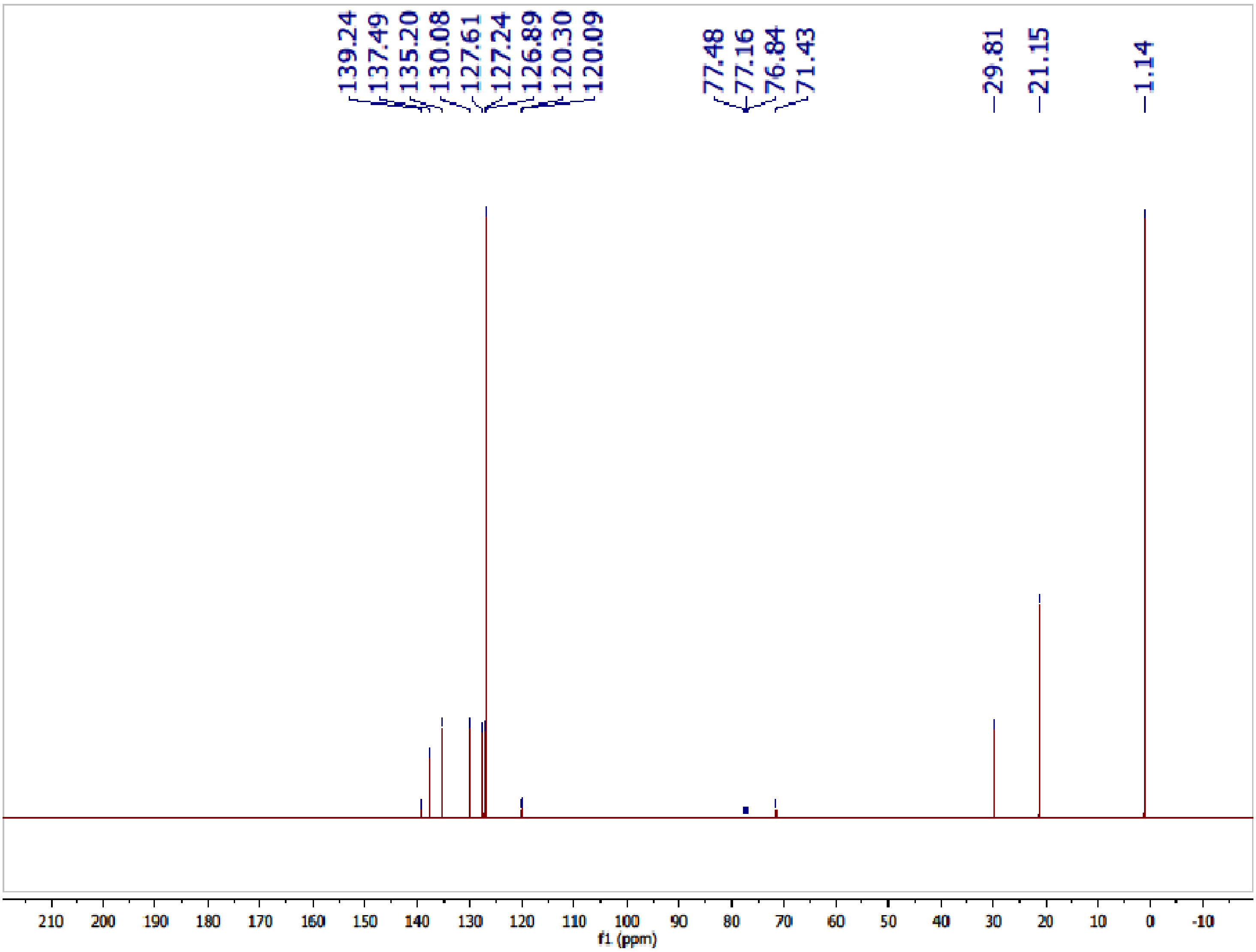

Figure S27. ^{13}C NMR spectrum of **5g** (Solvent: $CDCl_3$, IS: Mesitylene).

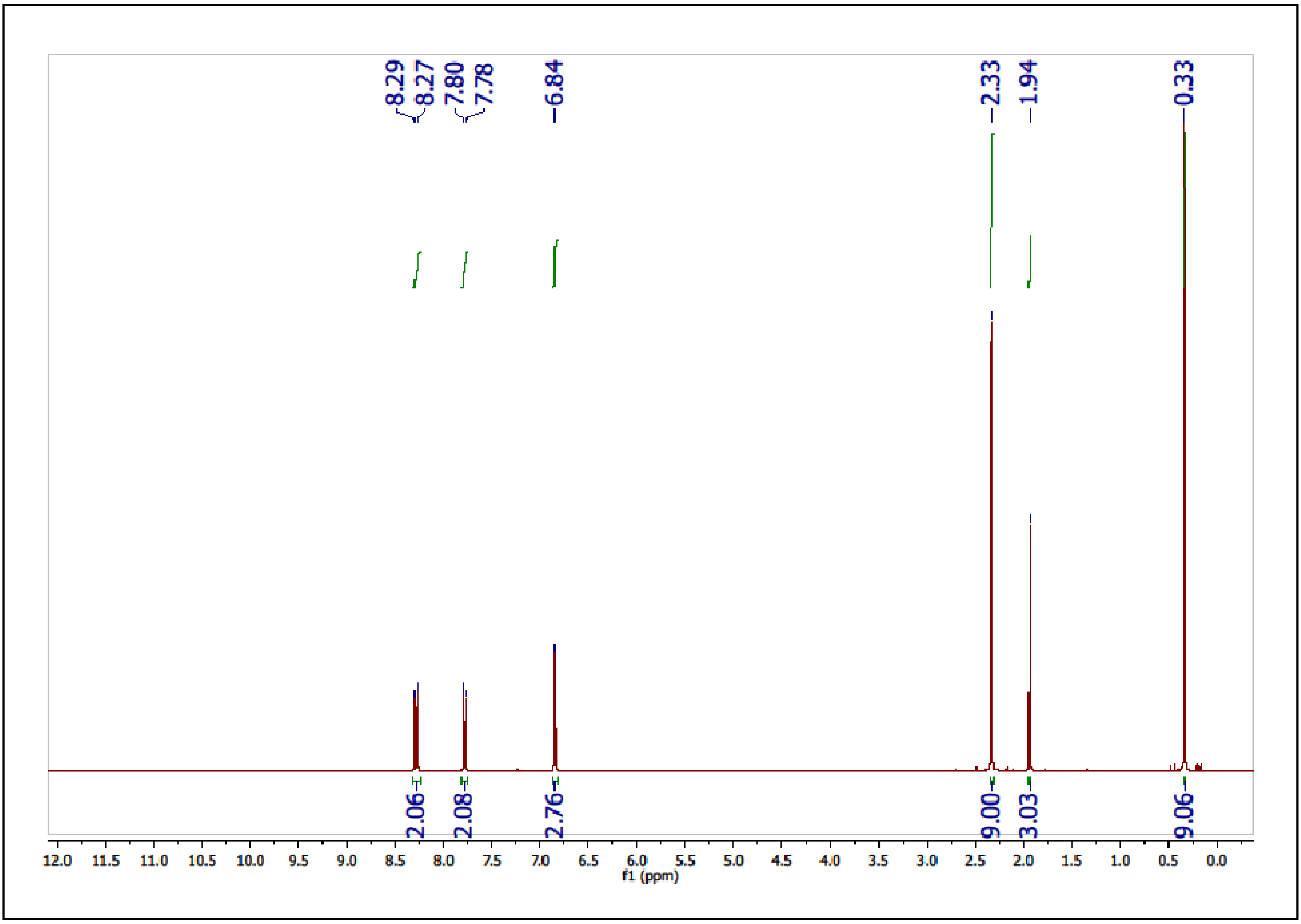

Figure S28. ^{1}H NMR spectrum of **5h** (Solvent: $CDCl_3$, IS: Mesitylene).

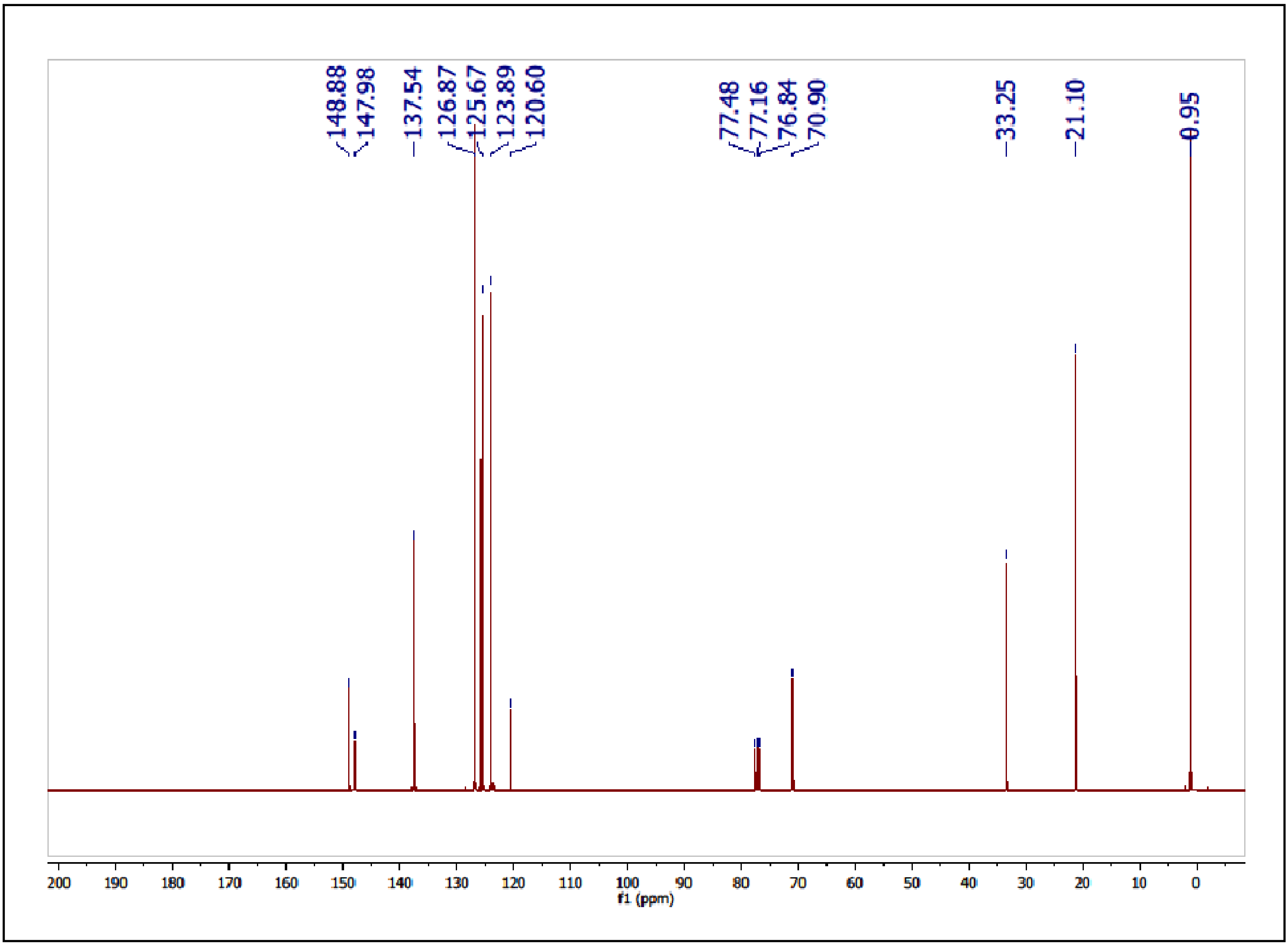

Figure S29. ^{13}C NMR spectrum of **5h** (Solvent: $CDCl_3$, IS: Mesitylene).

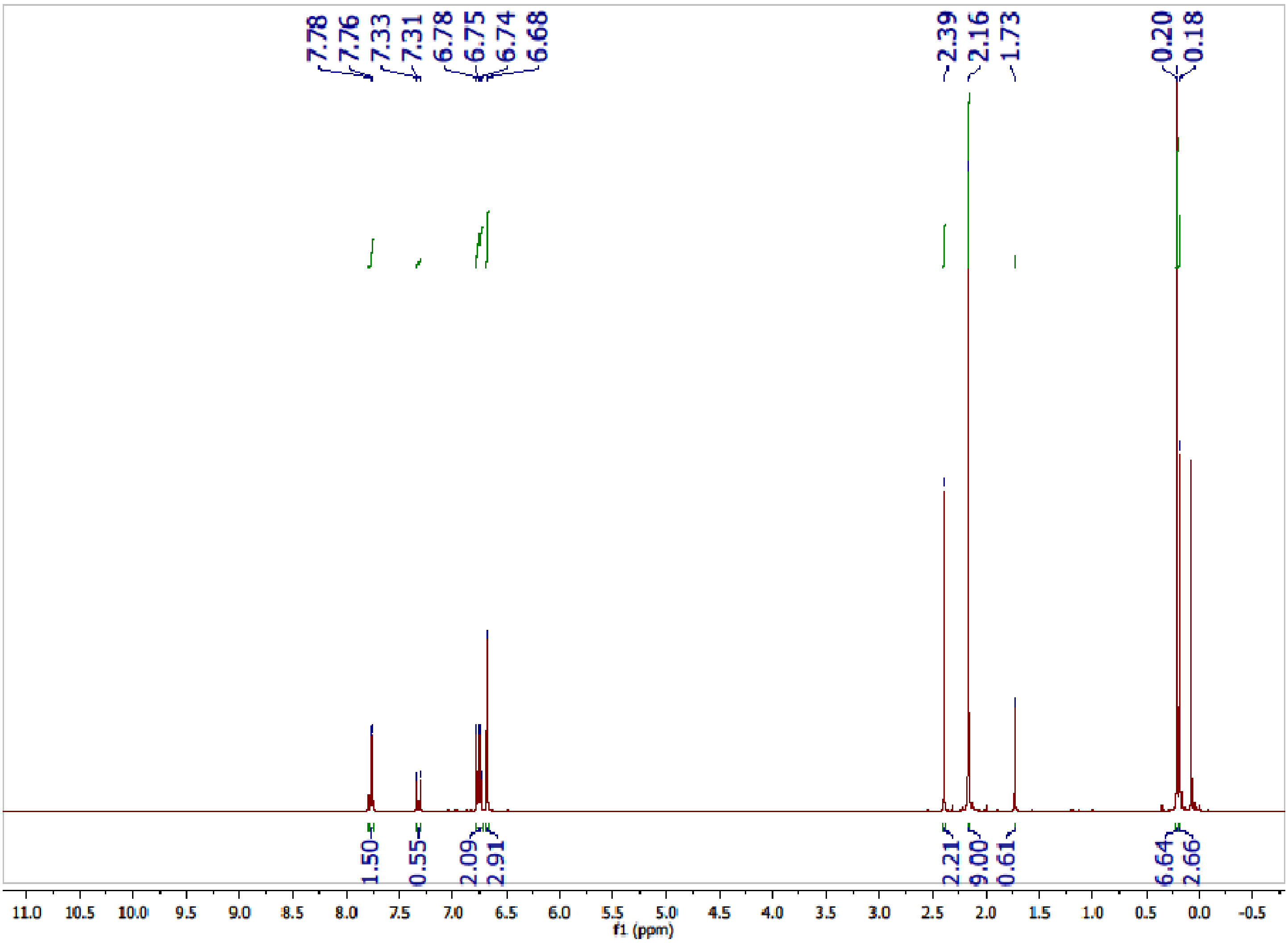

Figure S30. ^{1}H NMR spectrum of **5j** (Solvent: $CDCl_3$, IS: Mesitylene).

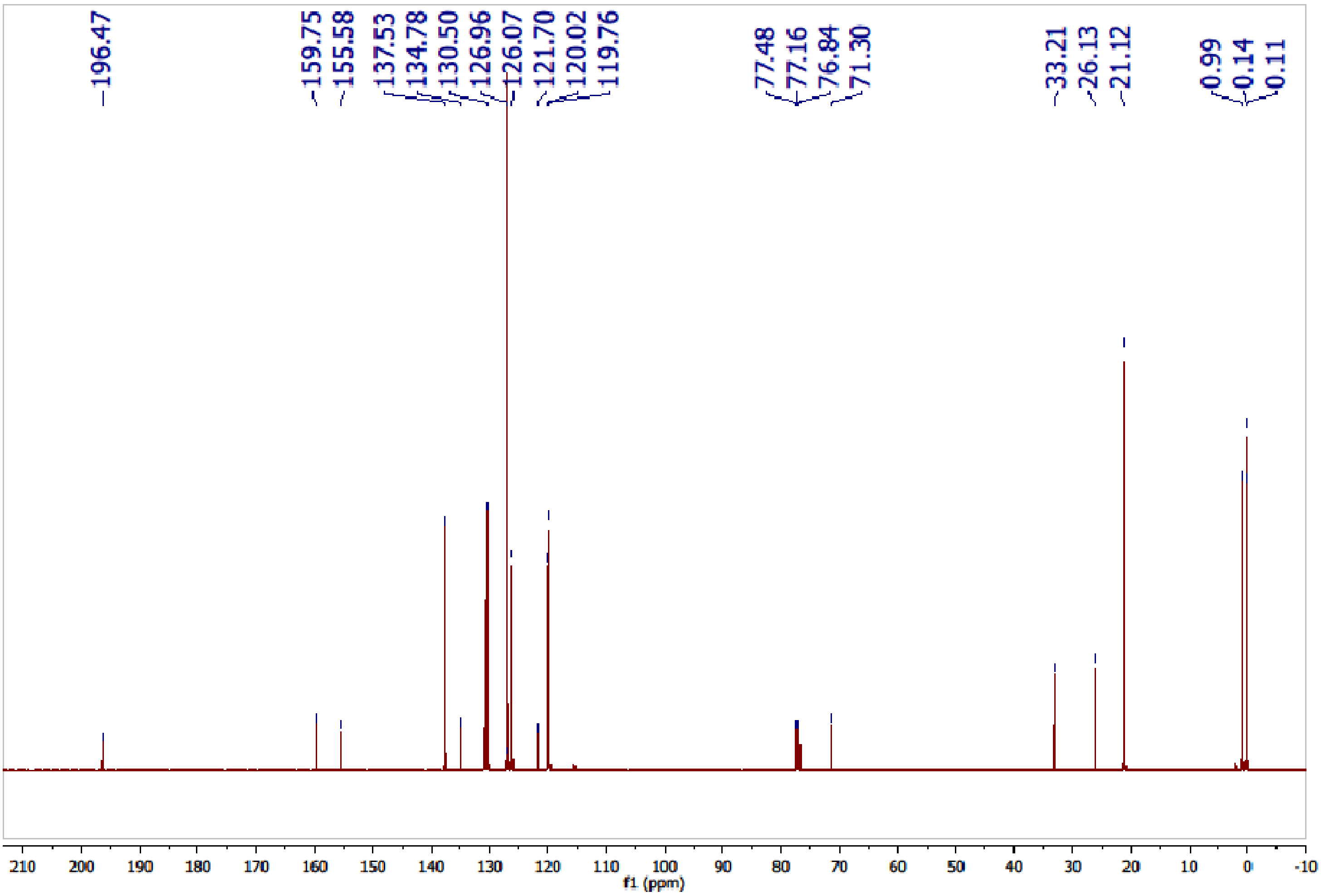

Figure S31. ^{13}C NMR spectrum of **5j** (Solvent: $CDCl_3$, IS: Mesitylene).

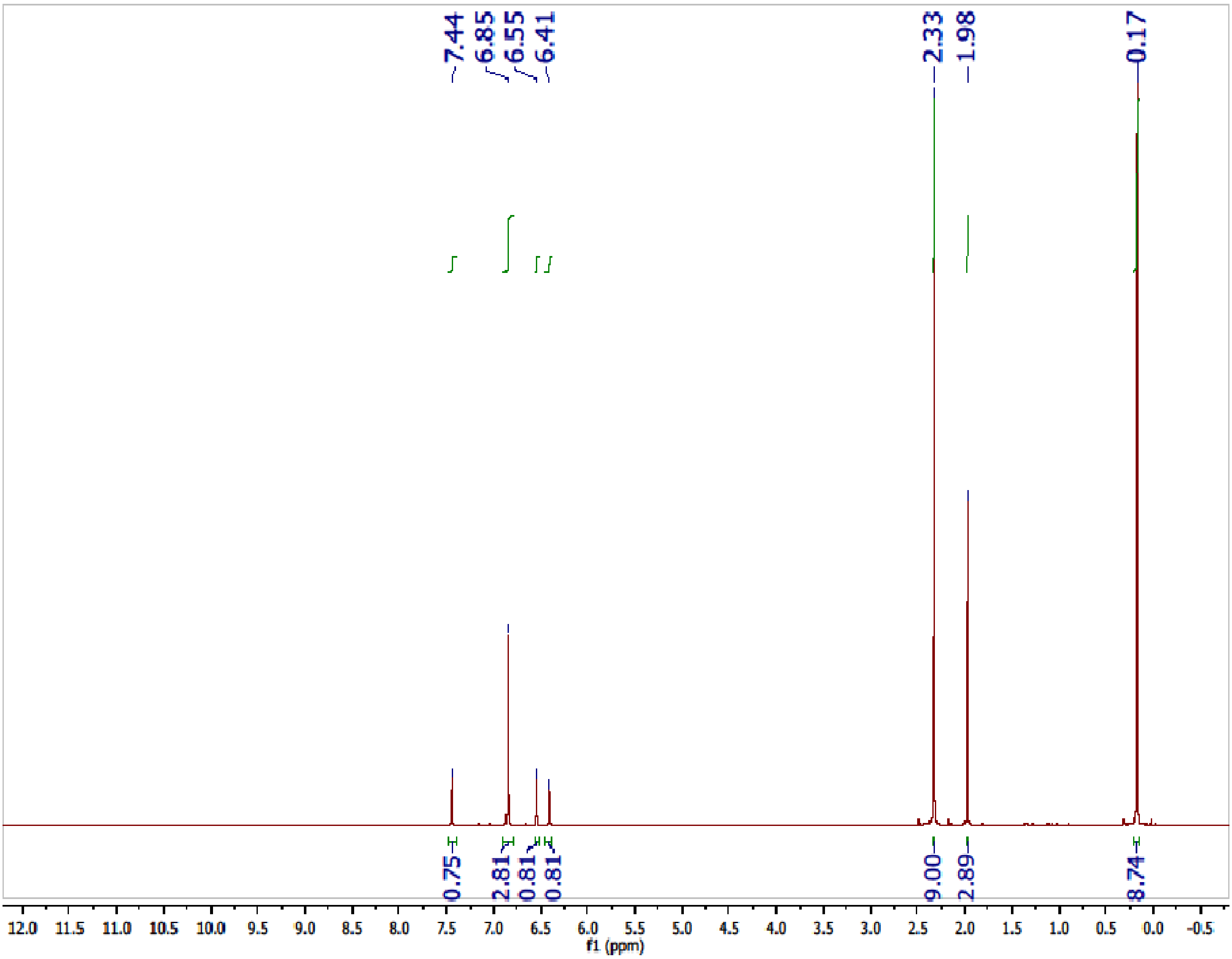

Figure S32. ^{1}H NMR spectrum of **5k** (Solvent: $CDCl_3$, IS: Mesitylene).

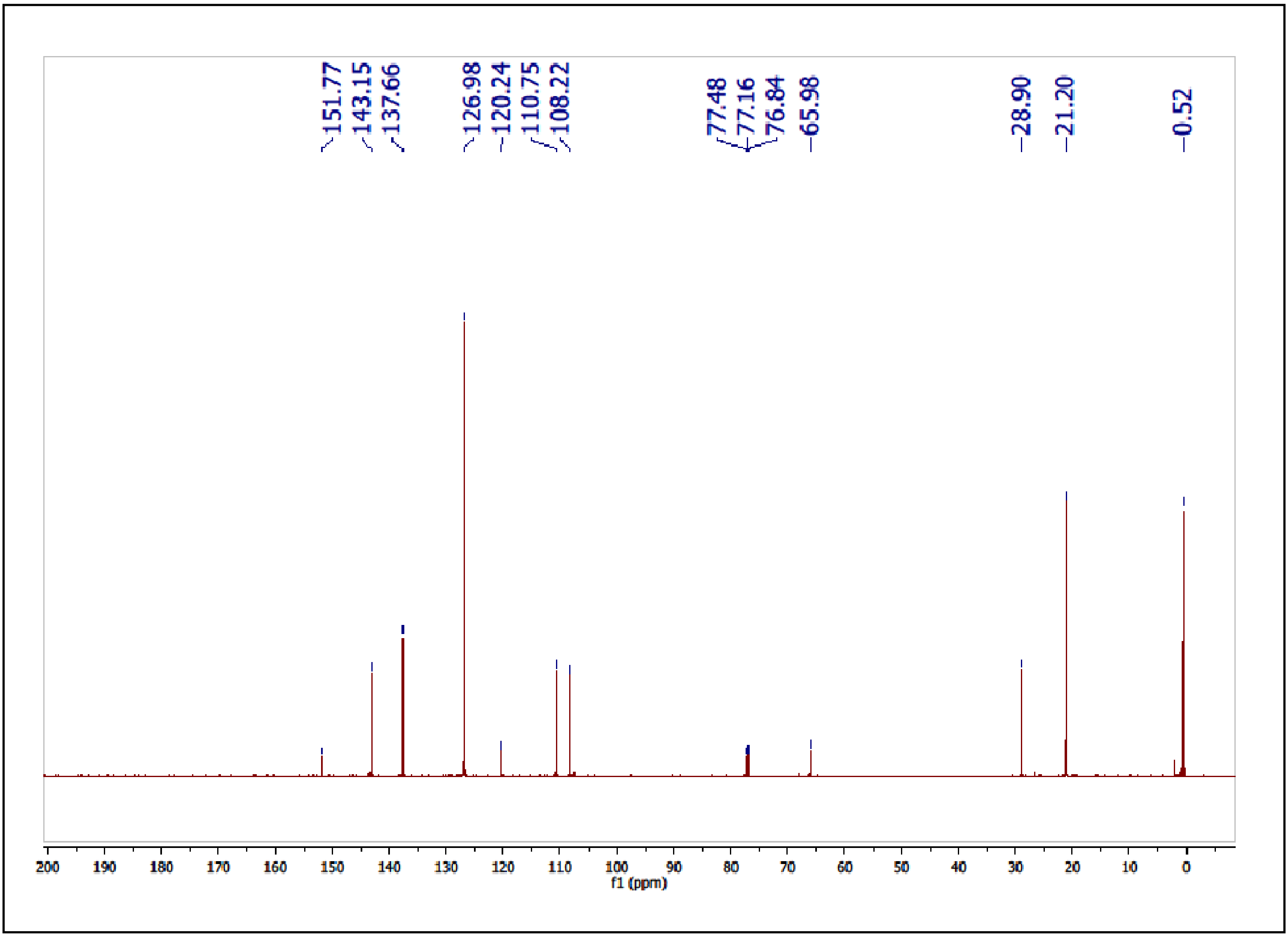

Figure S33. ^{13}C NMR spectrum of **5k** (Solvent: $CDCl_3$, IS: Mesitylene).

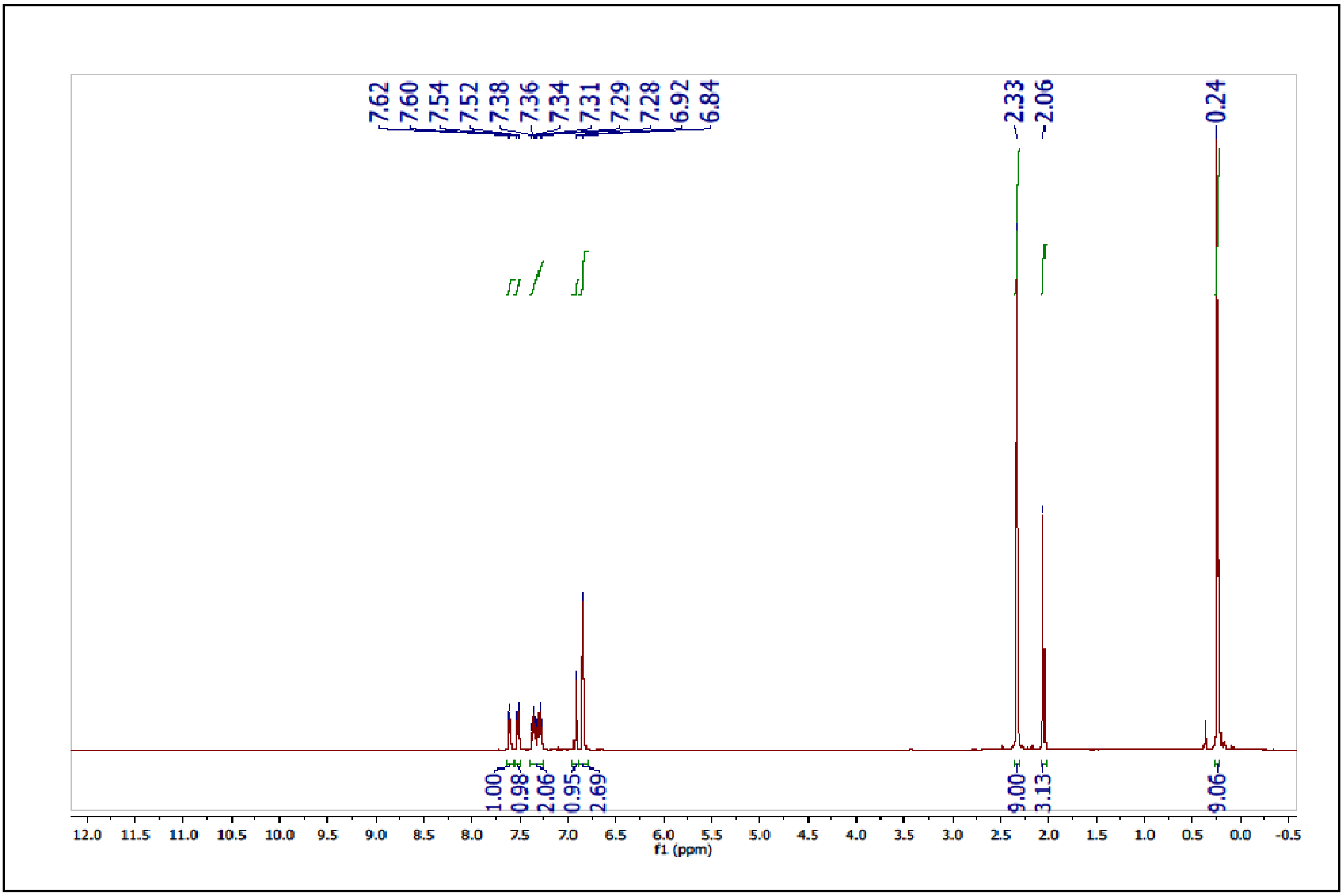

Figure S34. ^{1}H NMR spectrum of **5l** (Solvent: $CDCl_3$, IS: Mesitylene).

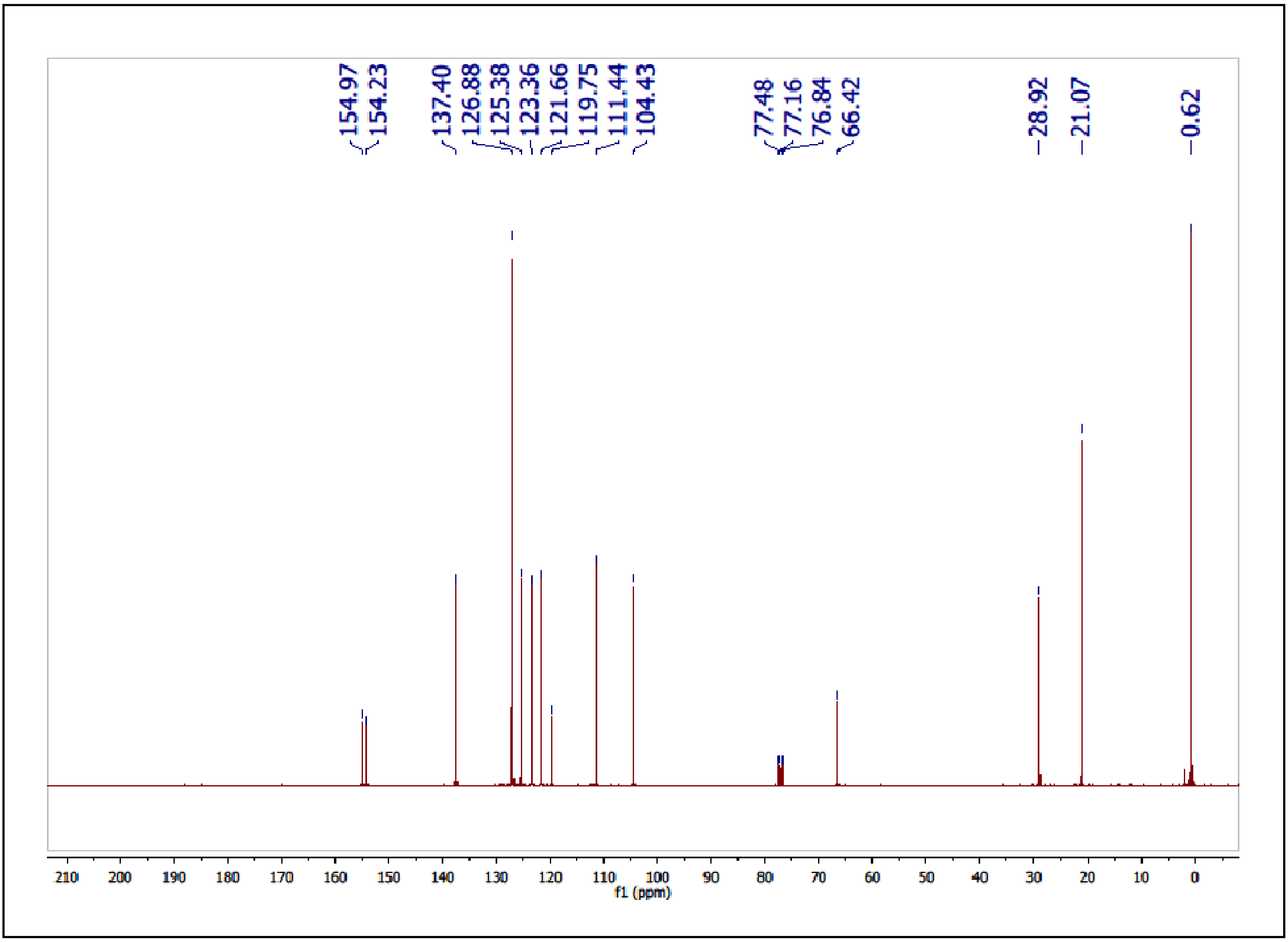

Figure S35. ^{13}C NMR spectrum of **5l** (Solvent: $CDCl_3$, IS: Mesitylene).

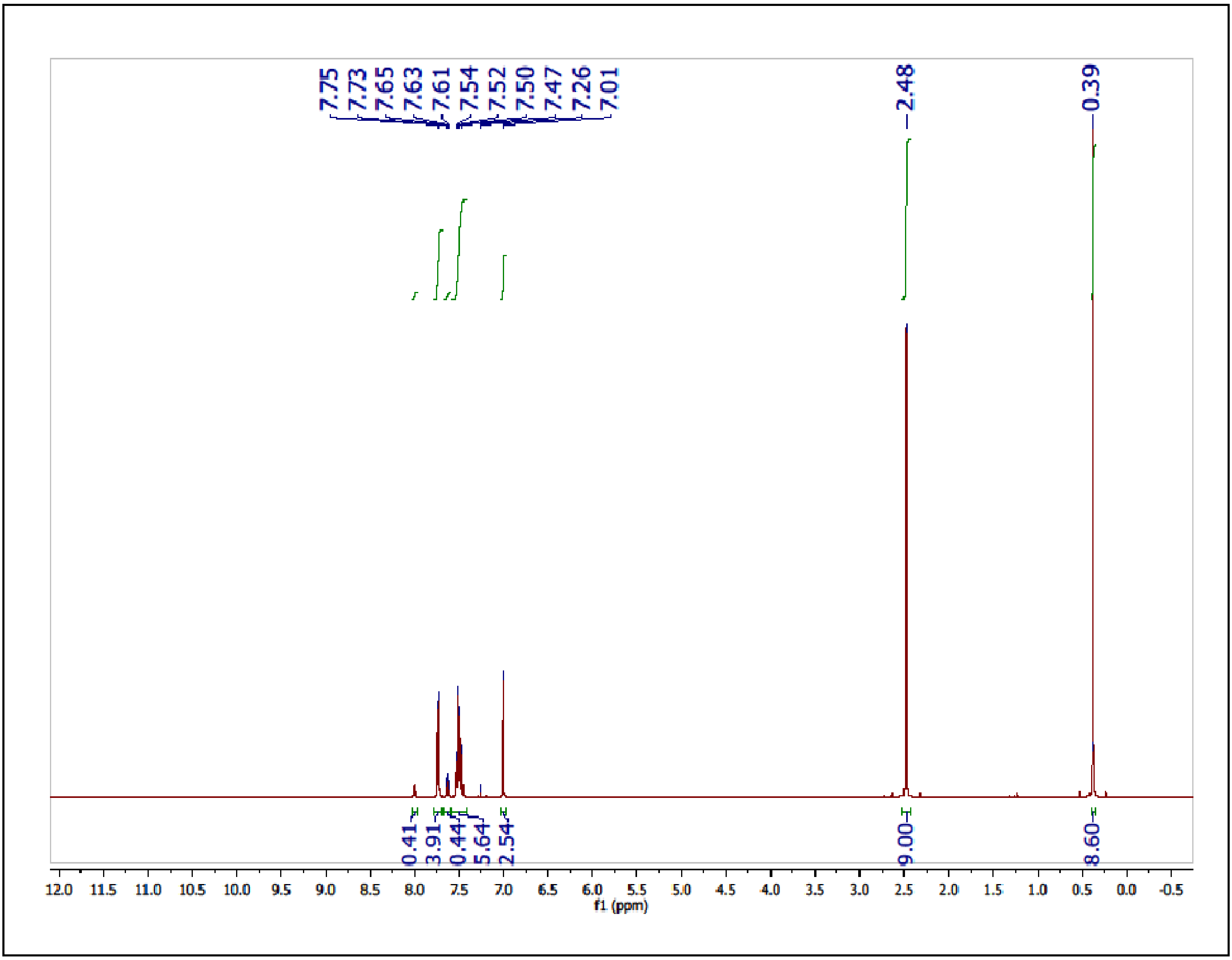

Figure S36. ^{1}H NMR spectrum of **5m** (Solvent: $CDCl_3$, IS: Mesitylene).

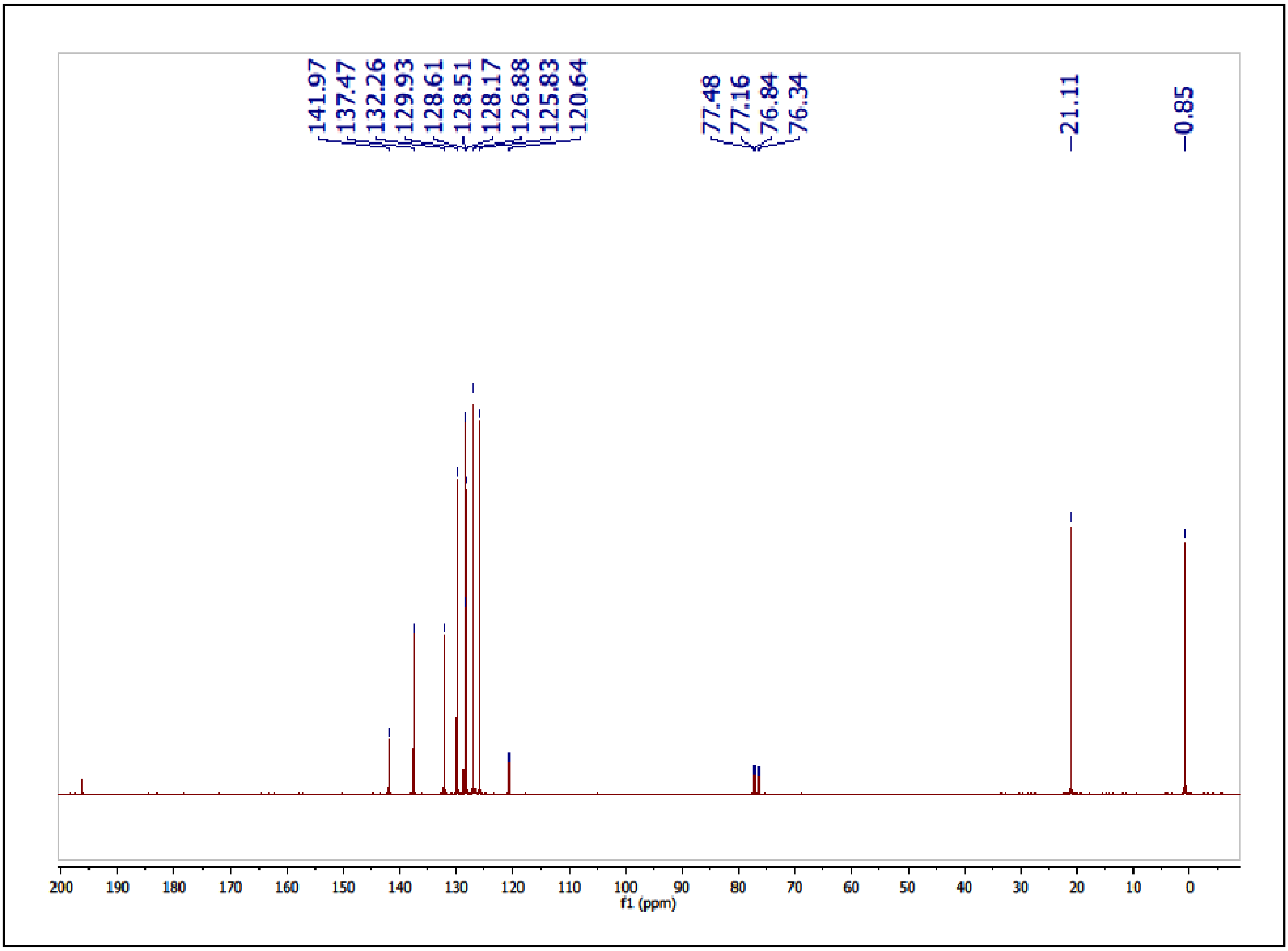

Figure S37. ^{13}C NMR spectrum of **5m** (Solvent: $CDCl_3$, IS: Mesitylene).

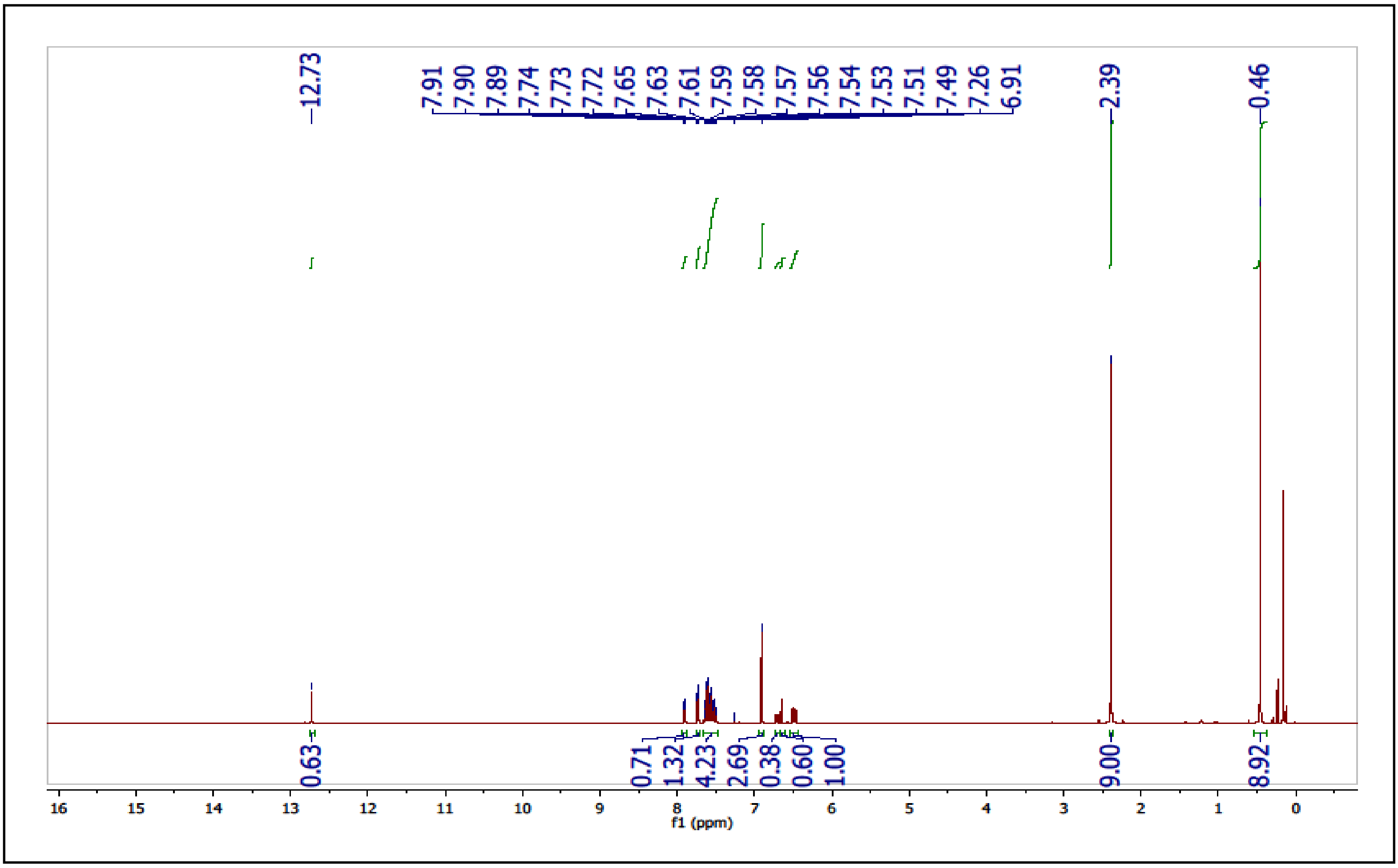

Figure S38. ^{1}H NMR spectrum of **5n** (Solvent: $CDCl_3$, IS: Mesitylene).

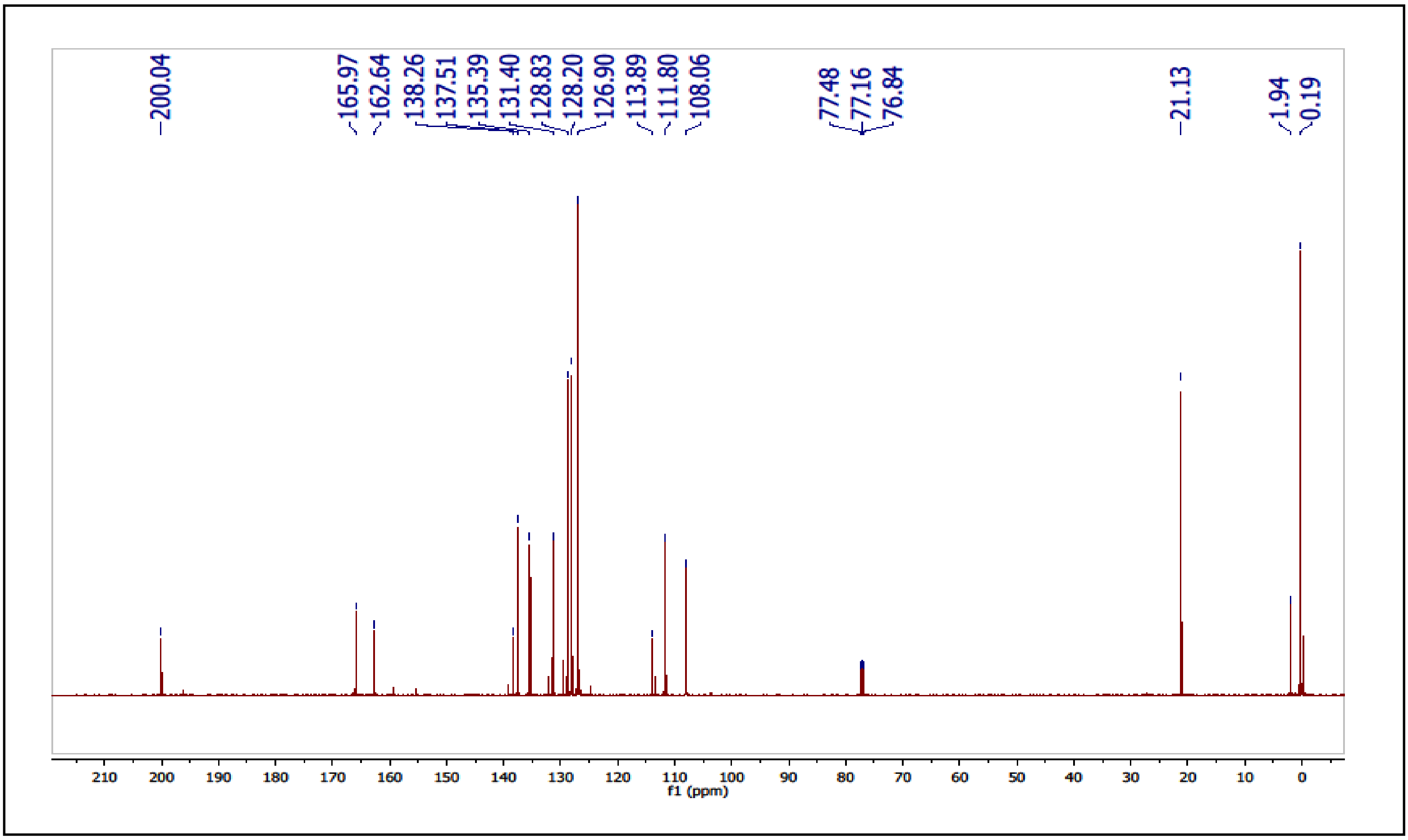

Figure S39. ^{13}C NMR spectrum of **5n** (Solvent: $CDCl_3$, IS: Mesitylene).

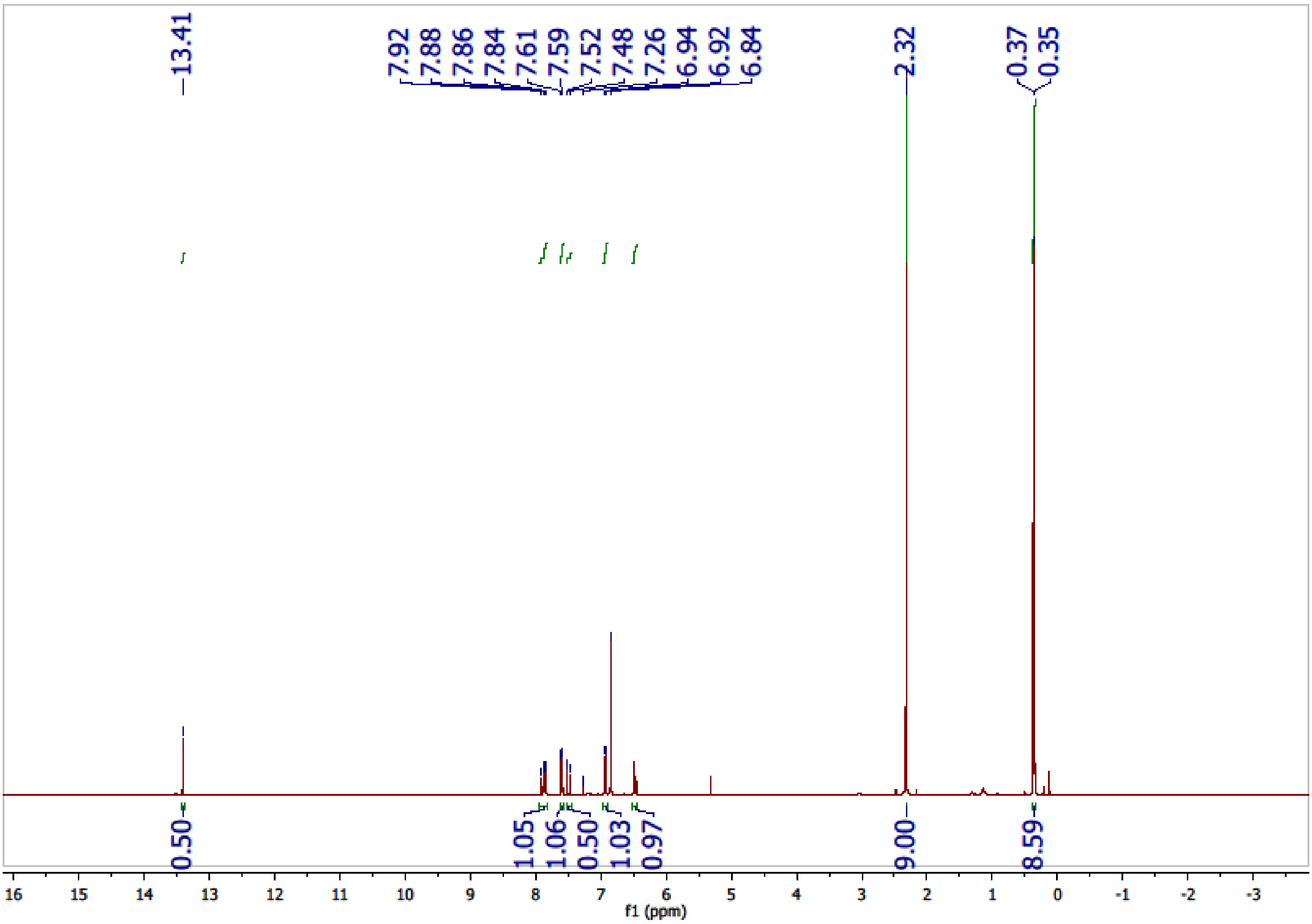

Figure S40. ^{1}H NMR spectrum of **5o** (Solvent: CDCl$_3$, IS: Mesitylene).

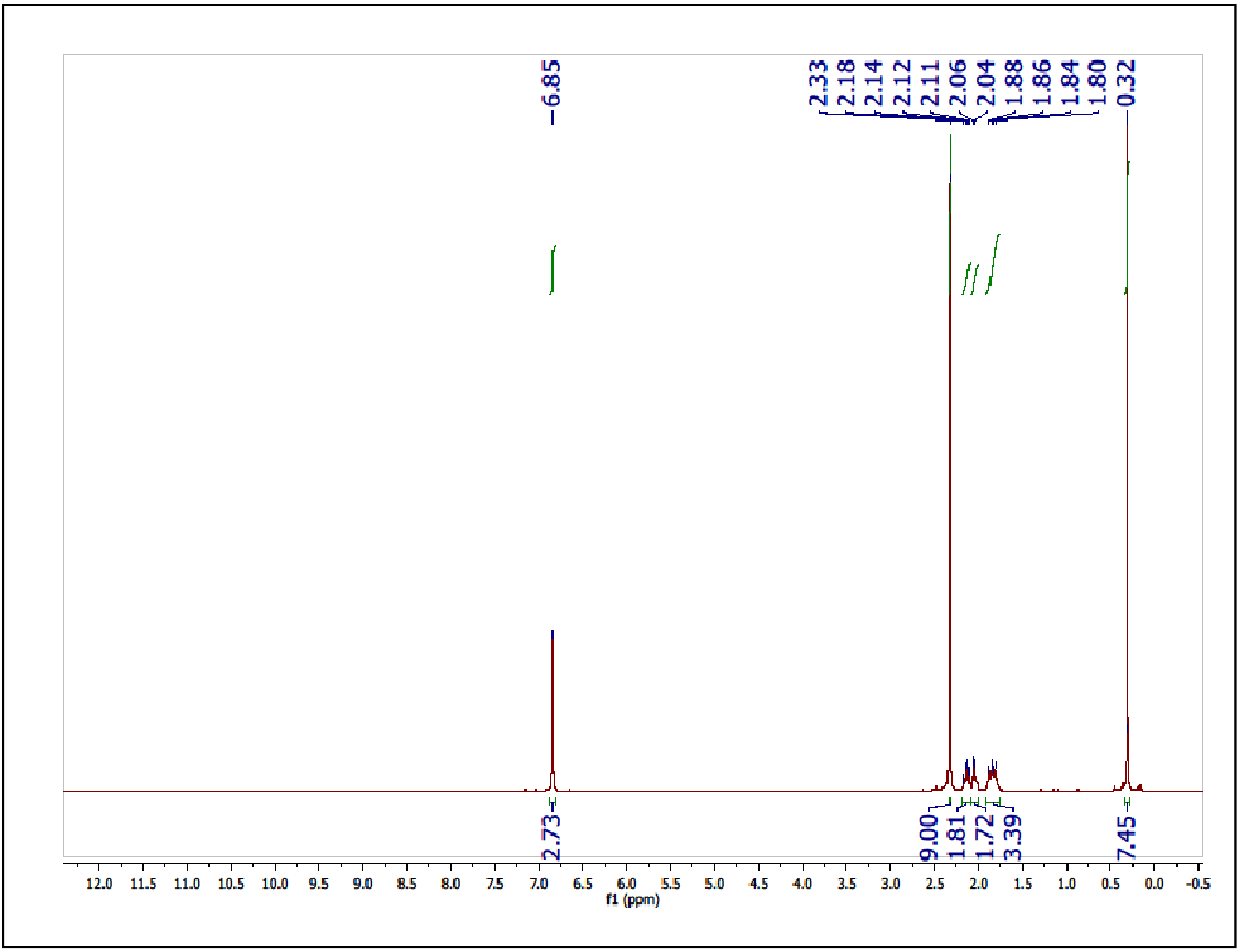

Figure S41. ^{1}H NMR spectrum of **5p** (Solvent: $CDCl_3$, IS: Mesitylene).

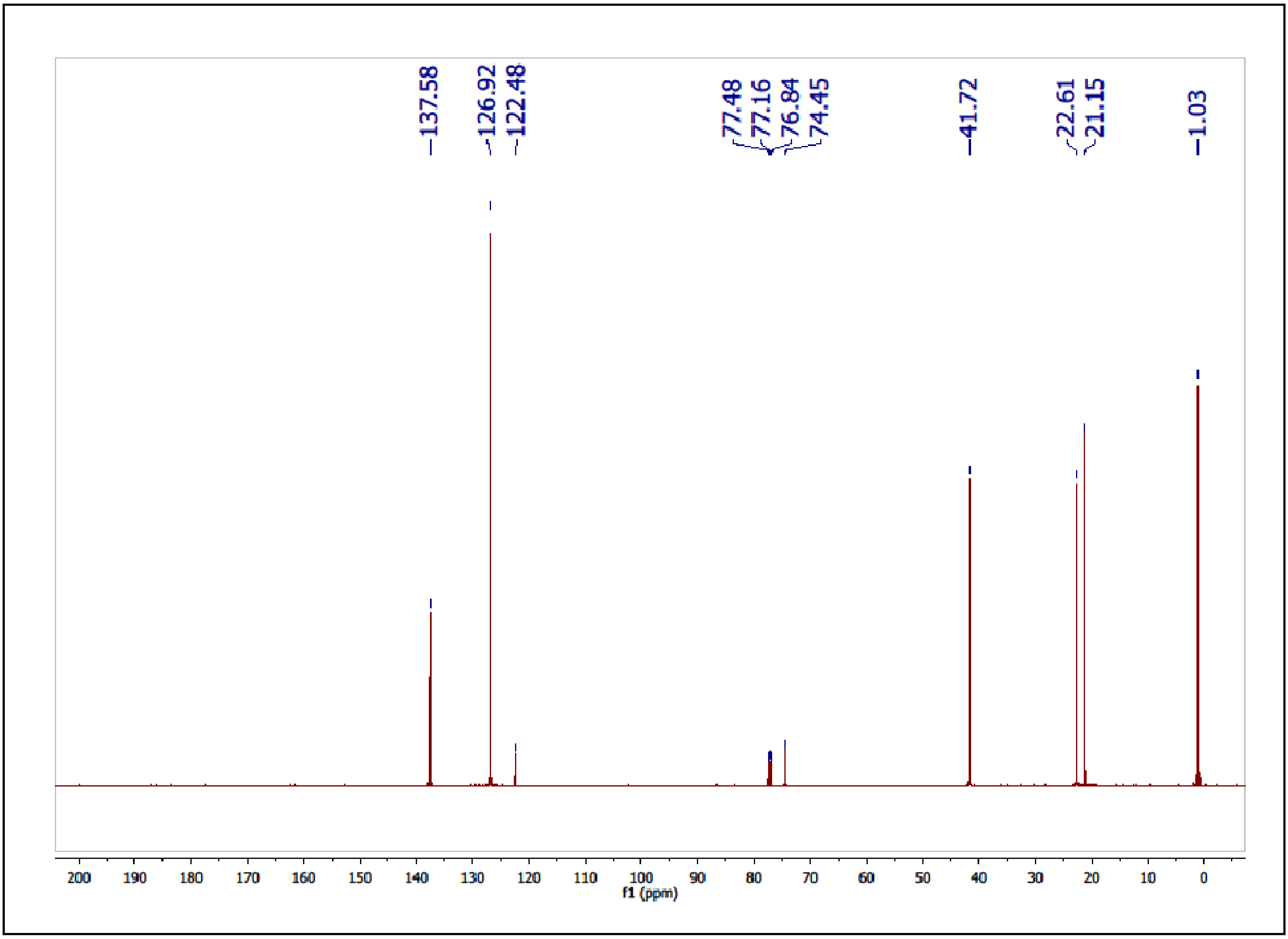

Figure S42. ^{13}C NMR spectrum of **5p** (Solvent: CDCl$_3$, IS: Mesitylene).

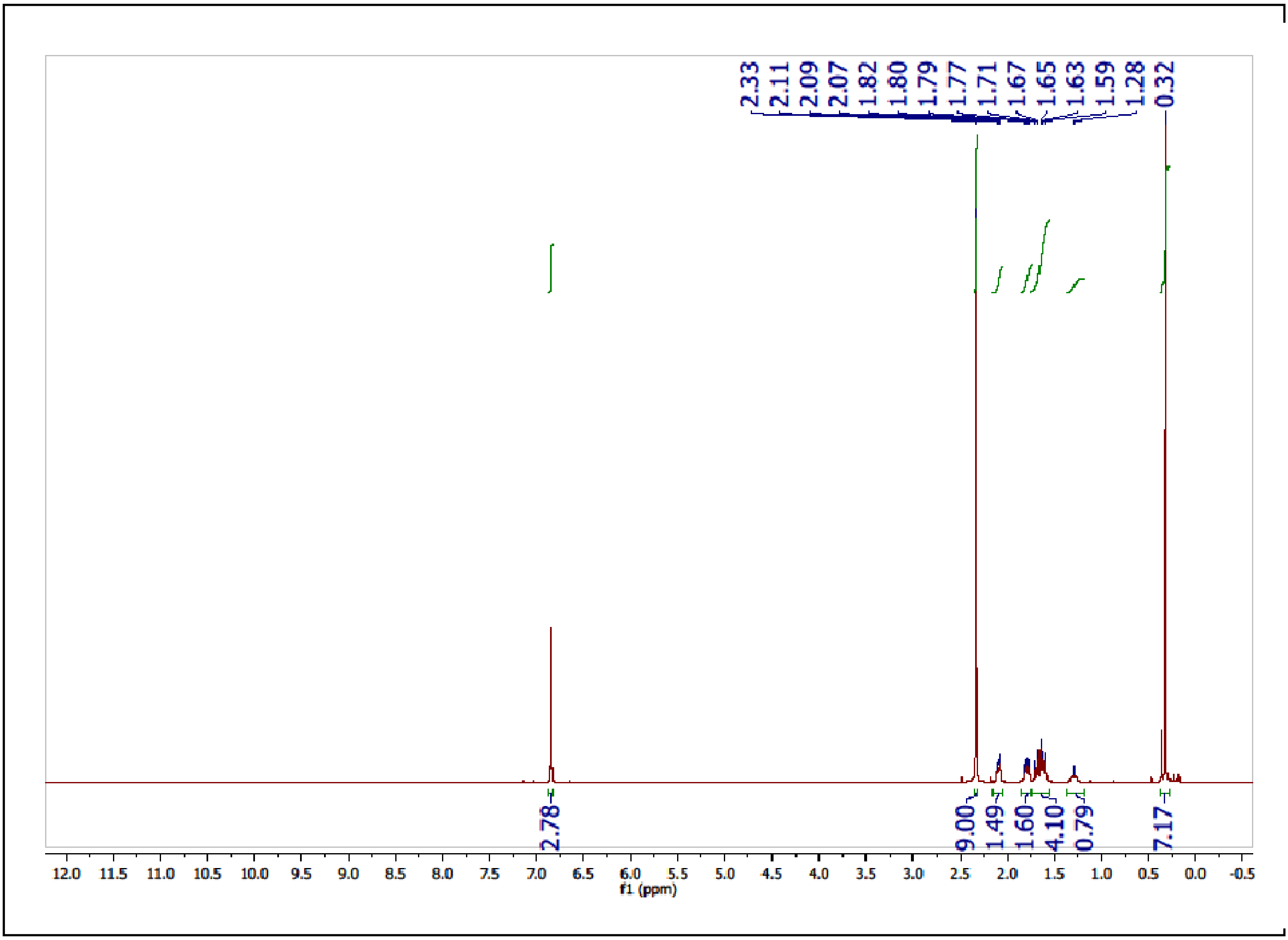

Figure S43. ^{1}H NMR spectrum of **5q** (Solvent: $CDCl_3$, IS: Mesitylene).

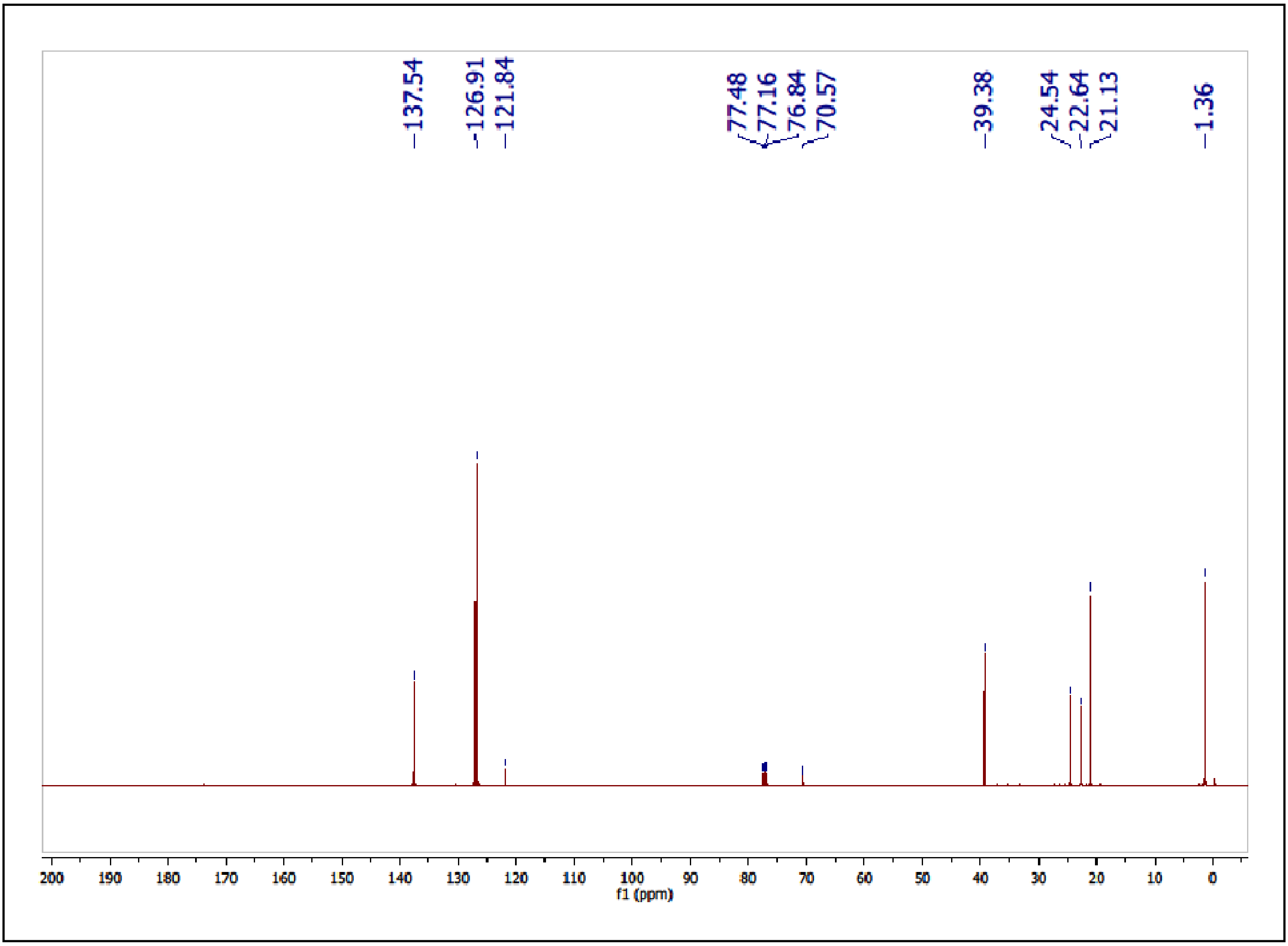

Figure S44. ^{13}C NMR spectrum of **5q** (Solvent: $CDCl_3$, IS: Mesitylene).

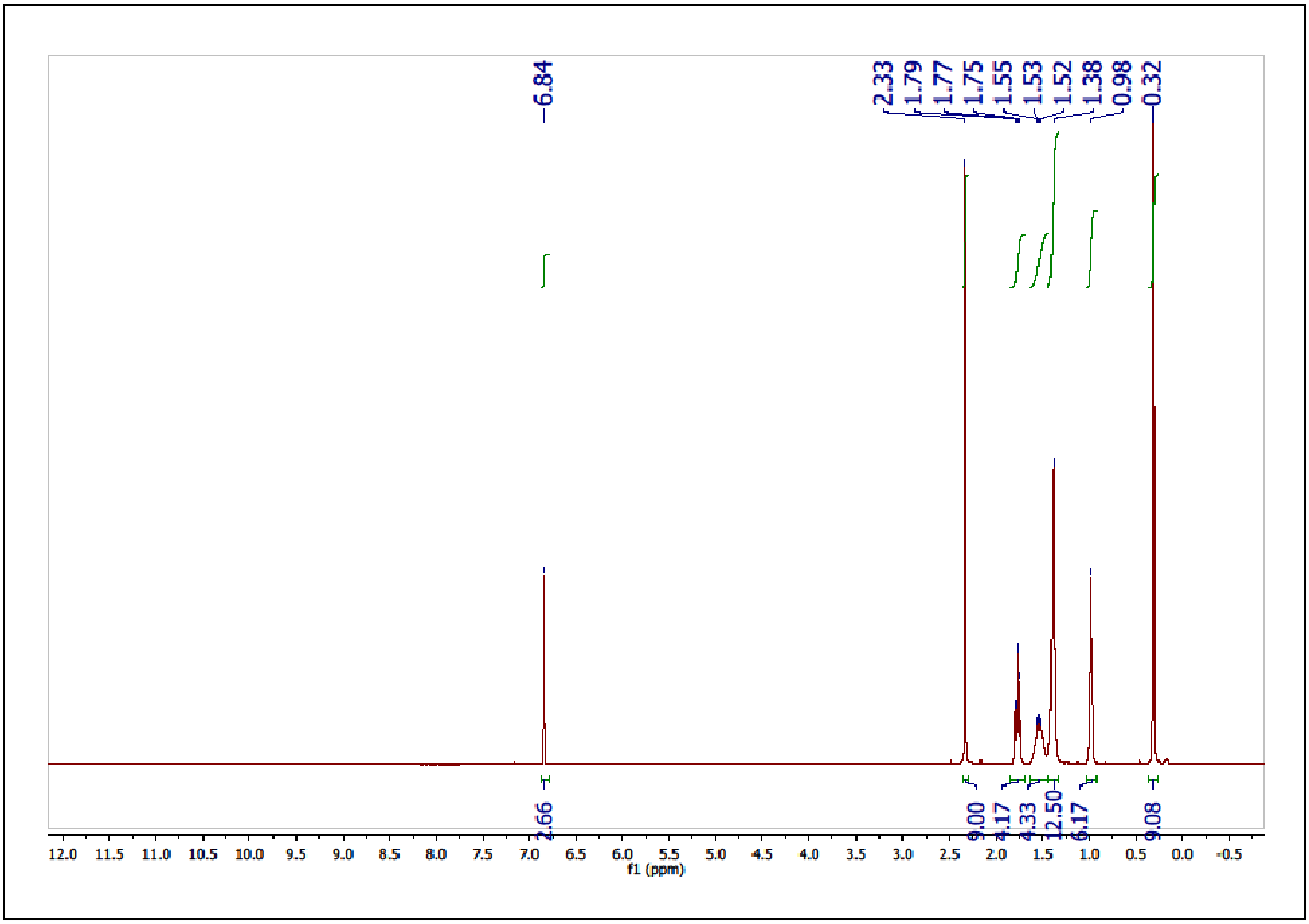

Figure S45. ^{1}H NMR spectrum of **5r** (Solvent: $CDCl_3$, IS: Mesitylene).

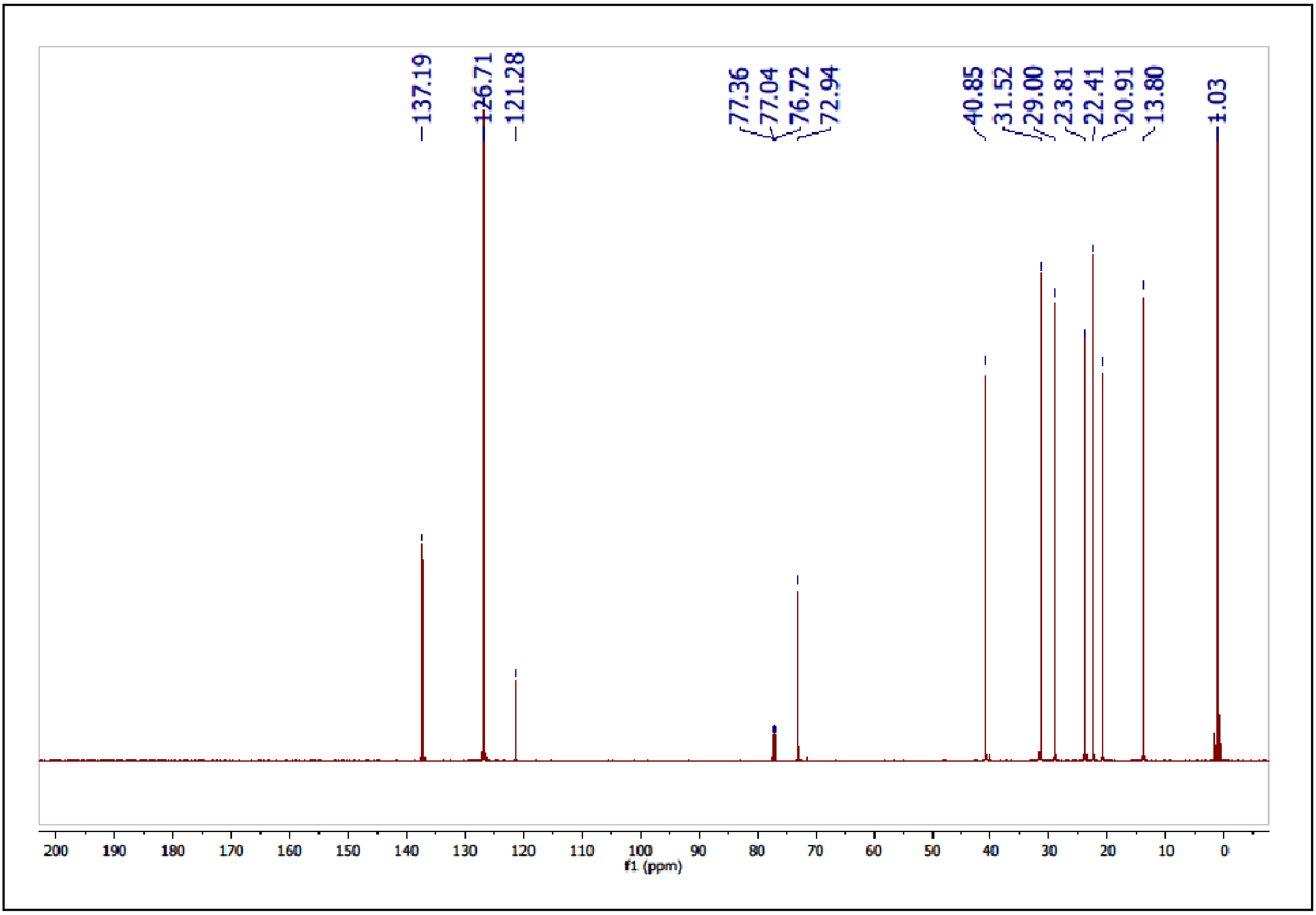

Figure S46. ^{13}C NMR spectrum of **5r** (Solvent: $CDCl_3$, IS: Mesitylene).

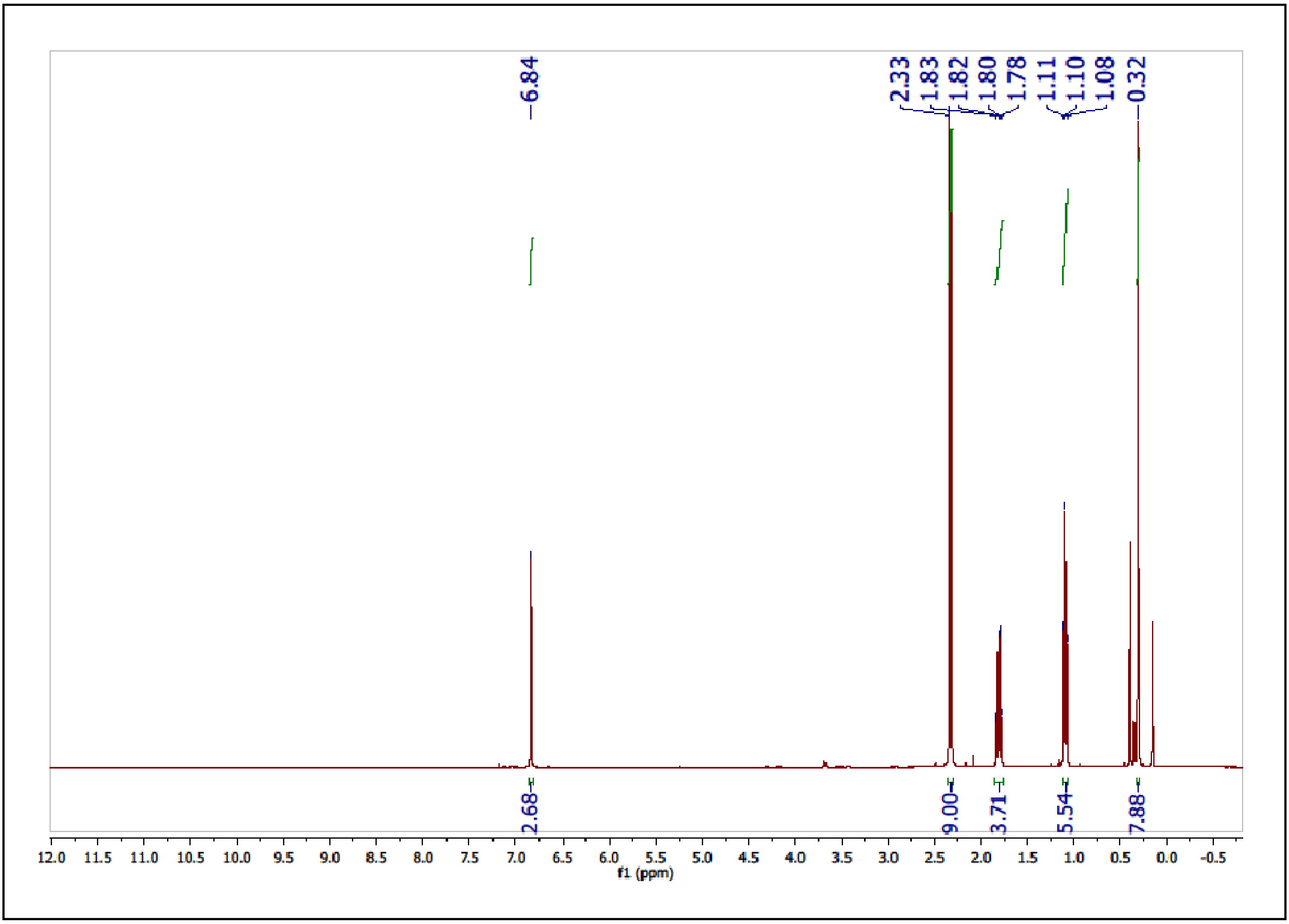

Figure S47. ^{1}H NMR spectrum of **5s** (Solvent: $CDCl_3$, IS: Mesitylene)

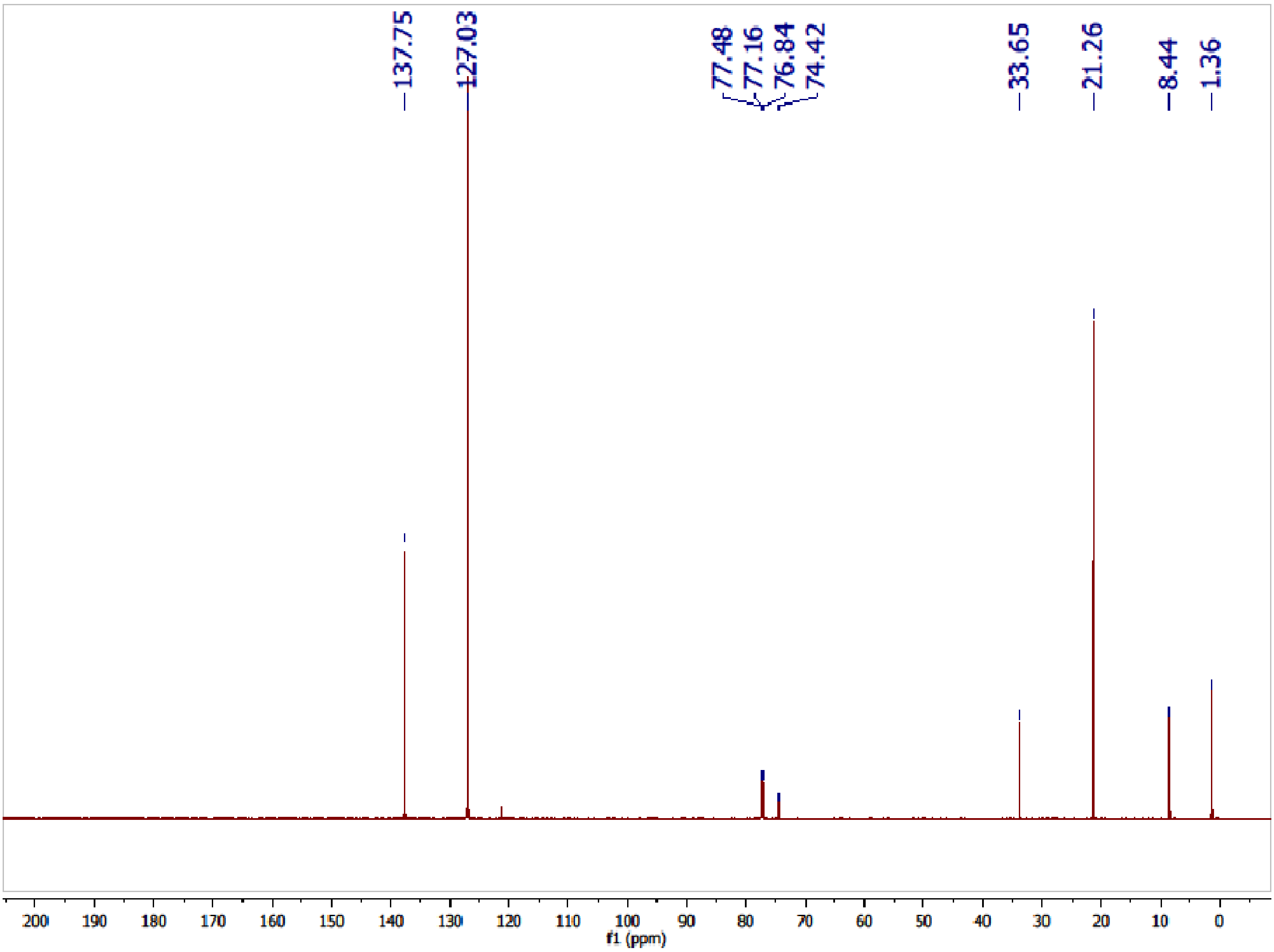

Figure S48. ^{13}C NMR spectrum of **5s** (Solvent: $CDCl_3$, IS: Mesitylene).

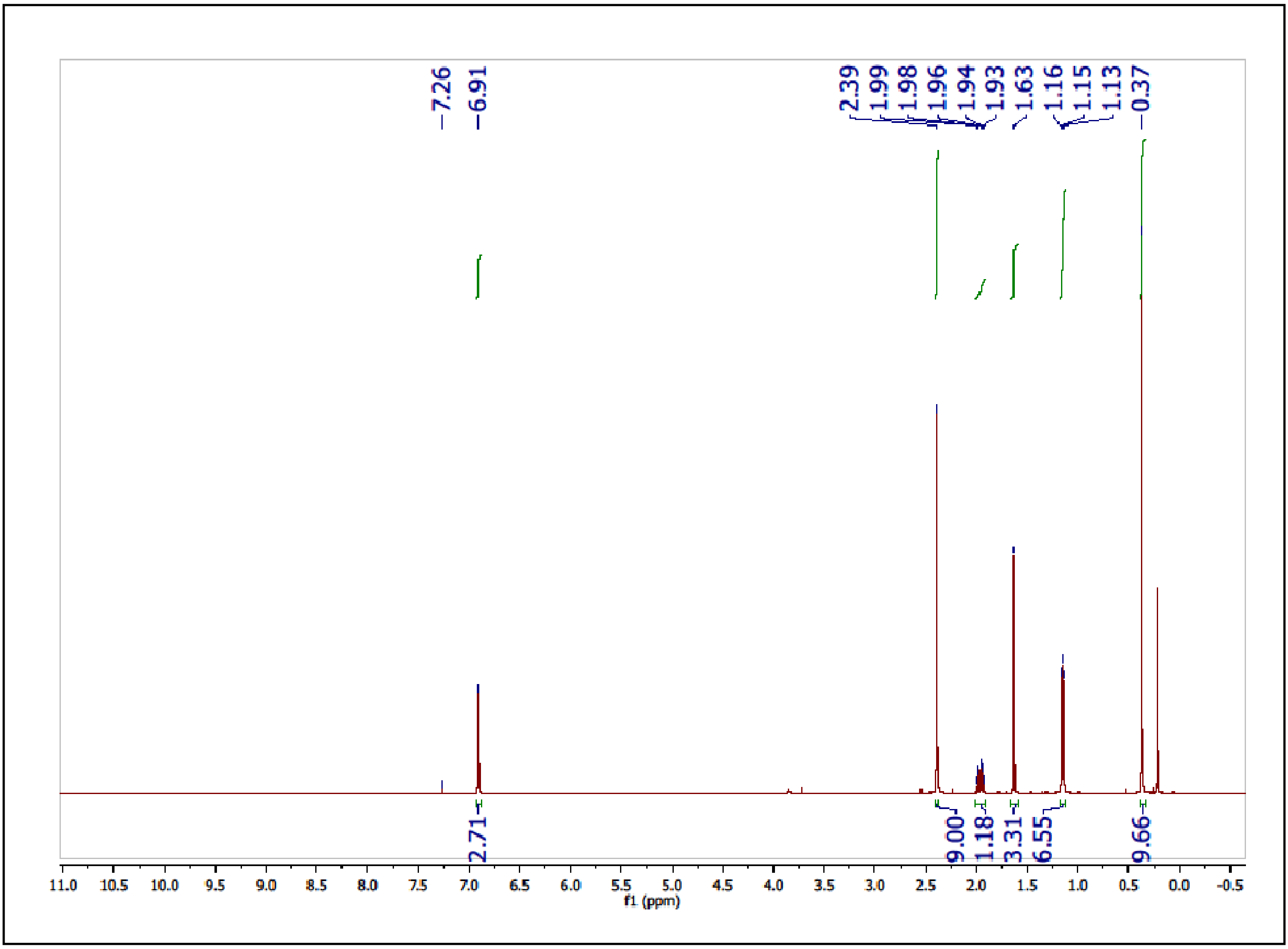

Figure S49. ^{1}H NMR spectrum of **5t** (Solvent: $CDCl_3$, IS: Mesitylene)

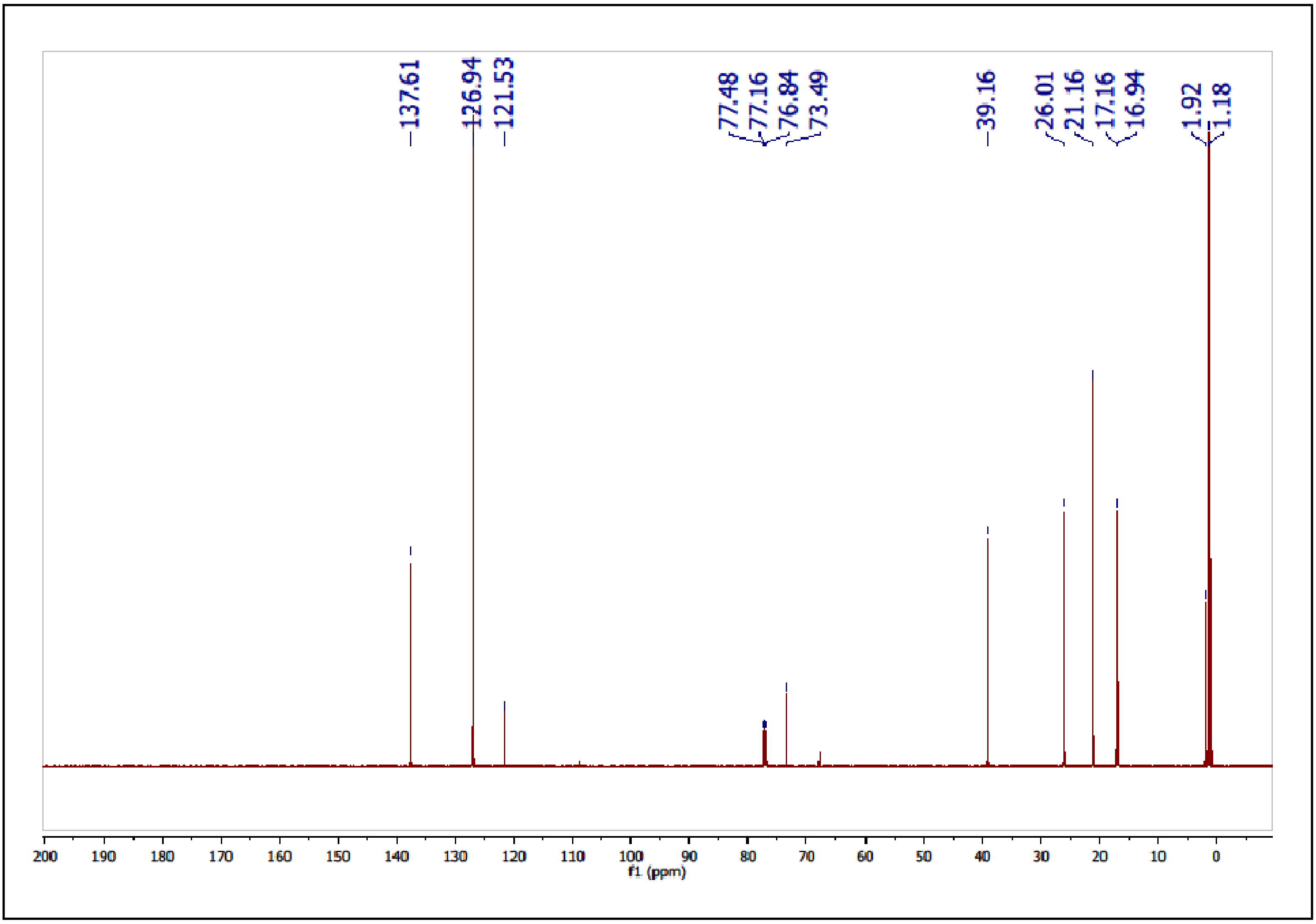

Figure S50. ^{13}C NMR spectrum of **5t** (Solvent: $CDCl_3$, IS: Mesitylene).

[S9]. NMR data for cyanosilylated products of ketones by catalyst 3.

(i) $\mathrm{PhCCH_3CNOSi(CH_3)_3}$ (5a) ^{1}H NMR (400 MHz, $\mathrm{CDCl_3}$) δ 7.39-7.51 (m, 4H, *Ph*), 1.91(s, 3H, TMSO-$\mathrm{C\mathit{H_3}CN}$), 0.24(s, 9H, $\mathrm{Si(\mathit{CH_3})_3}$), 2.33 (s, 9H, $\mathrm{Ph(C\mathit{H}_3)_3}$), 6.86 (s, 3H $\mathrm{C_6\mathit{H}_3(CH_3)_3}$); ^{13}C NMR (101 MHz, $\mathrm{CDCl_3}$) δ 1.01(s, $\mathrm{Si(\mathit{C}H_3)_3}$), 21.15(s, $\mathrm{Ph(\mathit{C}H_3)_3}$), 33.53(s, $\mathrm{PhC\mathit{C}H_3CNOSi(CH_3)_3}$), 71.59(s, $\mathrm{\mathit{C}CH_3(CN)OSi(CH_3)_3}$), 121.60(s, $\mathrm{CCH_3(\mathit{C}N)OSi(CH_3)_3}$), 124.58, 126.87, 128.60, 137.65, 141.12, 141.98 (represents carbon atom of the aromatic phenyl ring)

(ii) 4-$\mathrm{CH_3PhCCH_3CNOSi(CH_3)_3}$ (5b) ^{1}H NMR (400 MHz, $\mathrm{CDCl_3}$) *δ* 7.23-7.49(m, 4H, *Ph*), 1.89(s, 3H, TMSO-$\mathrm{C\mathit{H_3}CN}$), 0.23(s, 9H, $\mathrm{Si(\mathit{CH_3})_3}$), 2.41(s, 3H, 4-$\mathrm{C\mathit{H}_3PhCHCNOSi(CH_3)_3}$ 2.33 (s, 9H, $\mathrm{Ph(C\mathit{H}_3)_3}$), 6.85 (s, 3H $\mathrm{C_6\mathit{H}_3(CH_3)_3}$); ^{13}C NMR (101 MHz, $\mathrm{CDCl_3}$) *δ* 1.17 (s, $\mathrm{Si(\mathit{C}H_3)_3}$), 21.15(s, 4-$\mathrm{\mathit{C}H_3PhCCH_3CNOSi(CH_3)_3}$), 33.63(s, $\mathrm{Ph(\mathit{C}H_3)_3}$), 71.63(s, $\mathrm{\mathit{C}CH_3(CN)OSi(CH_3)_3}$), 121.73(s, $\mathrm{CCH_3(\mathit{C}N)OSi(CH_3)_3}$), 124.70, 127.02, 129.38, 137.79 (represents carbon atom of the aromatic phenyl ring) HRMS: Calcd for 4-$\mathrm{CH_3PhCCH_3CNOSi(CH_3)_3}$ *m/z* 233.12. Found: *m/z* 235.1684 [M+2H$^+$]

(iii) 3,4-$\mathrm{(CH_3)_2PhCCH_3CNOSi(CH_3)_3}$ (5C) ^{1}H NMR (400 MHz, $\mathrm{CDCl_3}$) *δ* 6.88-7.20 (m, 3H, *Ph*), 3.55-1.92(s, 3H, TMSO-$\mathrm{C\mathit{H_3}CN}$), 0.26(s, 9H, $\mathrm{Si(\mathit{CH_3})_3}$), 3.91, 3.95 (s, 2H, $\mathrm{Ph(C\mathit{H}_3)_2CCH_3CNOSiMe_3}$) 2.33 (s, 9H, $\mathrm{Ph(C\mathit{H}_3)_3}$), 6.85 (s, 3H $\mathrm{C_6\mathit{H}_3(CH_3)_3}$); ^{13}C NMR (101 MHz, $\mathrm{CDCl_3}$) *δ* 0.86(s, $\mathrm{Si(\mathit{C}H_3)_3}$), 20.96(s, $\mathrm{Ph(\mathit{C}H_3)_3}$), 33.26 (s, 3,4-$\mathrm{(CH_3)_2PhC\mathit{C}H_3CNOSiMe_3}$), 55.63 (s, $\mathrm{PhC\mathit{C}H_2CNOSi(CH_3)_3}$), 71.24(s, $\mathrm{\mathit{C}CH_3(CN)OSi(CH_3)_3}$), 118.97(s, $\mathrm{CCH_3(\mathit{C}N)OSi(CH_3)_3}$), 107.86, 110.67, 116.93, 121.47, 126.72, 134.29, 137.35, 148.91(represents carbon atom of the aromatic phenyl ring)

(iv) 4-$\mathrm{OCH_3PhCCH_3CNOSi(CH_3)_3}$ (5d) ^{1}H NMR (400 MHz, $\mathrm{CDCl_3}$) *δ* 6.94-7.54 (m, 4H, *Ph*), 1.89(s, 3H, TMSO-$\mathrm{C\mathit{H_3}CN}$), 0.23(s,9H, $\mathrm{Si(\mathit{CH_3})_3}$), 3.83(s, 3H, 4-$\mathrm{OC\mathit{H}_3PhCHCNOSi(CH_3)_3}$ 2.33 (s, 9H, $\mathrm{Ph(C\mathit{H}_3)_3}$), 6.85 (s, 3H $\mathrm{C_6\mathit{H}_3(CH_3)_3}$); ^{13}C NMR (101 MHz, $\mathrm{CDCl_3}$) *δ* 1.02 (s, $\mathrm{Si(\mathit{C}H_3)_3}$), 21.14(s, $\mathrm{Ph(\mathit{C}H_3)_3}$), 33.34(s, 4-$\mathrm{OCH_3PhC\mathit{C}H_3CNOSi(CH_3)_3}$), 55.11(s, 4-$\mathrm{O\mathit{C}H_3PhCCH_3CNOSi(CH_3)_3}$), 71.27(s, $\mathrm{\mathit{C}CH_3(CN)OSi(CH_3)_3}$), 121.73(s, $\mathrm{CCH_3(\mathit{C}N)OSi(CH_3)_3}$), 113.83, 126.01, 126.92, 134.01, 137.55, 159.84 (represents carbon atom of the aromatic phenyl ring) HRMS: Calcd *m/z* 249.11. Found *m/z* 249.1580 [$\mathrm{M^+}$].

(v) $\mathbf{4\text{-}BrPhCCH_3CNOSi(CH_3)_3}$ (5e) ^{1}H NMR (400 MHz, $\mathrm{CDCl_3}$) δ 7.45-7.56 (m, 4H, *Ph*), 1.87(s, 3H, $\mathrm{TMSO\text{-}C}H_3\mathrm{CN}$), 0.27(s, 9H, $\mathrm{Si(}CH_3)_3$), 2.33 (s, 9H, $\mathrm{Ph(C}H_3\mathrm{)_3}$), 6.85 (s, 3H $\mathrm{C_6}H_3\mathrm{(CH_3)_3}$); ^{13}C NMR (101 MHz, $\mathrm{CDCl_3}$) δ 1.07(s, $\mathrm{Si(}C\mathrm{H_3)_3}$), 21.22(s, $\mathrm{Ph(}C\mathrm{H_3)_3}$), 33.45(s, $\mathrm{4\text{-}BrPhC}C\mathrm{H_3CNOSi(CH_3)_3}$), 71.11(s, $C\mathrm{CH_3(CN)OSi(CH_3)_3}$), 121.12(s, $\mathrm{CCH_3(}C\mathrm{N)OSi(CH_3)_3}$), 122.39, 126.95, 131.83, 137.60, 141.31 (represents carbon atom of the aromatic phenyl ring) HRMS: Calcd *m/z* 297.0185. Found *m/z* 299.1817 [$\mathrm{M+2H^+}$].

(vi) $\mathbf{2\text{-}BrPhCCH_3CNOSi(CH_3)_3}$ (5f) ^{1}H NMR (400 MHz, $\mathrm{CDCl_3}$) δ 7.23-7.80(m, 4H, *Ph*), 2.07(s, 3H, $\mathrm{TMSO\text{-}C}H_3\mathrm{CN}$), 0.36(s, 9H, $\mathrm{Si(}CH_3)_3$), 2.33 (s, 9H, $\mathrm{Ph(C}H_3\mathrm{)_3}$), 6.86 (s, 3H $\mathrm{C_6}H_3\mathrm{(CH_3)_3}$); ^{13}C NMR (101 MHz, $\mathrm{CDCl_3}$) δ 1.14(s, $\mathrm{Si(}C\mathrm{H_3)_3}$), 21.15(s, $\mathrm{Ph(}C\mathrm{H_3)_3}$), 29.81(s, $\mathrm{2\text{-}BrPhC}C\mathrm{H_3CNOSi(CH_3)_3}$), 71.43(s, $C\mathrm{CH_3(CN)OSi(CH_3)_3}$), 126.89(s, $\mathrm{CCH_3(}C\mathrm{N)OSi(CH_3)_3}$), 127.24, 127.61, 130.08, 135.20, 137.49, 139.24 (represents carbon atom of the aromatic phenyl ring) HRMS: Calcd *m/z* 297.0185. Found *m/z* 299.1817 [$\mathrm{M+2H^+}$].

vii) $\mathbf{PhCCH_2BrCNOSi(CH_3)_3}$ (5g) ^{1}H NMR (400 MHz, $\mathrm{CDCl_3}$) δ 7.45-7.63 (m, 4H, *Ph*), 3.55-3.65(dd, 2H, $\mathrm{TMSO\text{-}C}H_3\mathrm{CN}$), 0.26(s, 9H, $\mathrm{Si(}CH_3)_3$), 2.33 (s, 9H, $\mathrm{Ph(C}H_3\mathrm{)_3}$), 6.85 (s, 3H $\mathrm{C_6}H_3\mathrm{(CH_3)_3}$); ^{13}C NMR (101 MHz, $\mathrm{CDCl_3}$) δ 0.80(s, $\mathrm{Si(}C\mathrm{H_3)_3}$), 21.19(s, $\mathrm{Ph(}C\mathrm{H_3)_3}$), 40.86(s, $\mathrm{PhC}C\mathrm{H_2BrCNOSi(CH_3)_3}$), 75.37(s, $C\mathrm{CH_3(CN)OSi(CH_3)_3}$), 118.97(s, $\mathrm{CCH_3(}C\mathrm{N)OSi(CH_3)_3}$), 125.40, 126.93, 128.85, 129.69, 137.56, 138.35 (represents carbon atom of the aromatic phenyl ring) HRMS: Calcd HRMS: Calcd *m/z* 297.0185. Found *m/z* 299.1786 [$\mathrm{M+2H^+}$].

(viii) $\mathbf{4\text{-}NO_2PhCCH_3CNOSi(CH_3)_3}$ (5h) ^{1}H NMR (400 MHz, $\mathrm{CDCl_3}$) δ 7.78-8.29 (m, 4H, *Ph*), 1.94(s, 3H, $\mathrm{TMSO\text{-}C}H_3\mathrm{CN}$), 0.33(s, 9H, $\mathrm{Si(}CH_3)_3$), 2.33 (s, 9H, $\mathrm{Ph(C}H_3\mathrm{)_3}$), 6.84 (s, 3H $\mathrm{C_6}H_3\mathrm{(CH_3)_3}$); ^{13}C NMR (101 MHz, $\mathrm{CDCl_3}$) δ 0.95(s, $\mathrm{Si(}C\mathrm{H_3)_3}$), 21.10(s, $\mathrm{Ph(}C\mathrm{H_3)_3}$), 33.25(s, $\mathrm{4\text{-}NO_2PhC}C\mathrm{H_3CNOSi(CH_3)_3}$), 70.90(s, $C\mathrm{CH_3(CN)OSi(CH_3)_3}$), 120.60(s, $\mathrm{CCH_3(}C\mathrm{N)OSi(CH_3)_3}$), 123.89, 125.67, 126.87, 137.54, 147.98, 148.88 (represents carbon atom of the aromatic phenyl ring) HRMS: Calcd *m/z* 262.1012. Found *m/z* 261.2281 [$\mathrm{M^+}$].

(ix) $\mathbf{4\text{-}NO_2PhCCH_3CNOSi(CH_3)_3}$ (5i) - ^{1}H NMR (400 MHz, $\mathrm{CDCl_3}$) δ 6.65-6.73 and 7.82-7.84 (m, 4H, Ph), 2.52 (s, 3H, $\mathrm{TMSO\text{-}C}H_3\mathrm{CN}$), 0.37 (d, 9H, $\mathrm{Si(}CH_3)_3$), 4.23-4.42 (br, $\mathrm{\text{-}N}H_2$), 2.33 (s, 9H, $\mathrm{Ph(C}H_3\mathrm{)_3}$)

(x) 4-OHPhCCH$_3$CNOSi(CH$_3$)$_3$ (5j) ^{1}H NMR (400 MHz, CDCl$_3$) δ 6.74-7.78 (m, 4H, *Ph*), 2.39(s, 3H, TMSO-C*H*$_3$CN), 0.20(s, 9H, Si(*CH*$_3$)$_3$), 2.16 (s, 9H, Ph(C*H*$_3$)$_3$), 6.68 (s, 3H C$_6$*H*$_3$(CH$_3$)$_3$); ^{13}C NMR (101 MHz, CDCl$_3$) δ 0.14(s, Si(*C*H$_3$)$_3$), 21.12(s, Ph(*C*H$_3$)$_3$), 33.21(s, 4-OHPhC*C*H$_3$CNOSi(CH$_3$)$_3$), 71.30(s, *C*CH$_3$(CN)OSi(CH$_3$)$_3$), 119.76(s, CCH$_3$(*C*N)OSi(CH$_3$)$_3$), 120.02, 126.96, 130.50, 137.53, 159.75 (represents carbon atom of the aromatic phenyl ring) HRMS: Calcd *m/z* 235.1029. Found *m/z* 235.9781 [M$^+$].

(xi) C$_4$H$_3$CCH$_3$CNOSi(CH$_3$)$_3$ (5k) - ^{1}H NMR (400 MHz, CDCl$_3$) *δ* 6.41(s, 1H Ar*H*), 6.55 (s, 1H, Ar*H*), 7.44 (s, 1H, Ar*H*), 1.98(s, 3H, -C*H*$_3$CCNOSiMe$_3$), 0.17 (s, 9H, -Si(C*H*$_3$)$_3$), 2.33 (s, 9H, Ph(C*H*$_3$)$_3$); ^{13}C NMR (101 MHz, CDCl$_3$) *δ* 0.52(s, Si(*C*H$_3$)$_3$), 28.90(s, *C*H$_3$CCNOSiMe$_3$), 65.98(s, CH$_3$*C*CNOSiMe$_3$), 120.24(s, CH$_3$C*CN*OSiMe$_3$) 108.22, 110.75, 143.15, 151.77 (s, Ar*H*), 21.20, 126.98, 137.66 (s, Mesitylene). ESI-MS: Calcd for C$_4$H$_3$CCH$_3$CNOSi(CH$_3$)$_3$ *m/z* 209.09. Found: *m/z* 209.0616 [M$^+$]

(xii) PhC$_3$HCCH$_3$CNOSi(CH$_3$)$_3$ (5l)- ^{1}H NMR (400 MHz, CDCl$_3$) *δ* 6.92-7.62 (m, 5H, Ar*H*), 2.06 (s, 3H, -C*H*$_3$CCNOSiMe$_3$), 0.24 (s, 9H, -Si(C*H*$_3$)$_3$)); ^{13}C NMR (101 MHz, CDCl$_3$) *δ* 0.62 (s, -Si(*C*H$_3$)$_3$), 21.07(s, C$_6$H$_3$(*C*H$_3$), 28.92 (s, C$_6$H$_4$C$_3$HOCCNO*C*H$_3$), 66.42 (s, C$_6$H$_4$C$_3$HO*C*CNOCH$_3$), 104.43, 111.44, 121.66, 123.36, 125.38, 154.23, 154.97 (s, represents carbon atom of the aromatic phenyl ring), 126.88, 137.40 (s, Mesitylene).

(xiii) Ph$_2$CCNOSi(CH$_3$)$_3$ (5m)- ^{1}H NMR (400 MHz, CDCl$_3$) *δ* 7.47-7.75 (m, 4H, *Ph*), 0.39(s,9H, Si(*CH*$_3$)$_3$), 2.48 (s, 9H, Ph(C*H*$_3$)$_3$), 7.01 (s, 3H C$_6$*H*$_3$(CH$_3$)$_3$); ^{13}C NMR (101 MHz, CDCl$_3$) *δ* 0.85(s, Si(*C*H$_3$)$_3$), 21.11(s, Ph(*C*H$_3$)$_3$), 76.34(s, *C*Ph$_2$(CN)OSi(CH$_3$)$_3$), 120.64(s, CPh$_2$(*C*N)OSi(CH$_3$)$_3$), 125.83, 126.88, 128.17-129.93, 137.47, 141.97(represents carbon atom of the aromatic phenyl ring) HRMS: Calcd *m/z* 281.1236. Found *m/z* 282.1304 [M$^+$].

(xiv) Ph$_2$(OH)$_2$CCNOSi(CH$_3$)$_3$ (5n)- ^{1}H NMR (400 MHz, CDCl$_3$) *δ* 6.46-7.91 (m, 8H, Ar*H*), 0.47 (s, 9H, -Si(C*H*$_3$)$_3$), 12.73 (s, 1H, -O*H*), 2.39 (s, 9H, C$_6$H$_3$(CH$_3$)$_3$); ^{13}C NMR (101 MHz, CDCl$_3$) *δ* 0.19 (s, -Si(CH$_3$)$_3$), 108.06, 111.80, 113.89, 128.20, 128.83, 131.40, 135.39, 138.26, 162.64, 165.97, 200.04. ESI-MS: Calcd for Ph$_2$(OH)$_2$CCNOSi(CH$_3$)$_3$ *m/z* 313.11. Found: *m/z* 313.0223 [M$^+$]

(xv) Ph$_2$(OH)$_2$(CH)$_2$CCNOSi(CH$_3$)$_3$ (5o)- ^{1}H NMR (400 MHz, CDCl$_3$) *δ* 6.84-7.92 (m, 5H, Ar*H*), 0.35-0.37 (d, *J*=7.7Hz, 9H, --Si(C*H*$_3$)$_3$), 13.41 (s, 1H, -OH). ESI-MS: Calcd for **Ph$_2$(OH)$_2$(CH)$_2$CCNOSi(CH$_3$)$_3$** *m/z* 339.13. Found: *m/z* 341.2754 [M+2H$^+$]

(xvi) $C_5H_8CNOSi(CH_3)_3$ (5p) ^{1}H NMR (400 MHz, $CDCl_3$) δ 1.80-2.18 (m, 8H, *Cp*), 0.32(s,9H, $Si(CH_3)_3$), 2.33 (s, 9H, $Ph(CH_3)_3$), 6.85 (s, 3H $C_6H_3(CH_3)_3$); ^{13}C NMR (101 MHz, $CDCl_3$) δ 1.03(s, $Si(CH_3)_3$), 21.15 22.61(s, $Ph(CH_3)_3$), 41.65(s, C_4H_8), 74.45(s, $CC_4H_8(CN)OSi(CH_3)_3$), 126.92(s, $C_5H_8(CN)OSi(CH_3)_3$), HRMS: Calcd *m/z* 225.1549. Found *m/z* 224.1255 [M$^+$]

(xvii) $C_6H_{10}CNOSi(CH_3)_3$ (5q) - ^{1}H NMR (400 MHz, $CDCl_3$) δ 1.28-2.11 (m, 9H, $C_5H_{10}CCNOSiMe_3$), 0.32(s, 7H, $OSi(CH_3)_3$); ^{13}C NMR (101 MHz, $CDCl_3$) δ 1.36 (s, $Si(CH_3)_3$), 22.64, 24.54, 39.38 (s, $C_5H_{10}CCNOSiMe_3$), 70.57 (s, $C_5H_{10}CCNOSiMe_3$), 121.84 (s $C_5H_{10}CCNOSiMe_3$), 21.13, 126.91, 137.54 (s, Mesitylene). HRMS: Calcd *m/z* 297.0185. Found *m/z* 299.1786 [M+2H$^+$].

(xviii) $(CH_3(CH_2)_5)_2CCNOSi(CH_3)_3$ (5r) - ^{1}H NMR (400 MHz, $CDCl_3$) δ 0.32 (s, 9H, -$Si(CH_3)_3$), 0.98, 1.38, 1.52, 1.53, 1.55, 1.75, 1.77, 1.79 (26H, -$(CH_2)_5CH_3$), 2.33, 6.84 (Mesitylene); ^{13}C NMR (101 MHz, $CDCl_3$) δ 1.03 (s, -$OSi(CH_3)_3$), 13.80, 22.41, 23.81, 29.00, 31.52, 40.85 (s, -$(CH_2)_5CH_3$), 72.94 (s, $(CH_3(CH_2)_5)_2CCNOSiMe_3$), 121.28 (s, $(CH_3(CH_2)_5)_2CCNOSiMe_3$), 20.91, 126.71, 137.19 (s, Mesitylene). ESI-MS: Calcd for $(CH_3(CH_2)_5)_2CCNOSi(CH_3)_3$ *m/z* 297.25. Found: *m/z* 297.2372 [M$^+$].

(xix) $(CH_3CH_2)_2CCNOSi(CH_3)_3$ (5s) - ^{1}H NMR (400 MHz, $CDCl_3$) δ 1.08-1.11 (m, 6H, -CH_3), 1.78-1.83 (m, 4H, -CH_2), 0.32 (s, 8H, -$Si(CH_3)_3$), 2.33, 6.84 (Mesitylene); ^{13}C NMR (101 MHz, $CDCl_3$) δ 1.36 (s, -$Si(CH_3)_3$), 8.44 (s, -CH_2CH_3), 33.65 (s, -CH_2CH_3), 74.42 (s, $(CH_2CH_3)CCNOSiMe_3$), 121.1 (s, $(CH_2CH_3)CCNOSiMe_3$), 21.26, 127.03, 137.75 (s, Mesitylene). ESI-MS: Calcd for $(CH_3CH_2)_2CCNOSi(CH_3)_3$ *m/z* 185.12. Found: *m/z* 186.9572 [M+H$^+$].

(xx) $(CH_3)_2CCH_3CCNOSi(CH_3)_3$ (5t) - ^{1}H NMR (400 MHz, $CDCl_3$) δ 0.37 (s, 9H, -$Si(CH_3)_3$), 1.13-1.16 (m, 6H, -$CH(CH_3)_3$), 1.63 (s, 3H, $CH_3CNCOSiMe_3$), 1.93-1.99 (m, 1H, -$CH(CH_3)_3$); ^{13}C NMR (101 MHz, $CDCl_3$) δ 1.18 (s, -$Si(CH_3)_3$), 21.16 (s, $Ph(CH_3)_3$), 73.49 (s, $(CCH_3)CCNOSiMe_3$), 1.92, 16.94, 17.16, 26.01, 39.16 (s, aliphatic carbon atoms), 126.94, 137.61 (s, aromatic phenyl ring carbon atoms of Mesitylene).

[S10]. Kinetic study

Representative procedure for reaction rate determination: The order of the cyanosilylation reaction of ketones catalyzed by catalyst **3** has been determined by using the initial rates method. The rate of the reaction k_{obs} is mainly calculated from the slope of the graph, plotted as the concentration of the product formation versus time. Here the concentration of one of the substrates is varied while the other and the catalyst are kept constant. Mesitylene was used as the internal standard in each experiment. The rate k_{obs} has been determined from the ^{1}H NMR of each experiment. ^{1}H NMR spectra were collected every 5 mins starting from t=5 to t=25 mins. The value of the slope of each linear best-fit plot of [Product] vs Time is the value of k_{obs}. The reaction order concerning acetophenone is determined from the plot of k_{obs} vs. acetophenone concentration.

Initially, the catalyst (0.0025 mmoles) was taken in an NMR tube inside the glove box followed by the addition of TMSCN (0.25 mmoles) along with mesitylene and then acetophenone (in different mmoles) and $CDCl_3$ (0.5 ml) were added under argon. ^{1}H NMR spectra were recorded for each setup at various time intervals. All the concentrations of acetophenone and the concentration of catalyst and TMSCN are provided in the table below (Table S4). From the k_{obs} and concentration of acetophenone plot it is observed that with the increase in concentration of acetophenone, it follows the linear correlation with k_{obs}.

SI. NO.	**Catalyst (mmoles)**	**Acetophenone (mmoles)**	**TMSCN (mmoles)**	**k_{obs} values (10^{-2})**
1	0.0025	0.25	0.25	1.25
2	0.0025	0.30	0.25	1.25
3	0.0025	0.45	0.25	1.33
4	0.0025	0.50	0.25	1.42

Table [S4]. Initial rates (k_{obs}) for the cyanosilylation of ketone with TMSCN catalyzed by catalyst **3**, carried out under varying concentrations of acetophenone.

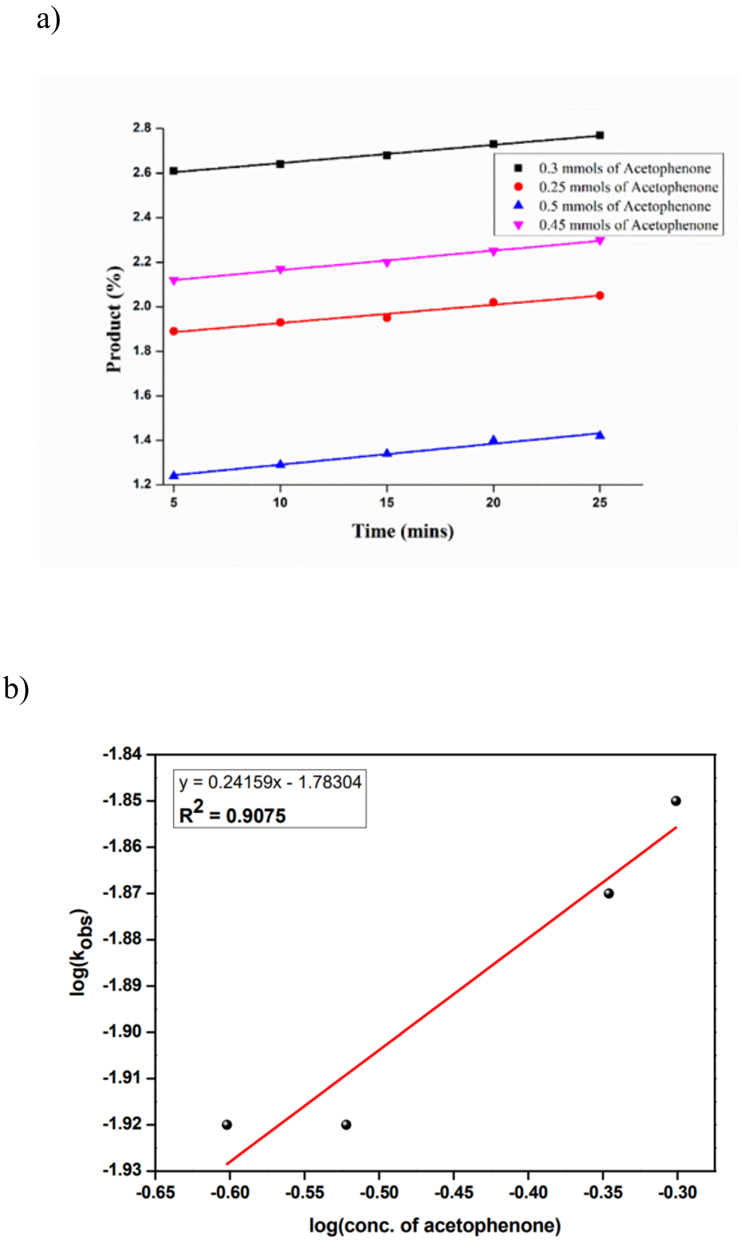

Figure S51. (a) The plot of Product (%) vs Time for the determination of the initial rate (k_{obs}) values.

(b) Plot of logk_{obs} vs log(conc. of acetophenone) for the determination of the order of the reaction.

The same experiment was done by varying the concentration of TMSCN and keeping the concentration of catalyst and acetophenone constant. Here also the catalyst (0.0025 mmoles) was taken in the NMR tube in the glove box and TMSCN (in different concentrations like 0.5 mmol, 1 mmol, 1.5 mmol), acetophenone (0.25 mmoles), mesitylene (0.25 mmoles) $CDCl_3$ (0.5 ml) were added to that NMR tube under argon atmosphere. ^1H NMR spectra were recorded after 5 mins intervals for each setup starting from t=5 to t=25 mins. In Table (S5) the varying concentrations of acetophenone and the concentration of catalyst and TMSCN as well as the value of k_{obs} are given. The plot of k_{obs} vs concentration of acetophenone indicates a linear correlation between the rate and the increase in acetophenone concentration.

SI. NO.	**Catalyst (mmoles)**	**Acetophenone (mmoles)**	**TMSCN (mmoles)**	**k_{obs} value (10^{-3})**
1	0.0025	0.25	0.5	8.8
2	0.0025	0.25	1.0	13
3	0.0025	0.25	1.5	16

Table [S5]. Initial rates (k_{obs}) for the cyanosilylation of acetophenone with TMSCN catalyzed by catalyst **3**, carried out under varying concentrations of TMSCN a)

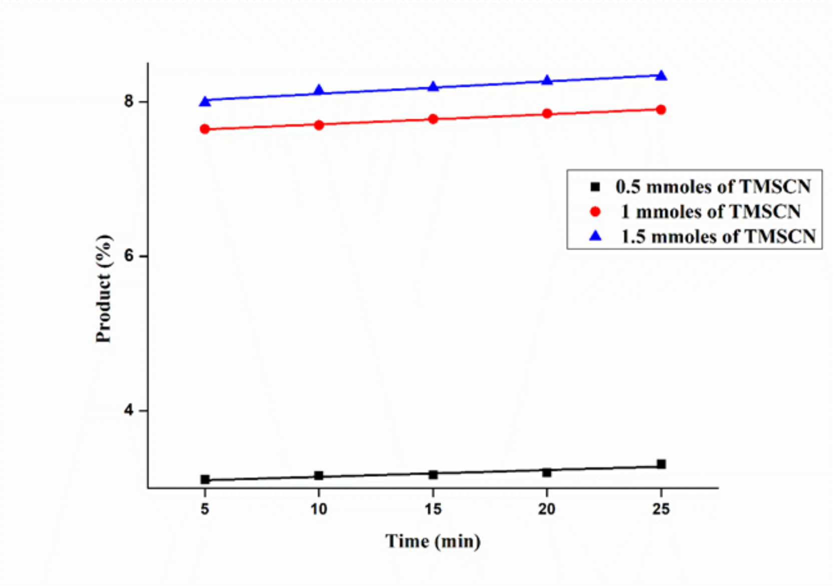

b)

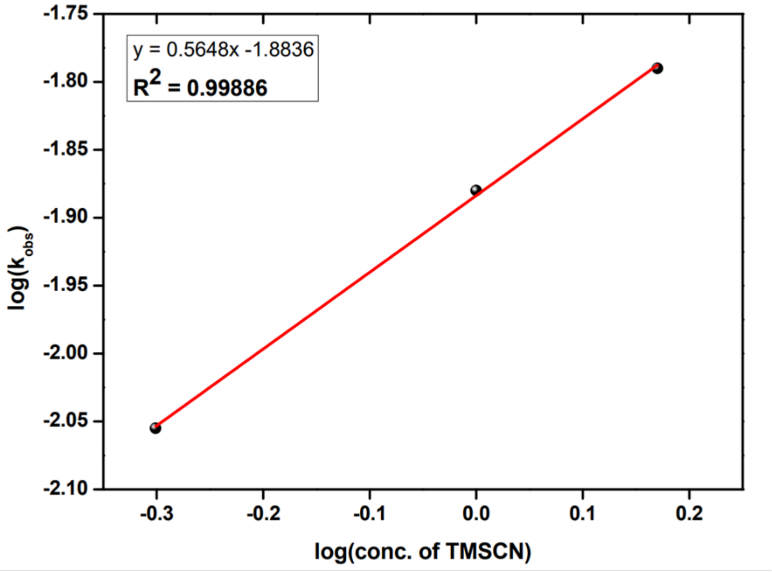

Figure S52. (a) The plot of Product (%) vs Time for the determination of the initial rate (k_{obs}) values.

(b) Plot of logk_{obs} vs log(conc. of TMSCN) for the determination of the order of the reaction.

The same experiment was done by varying the temperature and keeping the concentration of catalyst, acetophenone and TMSCN constant. Here the catalyst (0.00025 mmoles) was taken in the NMR tube in the glove box and TMSCN (0.25 mmol), acetophenone (0.25 mmoles), mesitylene (0.25 mmoles) and $CDCl_3$ (0.5 ml) were added to that NMR tube under argon atmosphere. ^1H NMR spectra were recorded after 5 mins intervals for each setup starting from t=5 to t=30 mins. Three sets of same experiments were performed at different temperature. In **Table (S6)** k was determined from plot of concentration of product vas time at all the three different temperatures. The plot of lnk vs 1/Temperature indicates a linear dependence between lnk and 1/Temperature (**Figure S52d**). Hence, the rate of the reaction follows Arrhenius behavior with temperature. We have calculated the activation energy (Ea) value from the slope of the lnk vs 1/Temperature curve which is 26.54 Kcal/mol. Theoretical calculations shows the activation energy is 31.3 Kcal/mol which is close to our experimental observation.

SI. NO.	Catalyst (mmoles)	Acetophenone (mmoles)	TMSCN (mmoles)	Temperature (K)	k value (10^{-3})
1	0.00025	0.25	0.25	293	1.6
2	0.00025	0.25	0.25	297	2.4
3	0.00025	0.25	0.25	301	5.3

Table [S6]. Initial rates (k) for the cyanosilylation of acetophenone with TMSCN catalyzed by catalyst **3**, carried out under varying temperatures.

c)

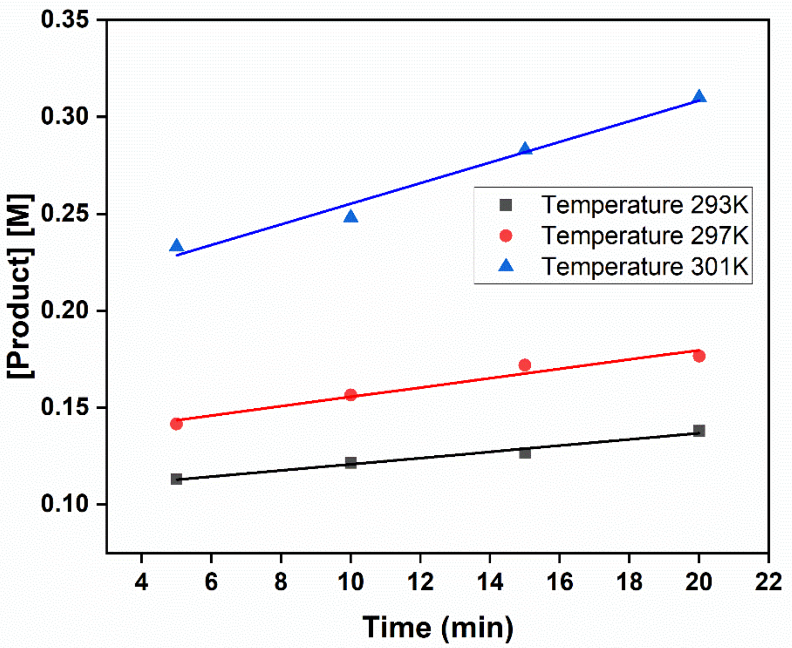

d)

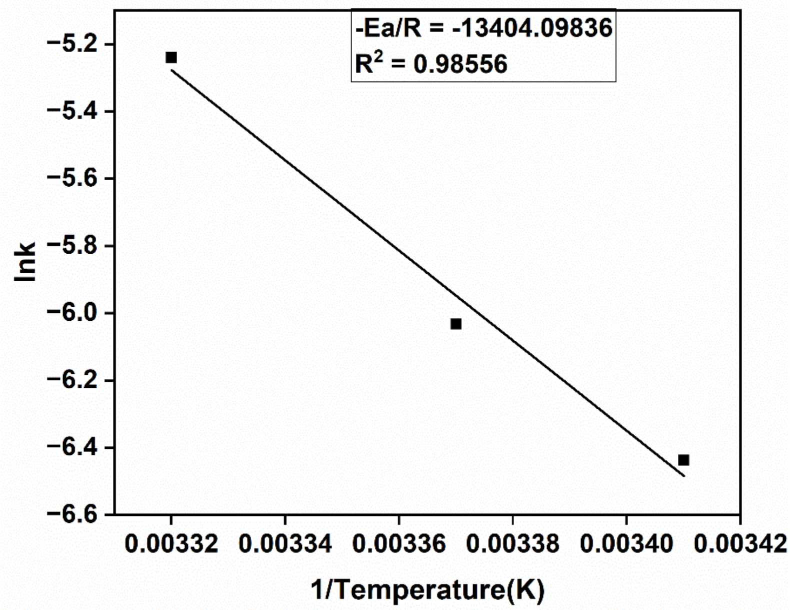

Figure S52. (c) The plot of Product [M] vs Time at different temperature for the determination of the initial rate (k_{obs}) values.

(d) Arrhenius Plot (lnk vs 1/Temperature) for the determination of the activation energy of the reaction.

[S11]. Experimental data and theoretical calculations to propose mechanistic pathway of cyanosilylation reaction.

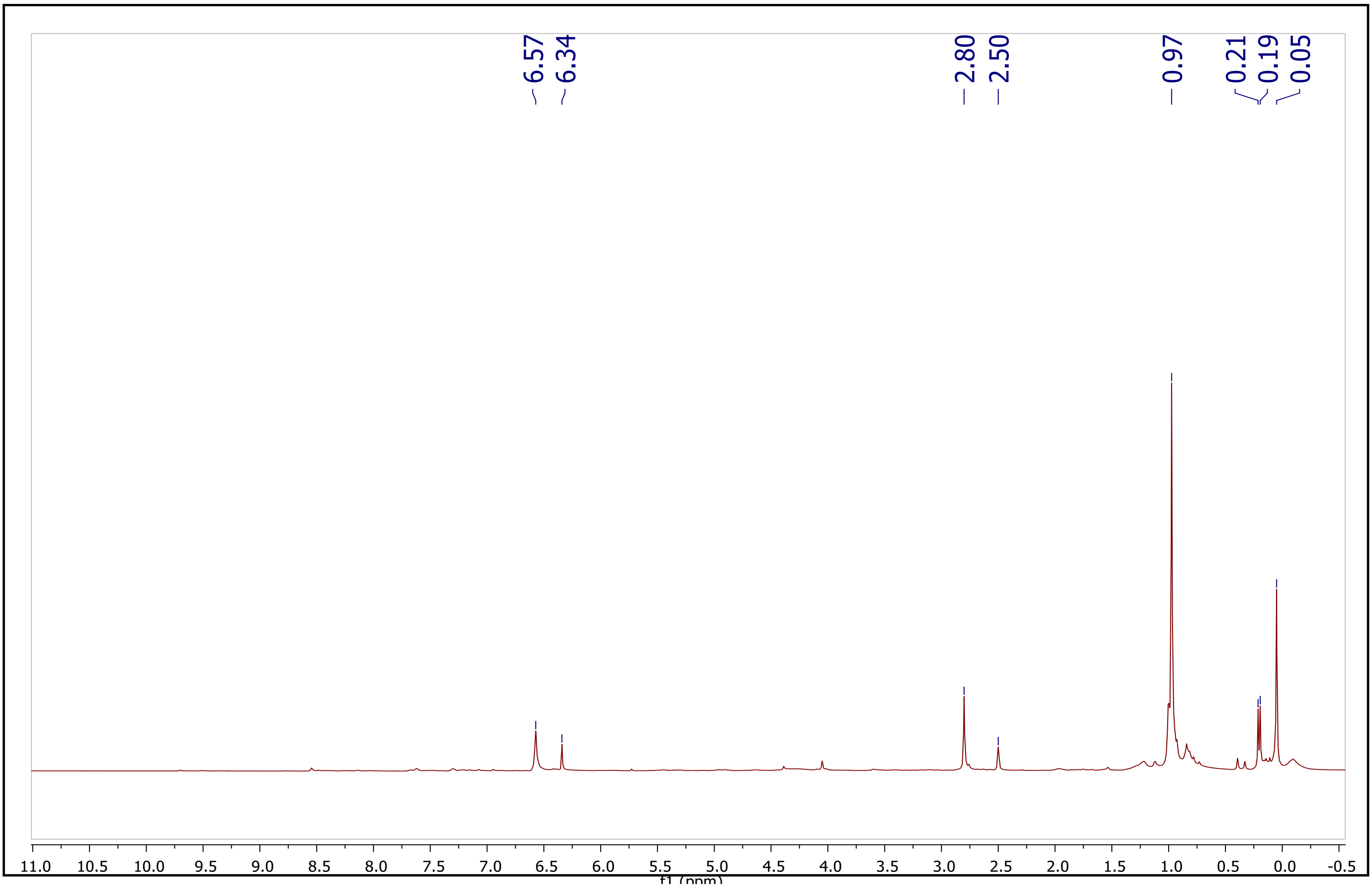

Figure S53. ^{1}H NMR spectrum of 1:1 reaction of catalyst and TMSCN

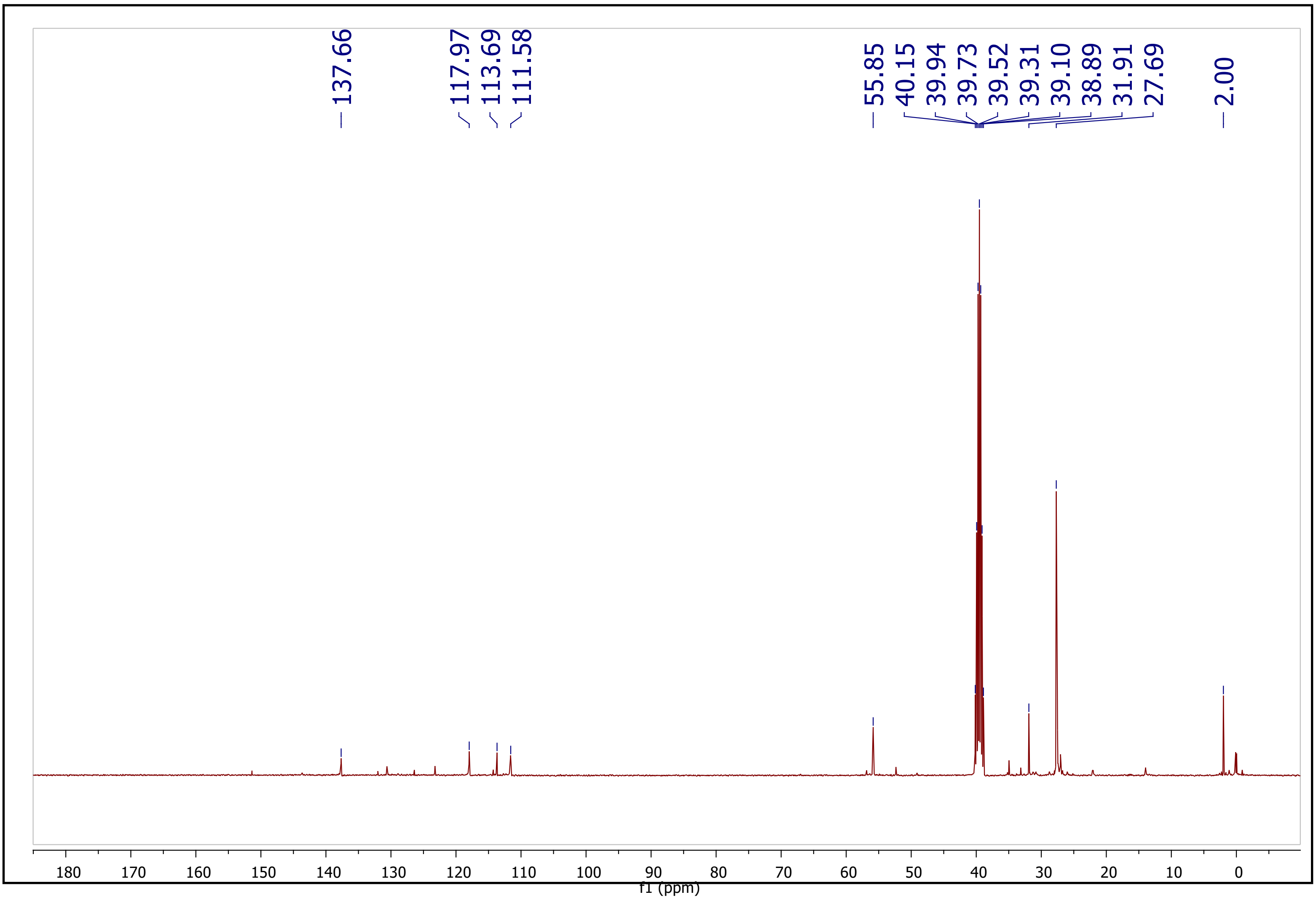

Figure S54. ^{13}C NMR spectrum of 1:1 reaction of catalyst and TMSCN

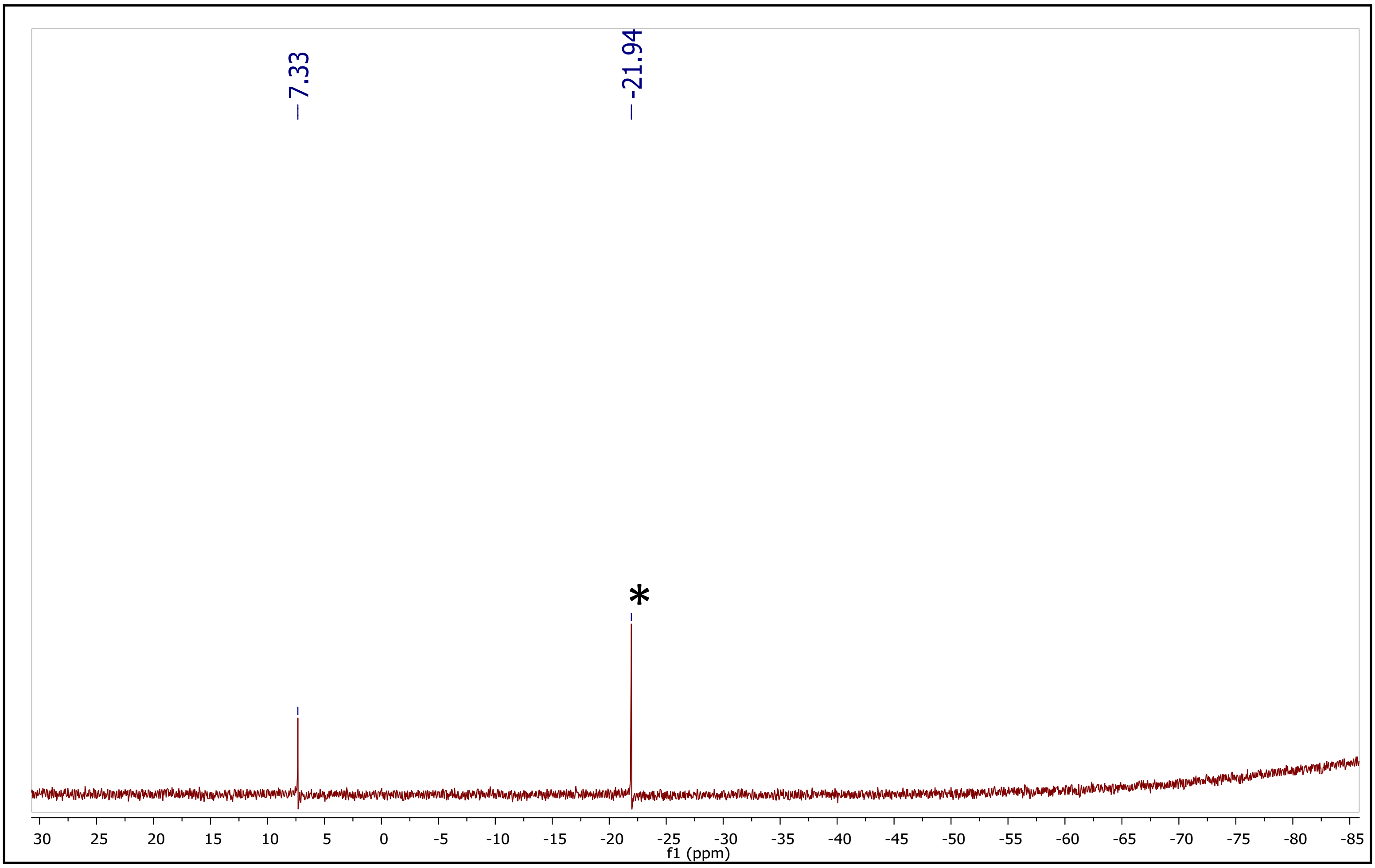

Figure S55. ^{29}Si NMR spectrum of 1:1 reaction of catalyst and TMSCN

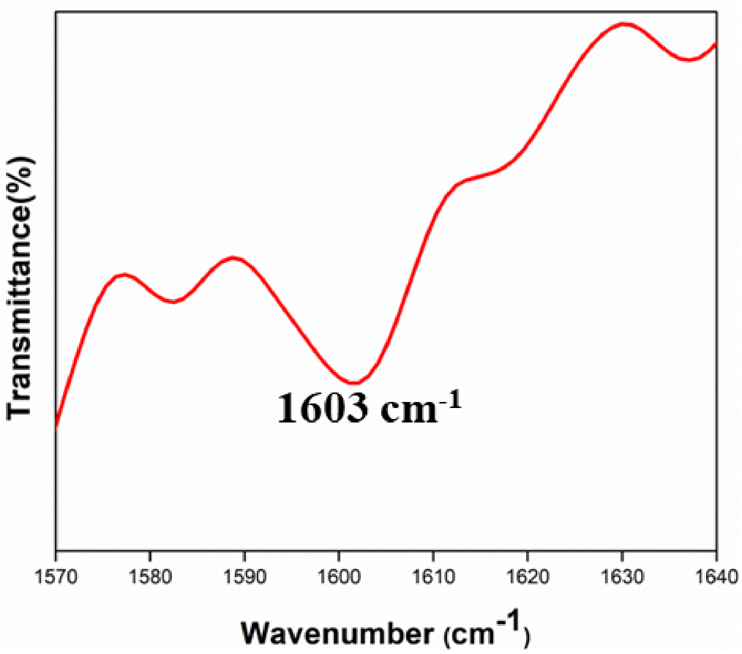

Figure S56. IR spectrum of 1:1 reaction of catalyst and TMSCN

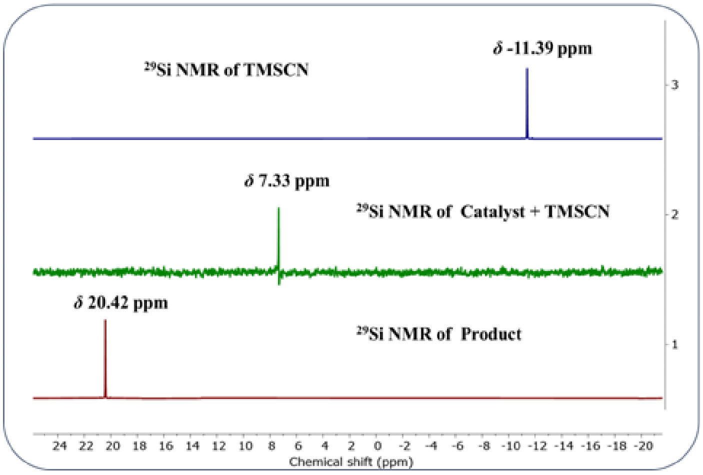

Figure S57. Stacked ^{29}Si NMR of TMSN, intermediate and the cyanosilylated product.

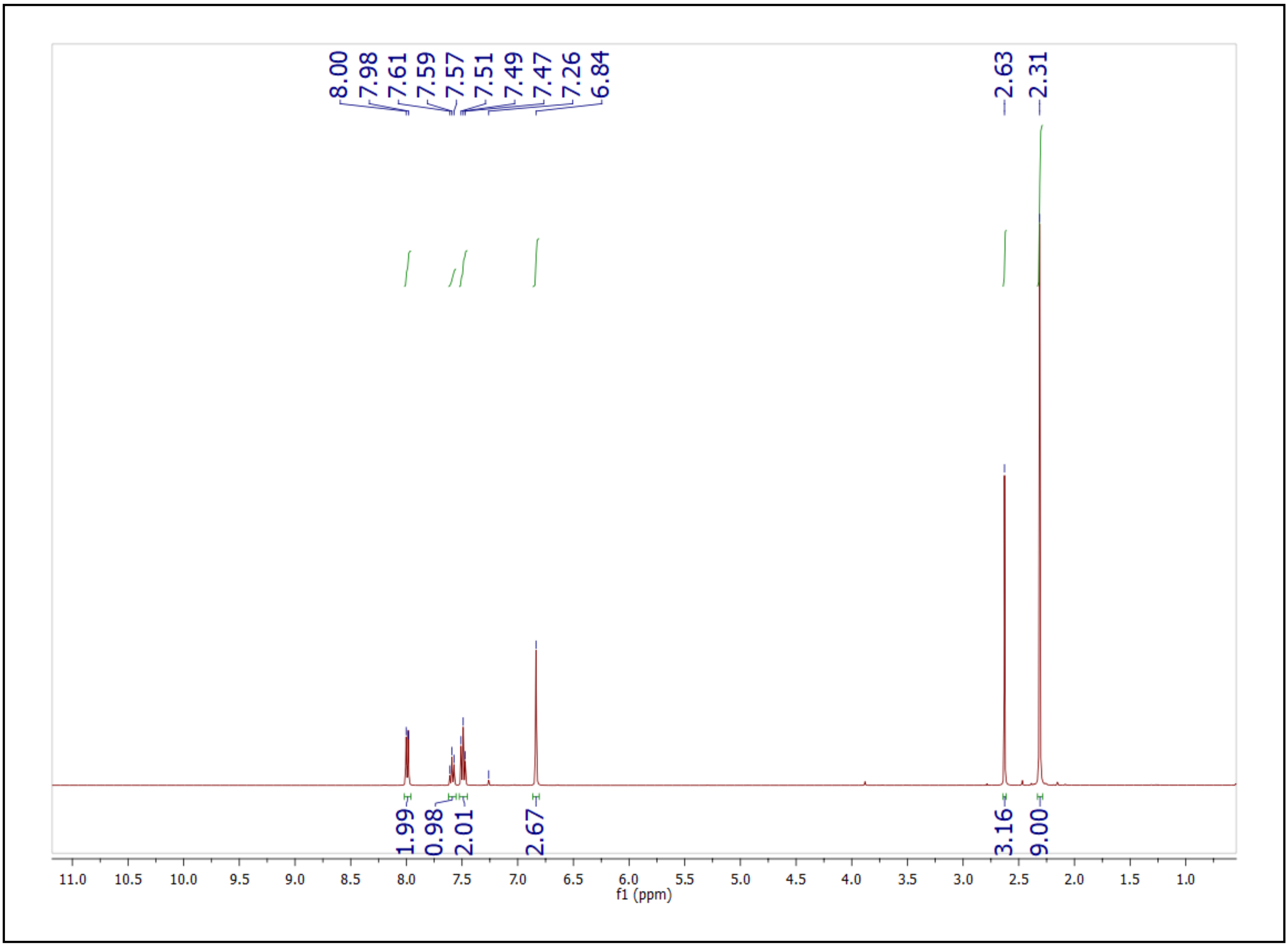

Figure S58. Cyanosilylation of acetophenone without using the catalyst.

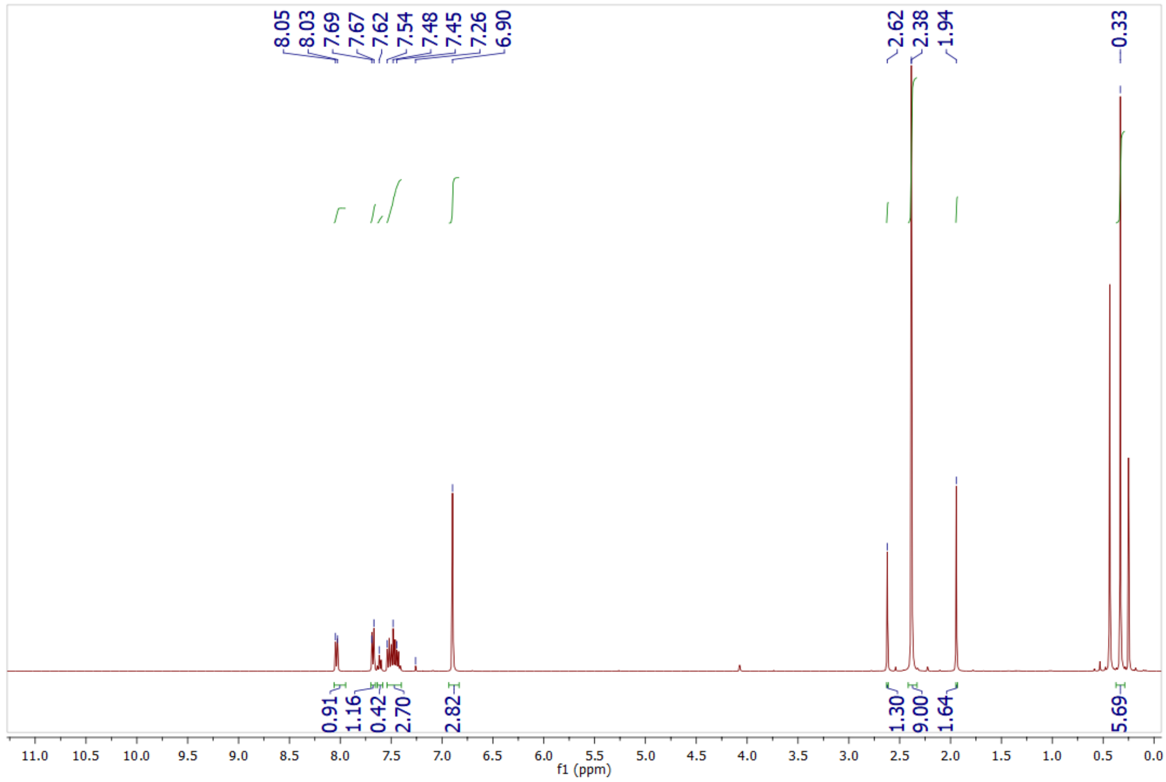

Figure S59. ^{1}H NMR of cyanosilylation of acetophenone with $AgSbF_6$ (0.5 mol%) using mesitylene as internal standard.

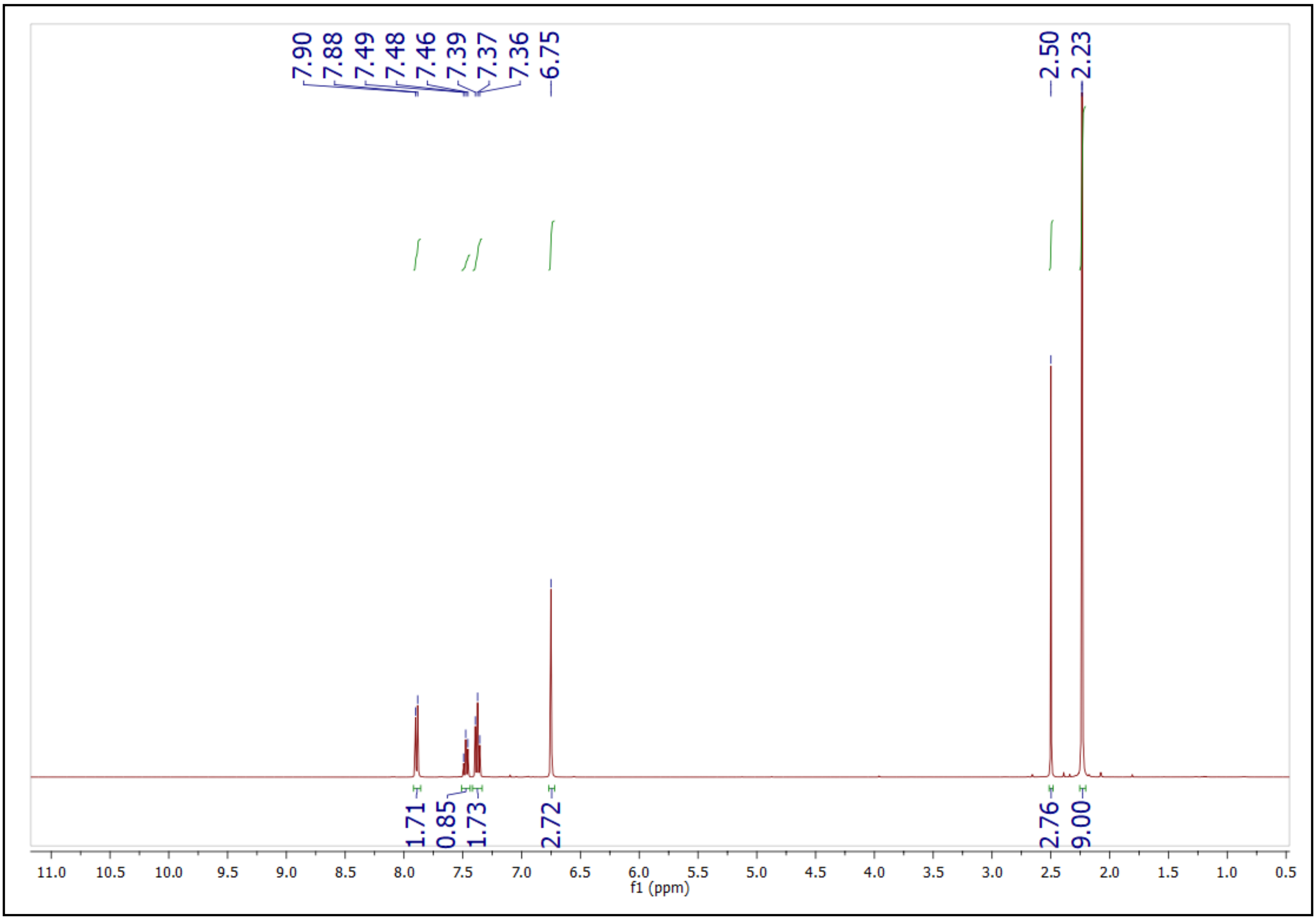

Figure S60. ^{1}H NMR of cyanosilylation of acetophenone with NaBarF$_4$ using mesitylene as internal standard

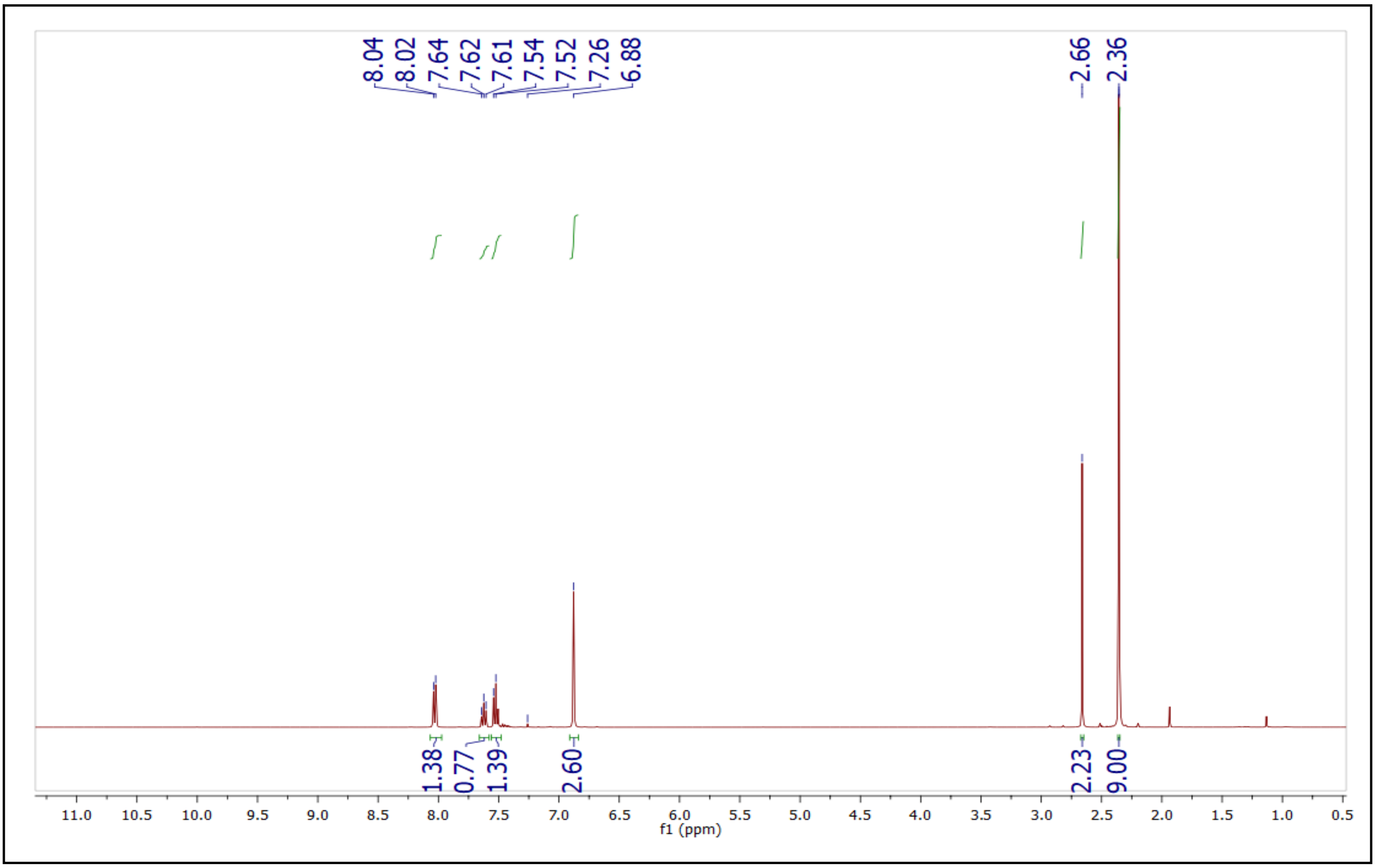

Figure S61. ^{1}H NMR of cyanosilylation of acetophenone as compound **2** as the catalyst using mesitylene as an internal standard.

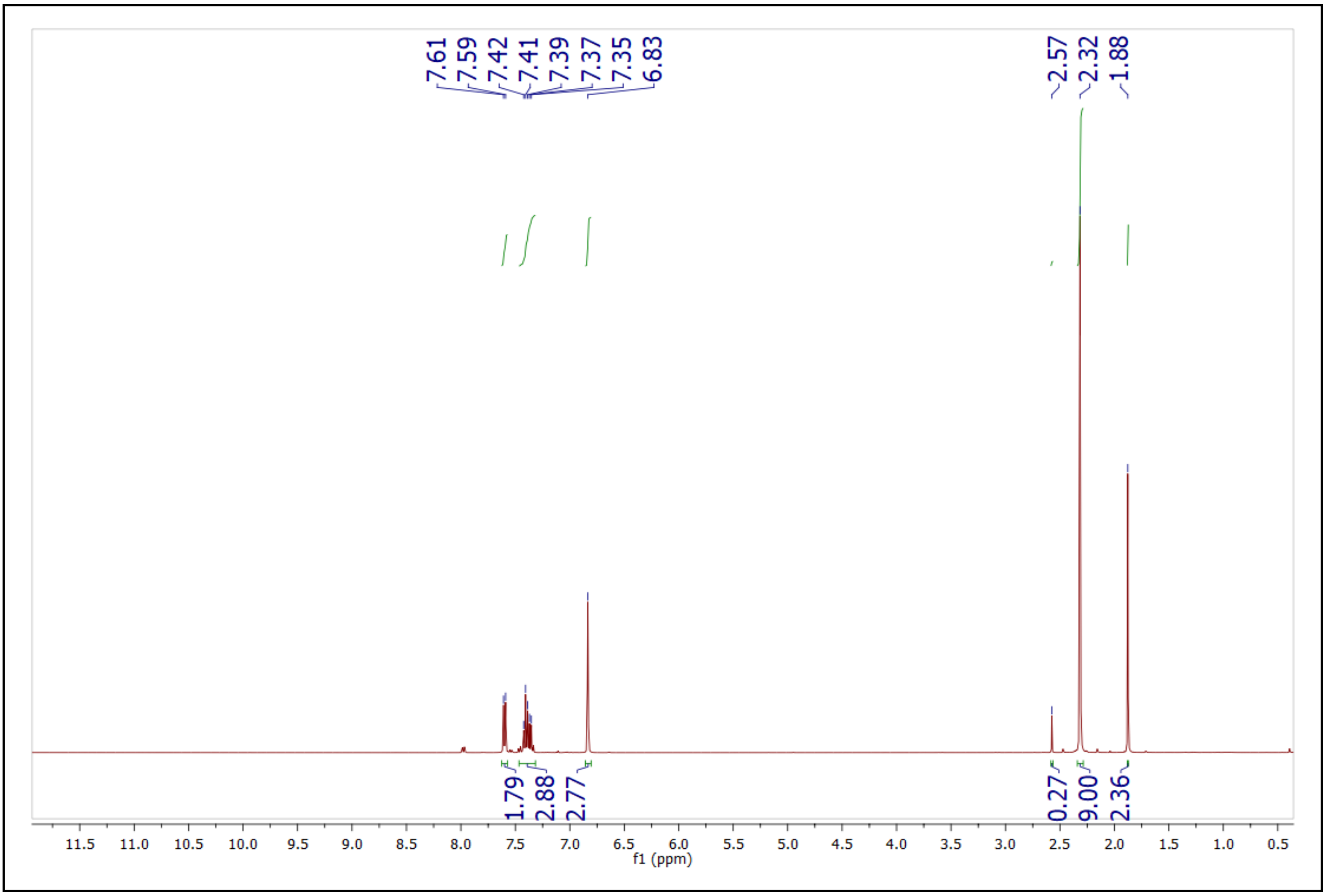

Figure S62. ^{1}H NMR of cyanosilylation of acetophenone using mesitylene as an internal standard in acetonitrile as a solvent.

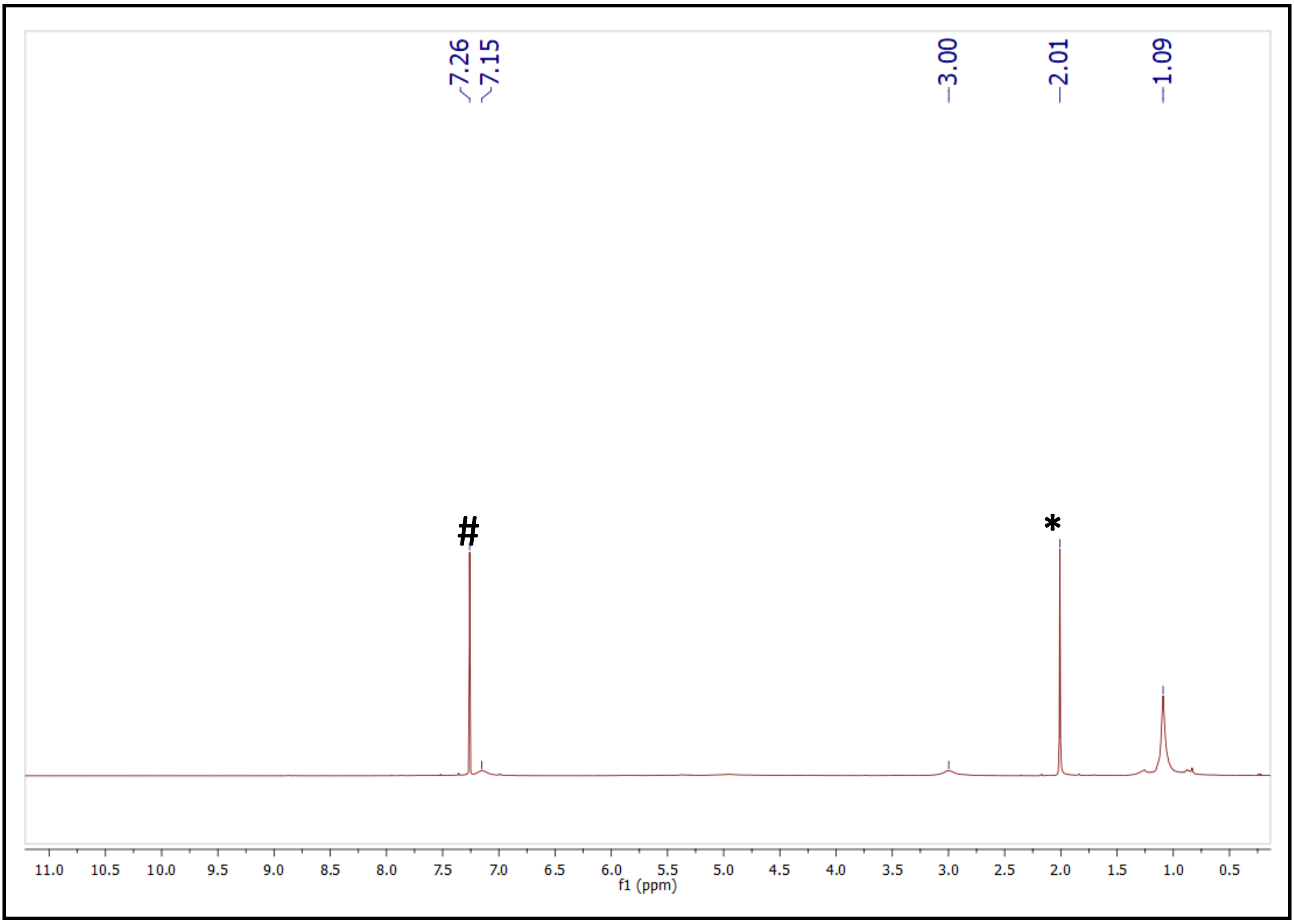

Figure S63. ^{1}H NMR of 1:1 reaction of catalyst **3** and acetonitrile in $CDCl_3$ (* - Acetonitrile, # - $CDCl_3$).

[S12]. Computational Details:

The electronic structure of all the systems studied is done by density functional theory. For geometry optimization M062X[2-3] exchange-correlation functional along with 6-311G(d,p) basis set is used for lighter atoms (C, H, B, N, O, F). For Bi, we have used lanl2dz basis set in combination with Stuttgart-Dresden pseudopotential. All optimized geometries are characterized by harmonic vibrational analysis to recognize the structures as minima (all positive frequencies) or transition states (one negative frequency). Transition states (TS) are verified through intrinsic reaction coordinate (IRC) calculations. All thermochemical data are estimated within the ideal gas-rigid rotor-harmonic oscillator approximation at 298.15 K and 1 atm pressure. SMD model is used to consider solvent effects.[4] Photophysical properties of these catalysts are calculated using time-dependent density functional theory (TD-DFT) methods using B3LYP-D3[4-8] exchange-correlation functional. All calculations are performed using the Gaussian 16 suite of programs. [9]

The approximation used in this DFT model:

1. The model catalysts **3m** is used for the mechanistic study, wherein the methyl groups replace the CH_2Bu substituent on the N center. Such modeling does not impose major changes in the electronic and structural properties of the catalyst and has been routinely used in simulations to reduce the computational cost. Due to this, however, it is possible that this model catalyst always lies in a higher energy state in the free energy profile and overestimates the activation barrier.
2. In our DFT calculations, the computed entropic corrections are scaled to 100% to consider the quenching of translational and rotational degrees of freedom in the solution phase. This entropic correction makes the overall activation barrier high.
3. All the thermochemical corrections are estimated using the ideal-gas-rigid rotor-simple harmonic oscillator approximations at 298.15 K and 1 atm pressure in our DFT study. This harmonic approximation also leads to the overestimation of the activation barrier.

Geometry optimized structures of all the compounds, reaction intermediates and transition states.

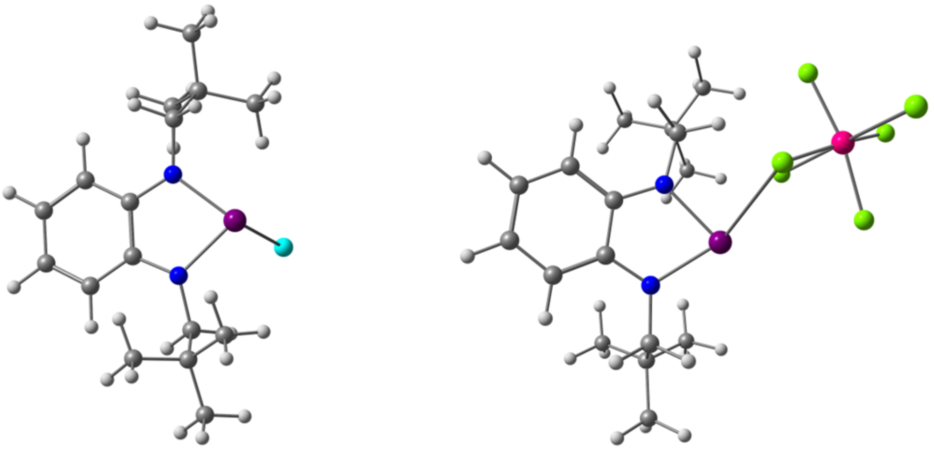

Compound **2**

Compound **3**

Figure S63. Geometry optimized structures of compound **2** and **3.** All the distances are shown in Å unit.

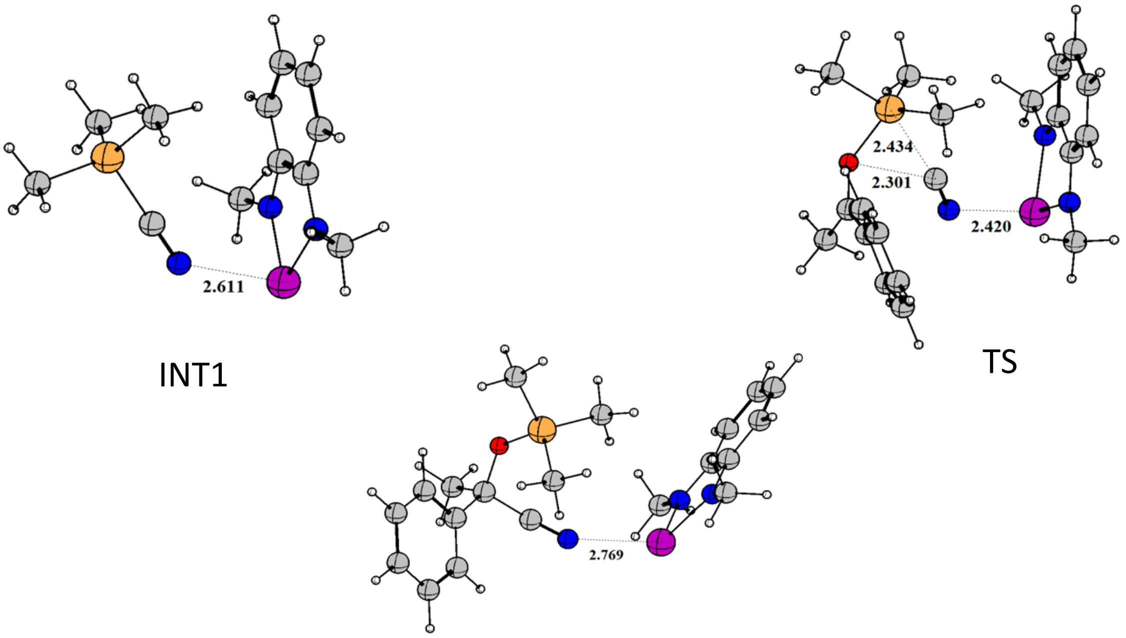

INT1

TS

INT2

Figure S64. Geometry optimized structures of all the intermediates and transition state for the cyanosilylation reaction of acetophenone catalyzed by **3.** All the distances are shown in Å units.

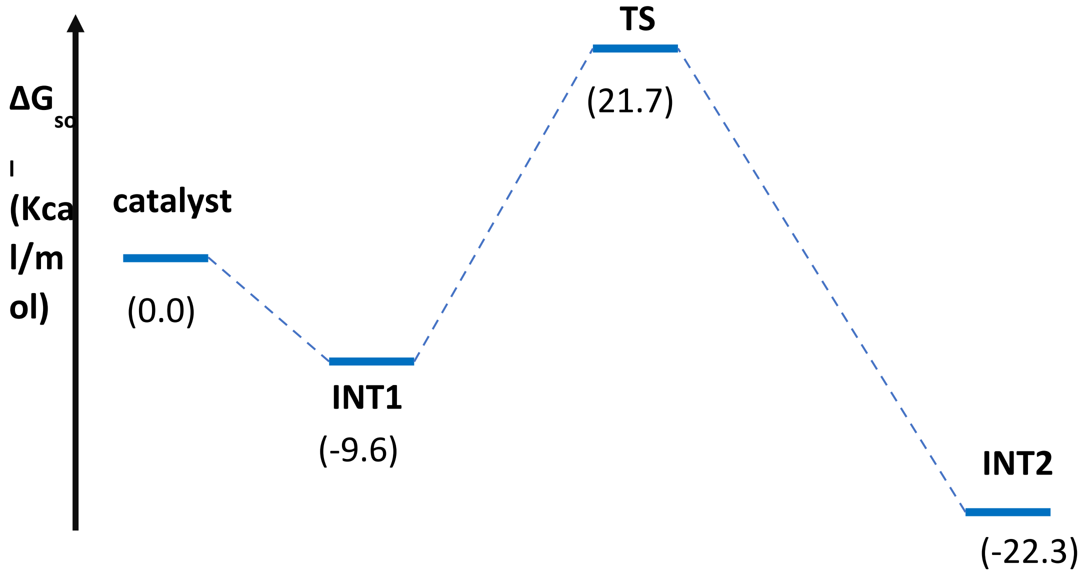

Figure S65. Relative solvent-corrected Gibbs free energy profiles for cyanosilylation of acetophenone catalyzed by **3.**

[S13]. References

1. N. Sen, P. Gothe, P. Sarkar, S. Das, S. Tothadi, S. K. Pati and S. Khan, *Chem. Commun.*, 2022, **58**, 10380-10383.
2. Y. Zhao and D. G. Truhlar, The M06 suite of density functionals for main group thermochemistry, thermochemical kinetics, noncovalent interactions, excited states, and transition elements: two new functionals and systematic testing of four M06-class functionals and 12 other functionals. *Theoretical chemistry accounts*, 2008, **120**, 215-241.
3. Y. Zhao and D. G. Truhlar, Density functionals with broad applicability in chemistry, *Accounts of chemical research*, 2008, **41**, 157-167
4. C. Lee, W. Yang and R. G. Parr, Development of the Colle-Salvetti correlation-energy formula into a functional of the electron density, *Physical review B*, 1988, **37**, 785.
5. S. Grimme, Accurate description of van der Waals complexes by density functional theory including empirical corrections, *Journal of computational chemistry*, 2004, **25**, 1463- 1473.
6. S. Grimme, Semiempirical GGA-type density functional constructed with a long-range dispersion correction, *Journal of computational chemistry*, 2006, **27**, 1787-1799.

7. S. Grimme, J. Antony, S. Ehrlich and H. Krieg, A consistent and accurate ab initio parametrization of density functional dispersion correction (DFT-D) for the 94 elements H-Pu, *The Journal of chemical physics*, 2010, **132**, 154104.
8. S. Grimme, S. Ehrlich, L. Goerigk, Effect of the damping function in dispersion corrected density functional theory, *Journal of computational chemistry*, 2011, **32**, 1456-1465
9. Frisch, M. J.; Trucks, G. W.; Schlegel, H. B.; Scuseria, G. E.;Robb, M. A.; Cheeseman, J. R.; Scalmani, G.; Barone, V.; Mennucci,B.; Petersson, G. A. et al.Gaussian 16, revision A.03.2016; GaussianInc.: Wallingford, CT.

Coordinates of the Intermediates and Transition states in XYZ format

Bi	-0.00007000	-1.38141100	0.13900400
Cl	-0.00022700	-2.01946600	2.50840000
N	1.30905200	0.14395400	0.21224200
N	-1.30905300	0.14405800	0.21203500
C	3.52365900	-0.03420300	-1.00214400
C	1.39186400	2.56371300	0.75788400
H	2.47296700	2.58085800	0.75134800
C	4.99415500	-0.32017700	-0.68380100
H	5.11669800	-1.30913600	-0.23261200
H	5.39584400	0.42222200	0.01160800
H	5.59739600	-0.28821000	-1.59451700
C	0.69295000	3.73818400	1.02543300
H	1.24161700	4.64926300	1.22897500
C	-2.98936200	-1.11549200	-1.94603700
H	-1.96561000	-0.89453500	-2.26098000
H	-3.60369600	-1.17243800	-2.84816400
H	-3.00600200	-2.10244300	-1.46992800
C	-4.99416900	-0.31970000	-0.68390800

H	-5.11692900	-1.30849800	-0.23237300
H	-5.59731600	-0.28798700	-1.59469300
H	-5.39582200	0.42298700	0.01119300
C	2.74672500	-0.07044800	0.33037500
H	2.91706800	-1.05186700	0.79299300
H	3.17011900	0.65757300	1.02869900
C	-0.69277800	3.73825900	1.02526600
H	-1.24139900	4.64940600	1.22862500
C	-3.52358600	-0.03408900	-1.00218900
C	-0.71018500	1.37904000	0.49296600
C	3.39301500	1.33388500	-1.67541400
H	3.88993800	1.32439100	-2.64939500
H	3.85824100	2.11759300	-1.07169800
H	2.34380400	1.59870500	-1.82776600
C	0.71025600	1.37896300	0.49310700
C	-3.39257800	1.33382700	-1.67570700
H	-3.85783600	2.11773400	-1.07231400
H	-3.88925800	1.32416800	-2.64981700
H	-2.34327800	1.59843200	-1.82784400
C	-2.74675200	-0.07027100	0.33033500
H	-3.17005600	0.65782200	1.02864500
H	-2.91714200	-1.05166300	0.79294400
C	-1.39174100	2.56385400	0.75754400
H	-2.47284100	2.58108400	0.75078500
C	2.98942200	-1.11533000	-1.94629800
H	3.60435200	-1.17267400	-2.84800700
H	1.96602300	-0.89380600	-2.26194800
H	3.00519100	-2.10228800	-1.47017200

NbBiSbF6

Bi	-0.38623200	-0.48249900	-0.32968000
N	-1.11389000	1.38961200	-0.48925700
N	-2.36681600	-0.87892300	-0.55338000
C	-2.48221000	1.46781400	-0.69730400
C	-3.21330800	2.65551300	-0.87904900
C	-3.16886400	0.22364200	-0.74996100
C	-2.89274300	-2.24512200	-0.54885200
C	-0.30382100	2.61211000	-0.36450900
C	-4.55025100	0.20051800	-1.00746500
C	-0.07991900	3.10597900	1.08467300
C	-5.23952200	1.37960900	-1.19130000
C	-4.56955400	2.60737800	-1.12302200
C	-3.29016800	-2.80039300	0.83855500
C	-3.75278700	-4.24441200	0.61209800
C	0.81525200	2.13040100	1.85207700
C	-2.08256500	-2.80089000	1.78012000
C	-1.40026700	3.29108300	1.83588400
C	-4.42340600	-1.98884400	1.47057500
C	0.64474500	4.45222600	0.96866800
Sb	3.29450100	-0.49092300	-0.17126500
F	3.97656700	1.04373300	0.65574800
F	1.82275800	0.61701800	-0.85978500
F	2.11033700	-0.74397200	1.30373200
F	2.34465800	-1.90539100	-1.00500200
F	4.25729200	-0.16200600	-1.73333500
F	4.57951600	-1.62643600	0.55148200
H	0.66978900	2.41608500	-0.81156400

H	-0.77091500	3.39905600	-0.95833700
H	1.77375500	1.97777300	1.35153400
H	1.01862200	2.52109300	2.85234000
H	0.34119600	1.15343300	1.99655200
H	0.03303300	5.18591200	0.43562400
H	0.86153600	4.85196200	1.96191000
H	1.59361200	4.34161900	0.43714600
H	-1.96503200	2.35607200	1.89124100
H	-1.19882800	3.62048700	2.85828100
H	-2.03498100	4.04440400	1.36272400
H	-3.73824800	-2.31633500	-1.23809900
H	-2.11474200	-2.90151400	-0.95486400
H	-1.21506600	-3.29304600	1.32653800
H	-1.79817000	-1.78655700	2.07443200
H	-2.32222800	-3.34225000	2.69821200
H	-2.94638300	-4.85959200	0.20325500
H	-4.07186000	-4.69285700	1.55556700
H	-4.59774500	-4.28334000	-0.08104500
H	-5.33504100	-2.04095100	0.86975200
H	-4.65575600	-2.38709600	2.46154600
H	-4.14830600	-0.93762000	1.58622500
H	-2.72079700	3.61514200	-0.83048700
H	-5.11720400	3.53061400	-1.26380500
H	-6.30407600	1.35321200	-1.38655300
H	-5.07677200	-0.74220700	-1.05411300

Int1

N	-1.22842719	0.88939291	-1.12771797
C	-0.04016308	1.36304141	0.87663863

C	0.38359245	2.75191433	-1.08549746
H	0.18882486	3.00720604	-2.11877028
C	-0.28974625	1.67794534	-0.48629727
C	1.55636188	3.16653468	0.98602013
H	2.27252138	3.74923436	1.55122822
C	0.89717677	2.11611942	1.59971535
H	1.08973811	1.88946752	2.64053728
C	1.29465499	3.48800510	-0.34983999
H	1.80963278	4.31814400	-0.81620481
N	-0.78389373	0.32397379	1.40574528
C	-0.53723043	-0.11962890	2.77338537
H	-0.71665112	0.69569331	3.47743678
H	-1.21154964	-0.93719753	3.02942710
C	-1.52375538	1.11697184	-2.53941704
H	-2.27974190	0.41019833	-2.88188259
H	-1.91283685	2.12659124	-2.68801948
Bi	-1.89107849	-0.68203681	0.00597974
H	-0.62535361	0.98386023	-3.14789492
H	0.49279683	-0.47237568	2.88576461
Si	3.34035278	-1.03855654	-0.25626597
C	3.47279115	0.51449922	-1.26836210
H	2.82063916	1.29384736	-0.86666590
H	4.50016504	0.88706208	-1.24138582
H	3.20771763	0.33988755	-2.31302596
C	4.29905082	-2.48669465	-0.91993975
H	5.36962579	-2.27354935	-0.86259767
H	4.10723098	-3.39309804	-0.34272017
H	4.05347715	-2.68512440	-1.96481427
C	3.57484123	-0.74648646	1.56860146

H	4.62248880	-0.50744142	1.76960195
H	2.97025826	0.09922838	1.90357702
H	3.31630272	-1.62776618	2.15899108
C	1.49613271	-1.55126801	-0.41544984
N	0.38618493	-1.85632969	-0.49495902

TS

C	-3.29466600	-2.27776500	0.36105100
C	-3.50933900	-0.98033400	-0.12302700
C	-4.24175500	-0.06009800	0.63548300
C	-4.74855500	-0.43249200	1.87157800
C	-4.50822100	-1.71292300	2.36002900
C	-3.77829400	-2.63357700	1.60827500
C	-3.03921100	-0.60013400	-1.45422600
O	-2.76429000	0.57861000	-1.74768400
Si	-2.04691400	2.06254500	-0.93106100
C	-0.58843400	2.56183400	-1.98217500
C	-0.78786300	-0.01071400	-0.72684400
N	-0.18978200	-0.98568300	-0.97963000
C	-3.48323000	3.16858500	-1.42416300
C	-1.83438100	2.17380700	0.92140500
H	-4.44582000	0.92779900	0.23962300
H	-5.33421900	0.27061500	2.44978100
H	-4.90091100	-2.00135600	3.32756400
H	-3.60029400	-3.62908500	1.99446200
H	-2.72611900	-2.98906700	-0.22586600
H	-3.24100200	4.20104100	-1.15391000
H	-3.66266800	3.14504900	-2.50153000

H	-4.42339200	2.92226400	-0.92381600
H	-2.41214000	3.00609200	1.33078500
H	-2.10741400	1.26052100	1.44884300
H	-0.77164400	2.34793000	1.11938700
H	-0.65528700	3.62221200	-2.23783500
H	0.34136800	2.38005700	-1.44109100
H	-0.57063200	1.98872800	-2.91212400
N	2.66509200	0.65892100	-0.59742500
C	1.09908500	-1.48937800	2.50556300
C	3.19673400	1.31621300	-1.78422000
C	1.35255500	1.38790900	2.75138300
C	1.41419600	2.77365000	2.78353300
C	1.87974400	3.48636600	1.68033700
H	3.51108500	0.56938300	-2.51439800
H	2.45131700	1.96392300	-2.25562300
H	0.04213800	-1.21528600	2.59840800
H	1.16319600	-2.54773900	2.24810100
H	2.66260300	3.37889300	-0.31377900
H	1.92518600	4.56745600	1.71193600
H	1.09401200	3.30033800	3.67349100
H	0.98807300	0.84389400	3.61281800
H	1.58905000	-1.35686800	3.47309300
H	4.07205700	1.91559300	-1.52167900
C	-2.93967400	-1.61518900	-2.53762000
H	-3.77614100	-2.31235400	-2.51155100
H	-2.86733200	-1.11675000	-3.50137300
H	-2.01139500	-2.17219400	-2.36339400
Bi	2.14291200	-1.32087700	-0.42955700
N	1.75576500	-0.68738900	1.48426000

C	2.24561200	1.42203100	0.48713800
C	2.29432800	2.81862800	0.53636000
C	1.76440400	0.69628900	1.60826700

Int2

C	-4.85783600	0.86635100	0.23369400
C	-4.01401000	-0.00877800	-0.44742200
C	-4.20558700	-1.38263800	-0.33821600
C	-5.22700300	-1.88121600	0.46427900
C	-6.06018700	-1.00936900	1.15465400
C	-5.87667100	0.36473500	1.03434200
C	-2.93910900	0.59391100	-1.35358900
O	-2.43946900	1.80034700	-0.85003000
Si	-1.50300600	2.06442700	0.54018500
C	0.26966400	2.24117200	-0.03751700
C	-1.79633000	-0.36694800	-1.46635900
N	-0.87290000	-1.05182600	-1.50076300
C	-2.14148900	3.63200100	1.30145800
C	-1.66474800	0.61311900	1.72396000
H	-3.56188300	-2.07313500	-0.87413200
H	-5.37053100	-2.95135700	0.54819900
H	-6.85396200	-1.39839700	1.78008400
H	-6.53087500	1.04800300	1.56187300
H	-4.71326300	1.93597000	0.13268400
H	-3.15532500	3.50235000	1.68642300
H	-1.50591300	3.94919400	2.13214400
H	-2.15739500	4.43903400	0.56572100
H	-0.90087000	0.69621400	2.50411900
H	-2.64143900	0.60978500	2.21385000
H	-1.55683000	-0.36129000	1.23900800

H	0.98080300	2.16958900	0.79221100
H	0.52323200	1.47228100	-0.77245000
H	0.42319600	3.21027800	-0.51833500
N	2.60940000	-0.39809200	1.33093500
C	3.17907100	0.46131800	-0.79195400
C	4.23679000	1.44089400	1.19223500
H	4.36885300	1.48144900	2.26526600
C	3.34989600	0.50299100	0.62306300
C	4.78598100	2.23834700	-1.02437800
H	5.35278500	2.91557900	-1.65033800
C	3.92354000	1.34038300	-1.60610100
H	3.81047000	1.31331300	-2.68124700
C	4.94204100	2.29037200	0.37460700
H	5.62953100	3.00418900	0.80988000
N	2.25529900	-0.43060000	-1.26057000
C	1.99575900	-0.50621100	-2.69792700
H	1.24014600	-1.26126600	-2.89896000
H	1.62928800	0.45767100	-3.06220100
C	2.68306700	-0.41070900	2.78992300
H	2.02211600	-1.18128300	3.18792400
H	3.70196500	-0.63318600	3.11424600
H	2.37925600	0.55440200	3.20331100
H	2.91074100	-0.77047700	-3.23201200
C	-3.49262200	0.85823400	-2.75660300
H	-2.71557600	1.28691000	-3.38963400
H	-3.87693600	-0.06096100	-3.19993900
H	-4.30829400	1.57393100	-2.65306900
Bi	1.26446600	-1.52214100	0.19533600